MARS: REVIEW AND ANALYSIS OF VOLCANIC ERUPTION THEORY AND RELATIONSHIPS TO OBSERVED LANDFORMS

Lionel Wilson
Environmental Science Division
Institute of Environmental and Biological Sciences
Lancaster University, Lancaster, England

James W. Head III
Department of Geological Sciences
Brown University
Providence, Rhode Island

Abstract. We present a theoretical treatment of the ascent, emplacement, and eruption of magma on Mars. Because of the lower gravity, fluid convective motions and crystal settling processes driven by positive and negative buoyancy forces, as well as overall diapiric ascent rates, will be slower on Mars than on Earth, permitting larger diapirs to ascend to shallower depths. This factor also favors a systematic increase in dike widths on Mars by a factor of 2 and, consequently, higher effusion rates by a factor of 5. As a result of the differences in lithospheric bulk density profile, which in turn depend on differences in both gravity and surface atmospheric pressure, magma reservoirs are expected to be deeper on Mars than on Earth, by a factor of about 4. The combination of the lower Martian gravity and lower atmospheric pressure ensures that both nucleation and disruption of magma occur at systematically greater depths than on Earth. Although lava flow heat loss processes are such that no major differences between Mars and Earth are to be expected in terms of flow cooling rates and surface textures, the lower gravity causes cooling-limited flows to be longer and dikes and vents to be wider and characterized by higher effusion rates. Taken together, these factors imply that we might expect compositionally similar cooling-limited lava flows to be about 6 times longer on Mars than on Earth. For example, a Laki type flow would have a typical length of 200–350 km on Mars; this would permit the construction of very large volcanoes of the order of 500–700 km in diameter. For strombolian eruptions on Mars the main difference is that while the large particles will remain near the vent, the finer material will be more broadly dispersed and the finest material will be carried up into a convecting cloud over the vent. This means that there would be a tendency for broader deposits of fine tephra surrounding spatter cones on Mars than on Earth. On Mars, strombolian eruption deposits should consist of cones that are slightly broader and lower relative to those on Earth, with a surrounding deposit of finer material. Martian hawaiian cones should have diameters that are about a factor of 2 larger and heights that are, correspondingly, about a factor of 4 smaller than on Earth; central craters in these edifices should also be broader on Earth by a factor of up to at least 5. Grain sizes in Martian hawaiian edifices should be at least 1 order of magnitude finer than in terrestrial equivalents because of the enhanced magma fragmentation on Mars. Differences in the atmospheric pressure and temperature structure cause Martian plinian eruption clouds to rise about 5 times higher than terrestrial clouds for the same eruption rate. Essentially the same relative shapes of eruption clouds are expected on Mars as on Earth, and so the cloud-height/deposit-width relationship should also be similar. This implies that Martian fall deposits may be recognized as areas of mantled topography with widths in the range of several tens to a few hundred kilometers. A consequence of the lower atmospheric pressure is that Martian plinian deposits of any magma composition will be systematically finer grained than those on Earth by a factor of about 100, almost entirely subcentimeter in size. Basaltic plinian eruptions, rare on Earth, should be relatively common on Mars. The production of large-scale plinian deposits may not signal the presence of more silicic compositions, but rather may be linked to the enhanced fragmentation of basaltic magma in the Martian environment or to the interaction of basaltic magma with groundwater. The occurrence of steep-sided domes, potentially formed by viscous, more silicic magma, may be largely precluded by enhanced magma fragmentation. Pyroclastic flow formation is clearly inherently more likely to occur on Mars than on Earth, since eruption cloud instability occurs at a lower mass eruption rate for a given magma volatile content. For a given initial magma volatile content, eruption speeds are a factor of at least 1.5 higher on Mars, and so the fountains feeding pyroclastic flows will be more than twice as high as on Earth. Pyroclastic flow travel distances may be a factor of about 3 greater, leading to values up to at least a few hundred kilometers. Martian environmental conditions thus operate to modulate the various eruption styles and the morphology and morphometry of resulting landforms, providing new insight into several volcanological problems.

Copyright 1994 by the American Geophysical Union.

Reviews of Geophysics, 32, 3 / *August 1994*
pages 221–263
8755-1209/94/94RG-01113$15.00
Paper number 94RG01113

1. INTRODUCTION

Analysis of the images returned from the Mariner and Viking missions has produced abundant evidence for a variety of volcanic landforms on Mars [e.g., *Carr*, 1973, 1981; *Carr et al.*, 1977; *Greeley*, 1973; *Plescia and Saunders*, 1979; *Greeley and Spudis*, 1981; *Schaber et al.*, 1978; *Schaber*, 1982; *Hodges and Moore*, 1994]. One approach to understanding the styles of Martian volcanic activity represented by these landforms has been to compare the morphologies of Martian volcanic structures with those of terrestrial analogs. While useful, this method may overlook the potentially dramatic effects of differences between the terrestrial and Martian environments on eruptive processes [*Wilson and Head*, 1983; *Wilson*, 1984; *Mouginis-Mark et al.*, 1992]. As a result, we concentrate here on a different approach, that of initially considering the processes of ascent and eruption of magma on Mars from first principles and developing predictions of the types of volcanic landforms expected to be produced in the Martian lithospheric and atmospheric environment. We then compare these predictions with observed landforms [e.g., *Hodges and Moore*, 1994]. We follow the basic approach that we have utilized in analyzing the ascent and emplacement of magma on the Earth and Moon [*Wilson and Head*, 1981*a*, 1983; *Head and Wilson*, 1992*a*], and Venus [*Head and Wilson*, 1987, 1992*b*]. We first examine modes of magma production in the Martian interior and then assess processes of magma ascent, analyzing the shallow density structure of the crust and lithosphere and its potential influence on the production of zones of neutral buoyancy. Following this, we examine processes of gas exsolution at shallow depths and methods by which the range of eruption products is manifested in the creation and growth of deposits and landforms. Finally, we compare theoretical predictions with the range of landforms that have been revealed by Mars exploration and use these observations as a basis to investigate a number of problems in the thermal and volcanological history of Mars.

On the basis of an assessment of the crustal configuration of Mars and a theoretical treatment of the ascent and eruption of magma through this crust in the Martian gravity and atmospheric environment, we find that the full range of volcanic eruption styles observed on Earth is to be expected. It is clear, though, that Martian environmental conditions operate to modulate the various eruption styles and the morphology and morphometry of resulting landforms. Using these theoretical predictions as a basis, we compare observed deposits and landforms and find general agreement, as outlined above. In several cases we find that theory provides new insight into Martian volcanological problems. For example, the effects of gravity and cooling should cause compositionally similar cooling-limited flows on Mars to be about a factor of 6 longer than those on Earth, thus providing a potential explanation for the flows several hundred of kilometers long that build the major Martian edifices. Similarly, theoretical analysis of plinian air fall and pyroclastic flow emplacement provides a basis to distinguish these types of deposits in Martian volcanoes, and analysis of the geologic record supports the view that both types of eruptions took place around several Martian volcanic centers. This analysis also provides some perspective on several other problems in Martian geology and history.

GLOSSARY

Aa flow: lava flow characterized by a rough, jagged, and clinkery surface.

Allochthonous breccia: rock or deposit formed of angular fragmental material derived from nonlocal sources and transported to present location.

Autochthonous breccia: rock or deposit formed of angular fragmental material derived from local sources.

Carbonatite: a rock of magmatic origin containing at least 50% carbonate minerals and usually associated with alkalic rocks and kimberlites.

Hawaiian eruption: a type of basaltic volcanic eruption characterized by fountains of molten magma particles fragmented by expanding magmatic gas and forming fire fountains over the vent. The pyroclastic fragments may cool and form cinder cones and/or recollect to form effusive flows.

Kimberlite: an alkalic peridotite containing abundant phenocrysts of the minerals olivine and phlogopite mica in a fine-grained matrix; often associated with diamond deposits in continental areas on Earth.

Komatiite: a suite of igneous basaltic and ultramafic lavas and rocks with very high magnesium content; generally restricted to early Earth history.

Lahar: a mudflow or landslide of hot pyroclastic material on the flanks of a volcano.

Maar: a broad, low-relief volcanic cone formed by multiple shallow explosive volcanic eruptions.

Megaregolith: a thick outer fragmental soil layer formed from upper crustal rock comminuted and redistributed primarily by intense impact cratering processes typical of early planetary history. Grades down into autochthonous breccia and fractured in situ crust.

Pahoehoe flow: lava flow characterized by a ropy and billowy surface; smooth, relative to an aa flow.

Plinian eruption: explosive volcanic eruption characterized by magma which disrupts into very small fragments that become locked to an expanding gas plume rising buoyantly from the vent and producing widely dispersed ash and pumice deposits.

Pseudocrater: a small cratered cone which is not a primary volcanic vent but instead forms from explo-

sive disruption of lavas as they flow over a volatile-rich substrate.

Pyroclastic flow: a turbulent flow of hot gas and disrupted magmatic fragments (pyroclasts). These often form during the collapse of plinian eruption columns.

SNC meteorites: a group of differentiated meteorites for which the parent body is thought to be the planet Mars. SNC designates the key named members of the group (shergottites, nakhlites, and chassignites).

Strombolian eruption: a type of basaltic volcanic eruption in which magma erupts upon the intermittent explosive emergence of large gas bubbles from the vent. Forms spatter cones around the vent.

Tholeiite: a basalt characterized by the minerals orthopyroxene and pigeonite in addition to clinopyroxene and calcic plagioclase feldspar. Commonly found on the Earth's ocean floor.

2. PRODUCTION AND ASCENT OF MAGMA

2.1. Background

Whenever magma is produced by partial melting at depth in the Martian interior, it will tend to ascend to the surface as long as its density contrast with the surrounding materials is such as to produce positive buoyancy. As is the case on Earth, the ascent may occur in stages, with the magma pausing to form intrusive bodies within which it may undergo chemical and physical evolution, leading to a diversification of the range of possible eruption product compositions. Ascending magma may also interact and mix with the crust through which it passes.

Estimates of the composition of surface volcanic and crustal deposits, and thus melts, on Mars have been made from several approaches. First, the general density characteristics of Mars permit estimates of Martian mantle composition, which is suggested to have 2–3 times the iron content of the Earth's mantle, possibly resulting in partial melts emerging as iron-enriched basic or ultrabasic lavas [*McGetchin and Smyth*, 1978; *Goettel*, 1981]. Second, remote sensing data and laboratory analyses have provided evidence that many bright and dark albedo units [*Soderblom et al.*, 1978; *Arvidson et al.*, 1982] are best interpreted as basalts characterized by varying degrees of oxidation [*Adams and McCord*, 1969; *McCord et al.*, 1982]. In addition, more recent spectroscopic measurements show that the characteristics of the dark areas differ down to the limits of resolution, with variations consistent with a variety of pyroxene types and abundances (predominantly clinopyroxene) and almost no evidence for abundant olivine [*Singer et al.*, 1990; *Pinet and Chevral*, 1990; *Bibring et al.*, 1990; *Mustard et al.*, 1993]. Third, chemical analyses of surface soils at the two Viking lander sites did not fit any known terrestrial rock types and were interpreted to be soils modified by exogenous salts [*Toulmin et al.*, 1977] or volcanic gases [*Settle*, 1979]; the parent rocks were interpreted to be distinctly mafic in composition [*Clark et al.*, 1982]. Fourth, analysis of the characteristics of lava flows on Martian shield volcanoes and interpretation of their rheological properties suggest flows with yield strengths and viscosities which have been cited as evidence for mafic basalts [*Hulme*, 1976; *Moore et al.*, 1978; *Cattermole*, 1987] and basaltic andesites [*Zimbelman*, 1985*a*, *b*].

Information obtained through analysis of the characteristics of SNC meteorites interpreted to have been derived from Mars [*Wood and Ashwal*, 1981] represent a fifth approach. These materials are very similar to terrestrial basaltic and ultramafic rocks, and some can even be classified as komatiitic [*Baird and Clark*, 1981], leading to the conclusion that ultrabasic volcanism is more important on Mars than on the Moon and present-day Earth [*Treiman*, 1986]. On the basis of the characteristics of the SNC meteorites, the Martian mantle is also thought to have a high Fe/Mg ratio relative to the Earth [*Dreibus and Wanke*, 1984]. Experimental petrologic studies on melts derived from such mantle compositions showed evidence for tholeiitic, picritic, and komatiitic melts with increasing degrees of partial melting, but the relative abundances of these compositions could not yet be determined; at lower pressures and in the presence of carbonate, carbonatitic and possibly kimberlitic, primary magmas may form [*Bertka and Holloway*, 1989, 1990]. Analysis of the SNCs from the point of view of magmatic processes [*Longhi*, 1990] shows the parent magmas to be high-Fe, low-Al liquids with high densities (2750–2960 kg m^{-3}) and low viscosities (0.4–12.8 Pa s) [*Longhi and Pan*, 1988] and with the possible presence of CO_2. *Longhi and Pan* [1988] suggested that some of the SNCs could be related to each other by assimilation of a component rich in K and other incompatible lithophile elements; this and the lack of negative Eu anomalies in the parent magma compositions have been interpreted to favor interaction with an Earth continentallike crustal component on Mars during magma ascent. Apparently, flows and shallow intrusions represented by the SNC meteorites did not undergo significant hydrothermal alteration, and the parent magmas contained less H_2O than a typical terrestrial basalt [*Longhi*, 1992]; however, some samples show evidence of more abundant H_2O [*Rutherford*, 1991; *Johnson et al.*, 1991; *McSween and Harvey*, 1993]. Martian mantle chemical heterogeneity is hinted at by the isotopic heterogeneity of the SNC meteorites [*Jones*, 1986]. Finally, evidence for plinian eruption deposits [*Mouginis-Mark et al.*, 1982; *Greeley and Crown*, 1990; *Crown and Greeley*, 1993] suggests the possibility of silicic volcanism, although arguments have been made against the existence of silicic volcanism on Mars [*Francis and Wood*, 1982].

In summary, these data and approaches suggest

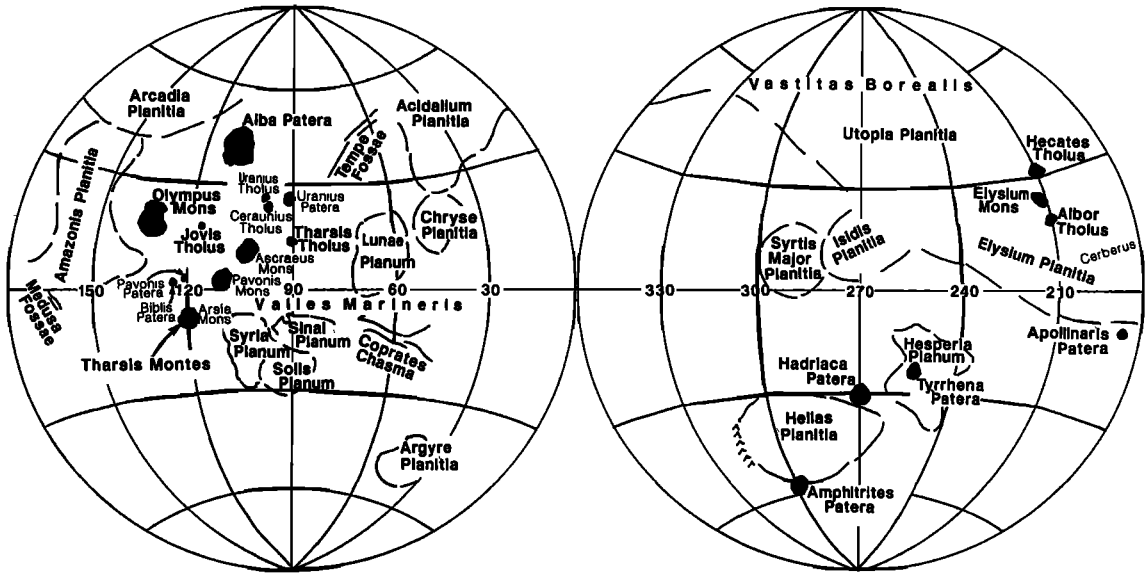

Figure 1a. Geography of Mars. Map of the major physiographic provinces and features on Mars, including the southern heavily cratered terrain, the northern lowlands, and the Tharsis and Elysium volcanic provinces. Solid black patches represent many of the major volcanic edifices on Mars. Tharsis Montes include Arsia, Pavonis, and Ascraeus. Modified from *Mutch et al.* [1976].

that the observed lava flows are likely to have basaltic to ultramafic compositions, with perhaps some of the shield volcano flows being more evolved in composition. Although remote sensing data suggest that basalt is widespread on the surface, there is some circumstantial evidence that the crust might contain more granitic components. For our analyses, we adopt a basaltic composition for mantle-derived melts and entertain the possibility of melts ranging out to komatiitic in composition. We also consider the possibility of compositionally evolved magmas derived from either (1) evolution in magma reservoirs (in situ processes) or (2) crustal contamination and mixing (ab initio processes). The well-established presence of the volatiles CO_2 and H_2O on the surface and in the atmosphere of Mars [*Owen*, 1992] suggests that it is appropriate to explore the consequences of at least these two volatiles being present in the variety of chemical types of ascending and erupting magma.

The crustal and lithospheric structure of Mars (Figures 1*a* and 1*b*) has been studied by a variety of techniques. Using the global gravity field, *Bills and Ferrari* [1978] inferred a mean global thickness of crust of assumed basaltic composition of 34–40 km, with maximum thicknesses under Tharsis (61–77 km) and minimum thicknesses under Hellas (8–10 km). The derivation of this thickness of basalt from the upper mantle strongly implies that upper mantle source regions for later partial melts will be more depleted than earlier ones and that there may be an evolutionary trend of compositions as a function of time and degree of upper mantle depletion. Indeed, the SNCs are known to be derived from a depleted mantle on the basis of isotopic [*Nakamura et al.*, 1982] and petrologic [*Longhi and Pan*, 1989] evidence, and they have young crystallization ages (probably <1.3 Ga). *Schubert et al.* [1992] link thermal evolution models to the derivation of crust as a function of time, estimating a maximum crustal thickness of 154 km for a fully differentiated Mars. We will return to the question of the relation of volcanic flux and thermal evolution.

The basic crustal configuration is modified by exogenic and surface processes (Figure 1*b*). These include the production of a megaregolith during the early bombardment history of Mars which, on the basis of the lunar analogy [*Short and Forman*, 1972; *Hartmann*, 1973; *Head*, 1976], would be characterized by an outer layer of allochthonous breccias (basin and crater ejecta ~1–2 km thick) [*Fanale*, 1976], an intermediate layer of autochthonous breccias (highly fractured and brecciated substrate up to about 10 km depth), and a deeper layer of fractured and cracked crustal material (down to about 25 km on the Moon). The depth to unmodified, compacted, or annealed crustal material is in the range of 8–12 km [*Clifford*, 1981, 1984, 1993] (Figure 2). There is clear evidence of water and water ice in the subsurface of Mars, and its presence will influence the structure of the uppermost crust, filling in voids and causing alteration of crustal mineralogy and production of clays and carbonates, etc., perhaps extending the porosity down to depths of 16 km [*Squyres et al.*, 1992]. This presence of groundwater and ground ice will also be important if magma resides in this realm or passes through it (Figure 3*a*), an issue discussed in section 2.4. In addition, in the uppermost layers of the crust, eolian, fluvial, volcanic, and mass-wasting deposits, will provide local to regional perturbations [*Carr*, 1979] to the megaregolith

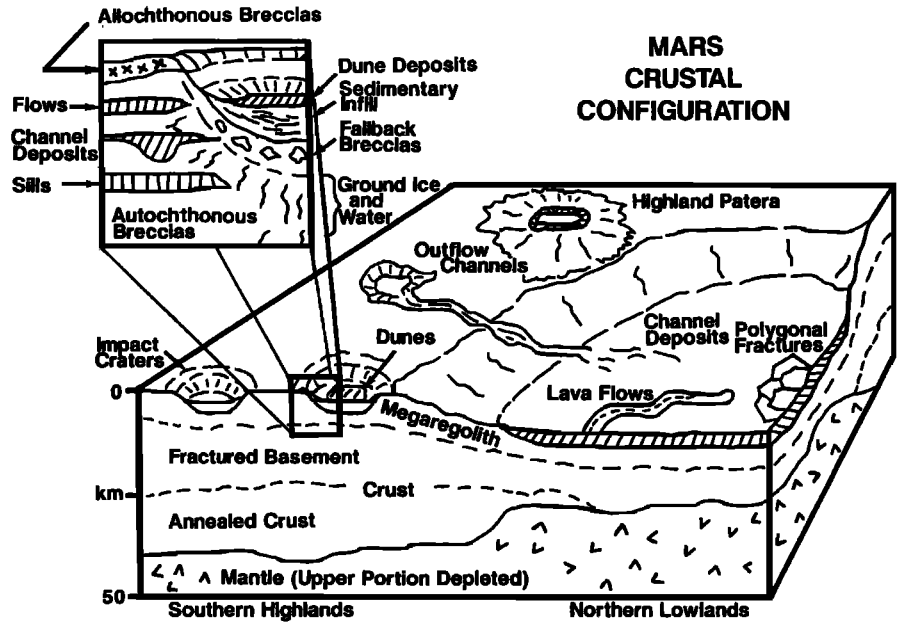

Figure 1b. Configuration of the crust of Mars indicating the basic crustal structure and the influence of exogenic and surface processes in modifying the density structure. The southern highlands and northern lowlands are illustrated schematically. Impact cratering on the ancient crust produces a megaregolith composed of autochthonous (in situ) and allochthonous (transported) breccias. This outer fragmental layer is then reworked by mass wasting and eolian processes and is further modified by the intrusion and extrusion of volcanic deposits. Ground ice and groundwater in the outer crust further add to the modification of the crust through chemical alteration, outflow and channel erosion, deposit emplacement, and the formation of fractured ground. The increase in pressure with depth causes the fractured basement to be annealed. The upper portion of the mantle is likely to be chemically depleted due to the derivation of the crust. Layer thicknesses are approximate. See Figure 2 for quantitative estimates of crustal density variation with depth.

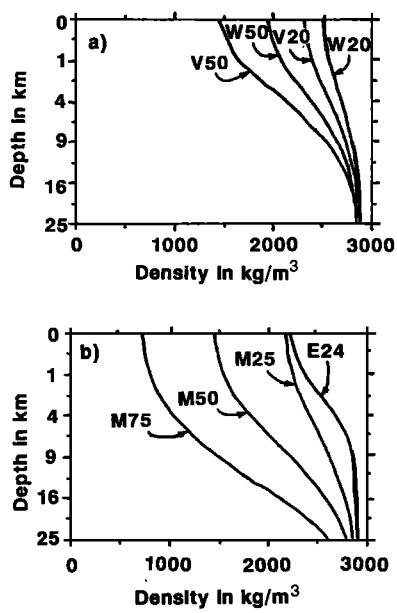

Figure 2. Variation of the density of the upper crust with depth (modified from *Clifford* [1981, 1984] and *Squyres et al.* [1992]). (*a*) Porosities of 20% and 50% voids without water (V20 and V50, respectively) and with water (W20 and W50, respectively) are shown. (*b*) Porosities of volcanic rocks on Mars of 25% (M25), 50% (M50), and 75% (M75) are shown, as well as a porosity of volcanic rocks on Earth of 24% (E24).

and outer crustal structure (Figure 1). Thus for individual regions the distribution of mapped geological units [*Tanaka et al.*, 1992*a*, *b*] is the best guide to the shallowest crustal structure.

Thermal history models predict a systematic thickening of the Martian lithosphere as a function of time [*Stevenson et al.*, 1983], but estimates of lithospheric thickness from the tectonic response to individual loads [*Comer et al.*, 1985] show spatial, as well as temporal, variations in elastic lithospheric thickness, with distinctly lower values beneath regions of major volcanic provinces. Thus although lithospheric thickness is generally increasing as a function of time and influencing the position of the brittle-ductile transition and the level of diapiric rise versus dike emplacement, prolonged phases of regional volcanism can clearly affect the regional thermal gradient and the position of the brittle-ductile transition as a function of time [*Solomon and Head*, 1990].

2.2. Magma Production, Ascent, and Creation of Primary and Secondary Reservoirs

We assume that the basic processes controlling partial melting of mantle materials and magma segregation at depth are the same on Mars as on Earth [*Elder*, 1987]: Rayleigh-Taylor instabilities [*Elder*, 1976] due to self-regenerating chemical, physical, and hence

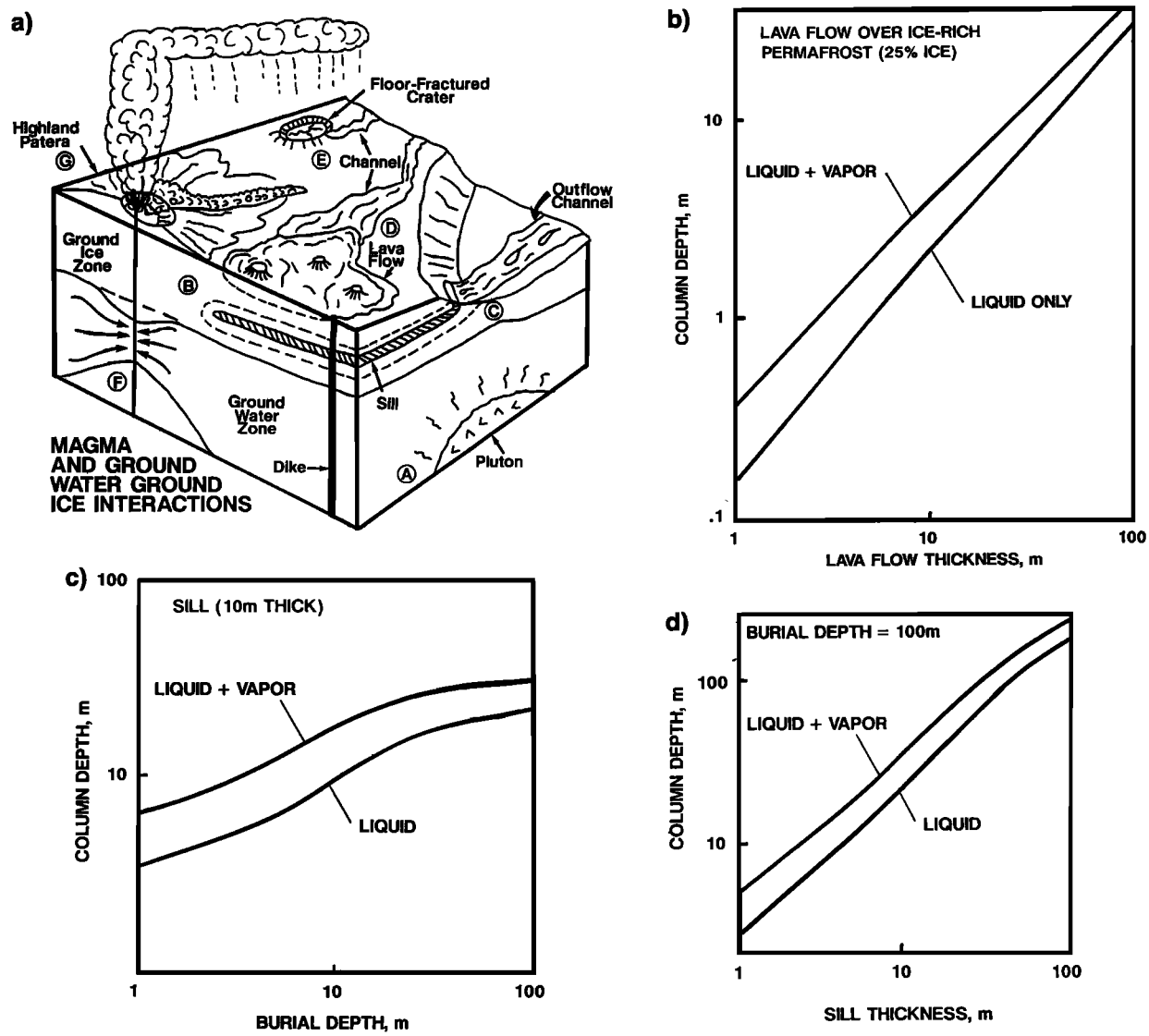

Figure 3. Relationship between ascending magma and the presence of groundwater and ground ice. (*a*) Magma and ground-ice/groundwater interactions. On the right, passive interactions are illustrated, in which a pluton radiates heat to the surroundings and locally creates an aureole of alteration (A). Lava flows emplaced on the surface (D) can convert underlying ground ice into water to create melting and channel formation or into steam to create local explosions and pseudocraters (shown as small cratered cones on the top of the flow). Sills emplaced at depth (B) can cause melting and release of groundwater at scarps to create outflow channels (C). Similar relations occur at shallow intrusions in crater floors (E). Active interactions result when magma rising in a dike incorporates groundwater into the conduit (F) and draws down the local groundwater table in the course of the eruption, often at very high flow rates. This enhances the formation of plinian eruption plumes (G) which can yield fallout deposits or extensive pyroclastic flows, and the formation of highland paterae. (*b*) Calculated column depth of liquid and liquid plus vapor generated by extrusion of a lava flow over an ice-rich (25% ice) permafrost, as a function of lava flow thickness, for (*c*) injection of a 10-m-thick sill, as a function of depth of burial, and for (*d*) injection of sills of various thicknesses at a depth of 100 m [after *Squyres et al.*, 1987].

thermal inhomogeneities cause localized regions of the mantle to ascend diapirically. The sizes, shapes, and spacings of these regions and their ascent rates are determined by the overall advective heat flux they represent and the physical properties of the bodies themselves and the surrounding materials [*Marsh and Carmichael*, 1974; *Fedotov*, 1977; *Marsh and Kantha*, 1978; *Spera*, 1980]. Partial melting occurs as a result of adiabatic decompression [*Oxburgh*, 1980] of the ascending mass, and melt segregation is driven by gradients in density, compaction, or deviatoric stress [*Sleep*, 1988].

Relatively deep magma reservoirs can form in several mantle environmental settings [*Head and Wilson*, 1992*b*]. Some of the most important ones result from the fusing of the head of a rising diapir or hot spot as

the adiabatic temperature reaches the melting point curve and voluminous pressure release melting occurs, producing a large, partially molten magma source region (a deep reservoir). The history of the reservoir is related to the evolution of the diapir or plume, the thermal and density structure of the material in which it occurs, and the instabilities that develop in the deep reservoir. Deep reservoirs also occur in conjunction with rift zones as a result of crustal thinning, localized mantle upwelling, and pressure release melting, related to regional extension or deeper patterns of mantle convection. Factors other than density can exert controls on the upward migration of plumes and magma batches. Ascending diapirs may stall upon encountering the rheological barriers of cooler more viscous surroundings such as the outer thermal boundary layer, the lithosphere. If the magma is still buoyant, instabilities may develop in the source region or the viscous lid and smaller diapirs may ascend; or, depending on the rheological properties of the country rock [*Rubin*, 1993], dikes may propagate from the stalled diapir or deep magma reservoir. In some cases, this material may migrate to the surface, causing eruptions; alternatively, it may stall in the crust, creating intrusions. Commonly, however, magma reaches shallow levels where it achieves a neutral buoyancy with the surrounding country rock because of the decreased density of the shallow crustal materials (Figures 1 and 2). If sufficient material reaches this level, a secondary reservoir centered on a neutral buoyancy level can be created, as is the case for Kilauea volcano [*Ryan*, 1987].

The details of the above processes depend on the exact nature of the physicochemical inhomogeneity of the Martian interior. Even though this knowledge is incomplete and sketchy, it is important to point out some general differences to be expected between Mars and the Earth. First, all conductive heat transfer processes in the Martian interior will occur at the same rate as on Earth, since these depend only on the thermal diffusivities of the constituent silicates, which are almost independent of composition. Second, at any given spatial size scale, all fluid convection motions (and consequent convective heat transfer) and crystal settling processes driven by positive or negative buoyancy will be slower on Mars than on Earth owing to the lower gravity; overall diapir ascent rates for bodies of a given size will also be slower for the same reason. Since heat loss from diapiric bodies is limited mainly by conductive heat transfer into the surrounding rocks, it is likely that the size scale of diapirs able to ascend to a given (shallow) level in the Martian lithosphere will be systematically larger than on Earth. We will return later to investigate the possibility that such bodies might form the nucleus of the major volcanic centers on Mars, such as the Tharsis volcanoes.

On Earth, magma from deeper sources ascends through the outermost ten to a few tens of kilometers of the lithosphere by generating brittle fractures in the surrounding rocks. The magma occupies these fractures to form dikes (which may or may not reach the surface) and sills. In zones where the country rock density variations cause large numbers of dikes to be localized, shallow magma reservoirs (commonly called magma chambers, though their geometry may be complex) may be formed. The temperatures, temperature gradients, and country rock physical properties expected in the outer parts of the Martian lithosphere [*Elder*, 1987; *Schubert et al.*, 1992] are sufficiently similar to those of the Earth to imply that similar processes should be involved; however, the difference in gravity between Mars and the Earth produces a number of systematic differences in the properties of dikes and ascent rates of magmas within them.

The width of the fissure system which opens to the surface in any particular eruption will be controlled by the amounts and spatial gradients of accumulated strain in the case of eruptions which are initiated by extensional regional tectonic forces or by the excess pressure in the magma reservoir in the case where this pressure initiates the eruption by exceeding the strength of the surrounding rocks. *Rubin and Pollard* [1987] have summarized the factors controlling the sizes, shapes, and stabilities against migration of dikes in planetary lithospheres, drawing on earlier work by *Weertman* [1971], *Johnson and Pollard* [1973], *Secor and Pollard* [1975], *Pollard and Muller* [1976], and *Pollard* [1976].

Wilson and Head [1988] and *Wilson and Parfitt* [1989, 1990] addressed the question of the influence of gravity on dike widths and eruption rates on the planets. They found that when dike propagation is limited by the requirement that the stress intensity at the dike tip overcomes the effective fracture toughness of the country rocks, the above treatments of dike shape and propagation imply that the mean width of a dike should be inversely proportional to the cube root of the acceleration due to gravity and its length perpendicular to the direction of magma motion should be inversely proportional to the gravity raised to the power 2/3. When motion is laminar, flow velocities of magmas in dikes are proportional to the total pressure gradient acting on the magma and to the square of the dike width; in turbulent motion the velocity is proportional to the square root of the product of the pressure gradient and dike width. Mass fluxes moving through dikes are proportional to the flow velocity and to the cross-sectional area perpendicular to flow. These relationships are discussed for eruptions on Earth, the Moon, and Venus by *Wilson et al.* [1980], *Wilson and Head* [1981*a*], and *Head and Wilson* [1986]. Collecting together all of the above relationships and the dependencies on gravity, it is implied that for the commonest circumstance of a magma being erupted to the surface from an overpressured magma reservoir,

the dike connecting it to the surface will be 1.35 times wider on Mars than on Earth and 1.8 times longer in outcrop. The magma flow speed when conditions are laminar will be 1.8 times greater than on Earth for the same excess reservoir pressure, and the discharge rate will be just less than 5 times greater. The corresponding figures when the magma motion is turbulent are a factor of 1.17 for flow speed and almost exactly 3 for eruption rate. Clearly, this will influence lava flow lengths and other eruption factors.

A lower limit on ascent speed is set by the requirement that the magma must not cool so much during its rise that its yield strength becomes large enough to prevent it moving through the fissure system [*Wilson and Head*, 1981*a*; *Delaney and Pollard*, 1982]. If Martian magmas erupt from shallow reservoirs in the upper several kilometers of the crust, the minimum mass effusion rates will be similar to those calculated for the Earth, since they are independent of the planetary gravity and magma viscosity [*Wilson and Head*, 1981*a*]: about 50 kg s^{-1} for eruptions through circular conduits and about 150 kg s^{-1} m^{-1} of fissure for dikelike conduits. If eruptions were to take place from the base of a thick (~50 km) Martian lithosphere, however, these estimates would increase in proportion to the travel distance [*Wilson and Head*, 1981*a*] to about 500 kg s^{-1} and 1500 kg s^{-1} m^{-1}, respectively.

The upper limit on magma ascent speed is set by the mean width of the widest dike that can be formed in a given stress environment. The above relationships suggest that if regional stress regimes are similar on Earth and Mars, eruption rates may be systematically higher on Mars by a factor of 5 for magmas of similar viscosity flowing in a laminar fashion and by a factor of 3 (independent of magma rheology) for very high discharge rate events where magma motion is turbulent; we show later that this will have a bearing on both the likely range of lengths of lava flows and on the likely rise heights and dispersal areas of explosive eruption clouds.

Secondary magma reservoirs commonly evolve with their centers at neutral buoyancy levels [*Rubin and Pollard*, 1987], that is, at depths where the magma density is equal to the density of the country rocks. Implicit in this statement is the idea that, on average, the magma in a chamber is less dense than the country rocks surrounding it in the lower part of the chamber and is more dense than the country rocks in the upper part of the chamber. In general, silicate mineral phases expand on melting, and so, the positive buoyancy of magma in the lower part of a chamber is to be expected. The negative buoyancy at higher levels is due to the fact that the shallower layers of country rock in volcanic areas are likely to consist of ancient lava flows, ash deposits, and other low-density material (Figures 1 and 2) which are either vesicular or poorly compacted (or both) and so have a significantly lower bulk density than they would have if completely compacted.

Shallow magma chambers are enlarged by the injection of melt from below. The melt bodies rise buoyantly from deeper zones of partial melting and accumulation as equant diapiric bodies or as much more elongated dikes. The geometry of the rising body is controlled by the rheology of the country rocks and the stress distribution in its vicinity, in turn a function of the density difference between the melt and its surroundings and the rise velocity. Each new melt body added to the existing reservoir brings with it a finite volume and a finite internal pressure in excess of the ambient lithostatic pressure. The new size, shape, and pressure state of the reservoir reflects a constantly readjusting balance between its internal volume and the stress state of the surrounding rocks [*Blake*, 1981].

One method of adjustment to the addition of new melt is a general enlargement of the chamber and the compression of its contents and the surrounding rocks. An alternative is the propagation away from the chamber wall of a dike or sill. If the distal end of a dike reaches the surface, causing an eruption, or if the proximal end of a dike or sill disconnects from the chamber wall and the magma propagates away as a separate intrusive body, the reservoir volume is reduced. But if a dike or sill remains connected to the wall and fails to intersect the surface, the net effect is simply a readjustment of the magma body to a new shape which involves a reduction in total stress. Clearly, the depths and detailed shapes of magma reservoirs are not controlled by hydrostatic forces alone. However, on average, the center of a reservoir is likely to reside at the level of neutral buoyancy.

2.3. Density Structure of the Shallow Crust and Lithosphere and Development of Neutral Buoyancy Zones

The density structure of the crust in which a reservoir forms and on which a volcano builds is crucial to the determination of reservoir depth and edifice growth [*Head and Wilson*, 1992*a*, *b*]. On the Moon the density barrier represented by the anorthositic highlands causes magma reservoirs to stabilize at the base of the crust at depths of about 60 km; shallow reservoirs are unimportant, and because of this, no major shields are found on the lunar surface [*Head and Wilson*, 1991, 1992*a*]. On Venus the anomalously high atmospheric pressure influences the gas exsolution of rising magma and thus the density structure of the shallow crust; at the lowest elevations and highest pressures, no neutral buoyancy levels are predicted to form, and magmas are likely to emerge directly from deep reservoirs to the surface, whereas at lower pressures, typical of higher elevations, neutral buoyancy zones are predicted to form and to favor the development of shallow reservoirs and volcanic shields [*Head and Wilson*, 1992*b*]. On Mars we need to consider

both the crustal composition and structure and the influence of the low atmospheric pressure (relative to Earth) on the degassing of rising magma and the density of the erupted products in the crustal column. The crust is apparently predominantly basaltic. The shallowest crust is complicated by various processes (Figures 1 and 2), but in general, the basic crust should have been constructed predominantly from earlier eruptions, in which case it could be mafic or ultramafic and its primary density influenced by the atmospheric pressure and near-surface degassing history. Once an edifice begins to grow, the surface layers are a mix of vesicular lava flows and pyroclastics modified by in situ weathering and surface activity (Figure 1). We assume both types of volcanic deposits are more vesicular than on Earth because of late stage degassing in the low-pressure atmosphere. The early stage degassing of the magma nearing the surface in the conduit will encourage formation of pyroclastics rather than lava flows under almost all conditions, but it is the late stage degassing at atmospheric pressure which determines the final porosity of the material deposited.

The variations of density $\rho(h)$ with depth h for basaltic volcanic regions on Earth have been obtained from seismic wave propagation measurements in Iceland and Hawaii [*Hill*, 1969; *Gudmundsson*, 1987] and can be conveniently modeled [*Head and Wilson*, 1992*b*] using a continuous density function derived by assuming that the compaction of void space is a function only of pressure. Assuming an exponential decay of fractional void space, $V(P)$, with increasing pressure P,

$$V = V_0 \exp(-\lambda P), \quad (1)$$

where V_0 is the void space fraction at the surface and λ is a constant. If ρ_∞ is the density of the country rock in its completely compacted state, it follows from the definitions of bulk density and void space that

$$\rho(V) = \rho_\infty(1 - V) \quad (2)$$

and that the bulk density of surface country rocks, ρ_{surf}, is given by

$$\rho_{surf} = \rho_\infty(1 - V_0). \quad (3)$$

Since any increase dP in the pressure P due to an increase dh in the depth h is given by $dP = \rho\, g\, dh$, equations (1), (2), and (3) can be combined to give

$$\rho(h) = \rho_\infty/[1 + \{V_0/(1 - V_0)\} \exp(-\lambda\rho_\infty gh)] \quad (4)$$

and

$$P(h) = \lambda^{-1} \ln [V_0 + (1 - V_0) \exp(\lambda\rho_\infty gh)]. \quad (5)$$

Thus the density and pressure variations with depth can be specified in terms of the three model parameters ρ_∞, λ, and V_0.

The variation of density with depth in basaltic regions on the Earth can be well fitted with $\rho_\infty = 2900$ kg m^{-3} and $\lambda = 1.18 \times 10^{-8}$ Pa^{-1} [*Head and Wilson*, 1992*b*]. We see no reason to expect the value of λ to vary systematically between the terrestrial planets as long as we are concerned with broadly similar silicate rocks. However, the value of ρ_∞ depends on the typical chemical composition of the material accumulating to form the volcanic edifice. For the Earth the value 2900 kg m^{-3} (consistent with an unvesiculated melt density of the same composition of 2600 kg m^{-3}) is appropriate for typical basaltic rocks, and a similar pair of values was assumed for Venus by *Head and Wilson* [1992*b*]. As described above for Mars, morphological evidence and Viking lander chemical data have generally been interpreted as implying a basaltic composition for much of the surface, for which a melt density of 2600 kg m^{-3} and $\rho_\infty \sim 2900$ kg m^{-3} would be appropriate. However, recent arguments described above [e.g., *Longhi and Pan*, 1989; *Longhi*, 1990] based on the chemistry of the SNC meteorites suggest the possibility of a more ultramafic composition, with a melt density of 2900 kg m^{-3}, so that $\rho_\infty \sim 3200$ kg m^{-3}.

The value to be adopted for V_0, the surface void space fraction of volcanic products, on Mars is also debatable. For Earth an average of $V_0 = 0.24$ is consistent with the seismic data [*Head and Wilson*, 1992*b*], so that $\rho_{surf} = 2200$ kg m^{-3}. For Venus, where the high atmospheric pressure at the surface reduces gas release from magmas [*Head and Wilson*, 1986; *Head and Wilson*, 1992*b*], the fact that exsolved gas is not released during explosive lava fountaining but is instead retained in the erupted lavas leads to the possibility of a very wide range of surface void space fractions. *Head and Wilson* [1992*b*] found that V_0 could lie anywhere in the range 0.02 to 0.65 for a plausible spread of combinations of magmatic H_2O and CO_2 contents, leading to values of ρ_{surf} between 2940 and 1045 kg m^{-3}. For Mars we assume that the low atmospheric pressure generally leads to enhanced magma vesiculation and fine-grained pyroclast formation [*Wilson et al.*, 1982], and we adopt V_0 over the wide range 0.25 to 0.75, coupled with a compact basalt density at great depth of $\rho_\infty = 2900$ kg m^{-3}; this implies that ρ_{surf} lies between 2175 and 725 kg m^{-3}; for a more ultramafic composition with $\rho_\infty = 3200$ kg m^{-3}, ρ_{surf} lies between 2400 and 800 kg m^{-3}.

These assumptions lead to the variations of country rock density with the depths given in Table 1. From these, depths of neutral buoyancy levels (given in Table 2) are derived by interpolating to find the depth at which the country rock density is equal to the unvesiculated melt density. The table also shows the depths of neutral buoyancy levels on Mars and Venus calculated on the assumption that this depth is proportional to the planetary gravity; the calculations show that because of the nonlinear variation of density with depth, magma reservoirs on Venus will be shallower

TABLE 1. Variation of Country Rock Bulk Density With Depth in the Shallow Lithosphere on Earth, Mars, and Venus Using the Stated Surface Void Fractions V_0 and the Value ρ_∞ = 2900 kg m^{-3} for the Density of Fully Compacted Country Rocks

Depth, km	Earth	Mars				Venus			
	(V_0 = 0.24)	V_0 = 0.25	V_0 = 0.325	V_0 = 0.5	V_0 = 0.75	V_0 = 0.125	V_0 = 0.15	V_0 = 0.2	V_0 = 0.25
0	2200	2175	1958	1450	725	2538	2465	2320	2175
1	2364	2244	2039	1545	798	2623*	2566*	2448	2327
2	2496	2308	2116	1639	875	2691	2646*	2552	2454
3	2600*	2367	2189	1732	957	2742	2708	2635*	2557*
4	2680	2422	2257	1822	1042	2782	2756	2700	2639*
5	2739	2472	2320	1909	1130	2812	2792	2749	2703
8	2840	2597*	2481	2148	1408	2864	2856	2837	2817
11	2878	2688	2604*	2345	1688	2885	2882	2875	2866
17	2897	2800	2757	2618*	2182	2898	2897	2896	2894
20	2899	2831	2802	2704	2372	2899	2899	2898	2898
25	2900	2863	2847	2792	2598*	2900	2900	2900	2900

Density values are in kilograms per cubic meter.
*Values close to the density assumed for the melts resident in magma chambers, 2600 kg m^{-3}.

than is implied by pure gravity scaling, while those on Mars will be deeper.

A further level of detail can be introduced into these calculations by taking account of the fact that at the depths found above for neutral buoyancy levels, magmas containing appreciable amounts of CO_2 will have begun to exsolve some of this gas, reducing their densities. We have used the pressure solubility law adopted by *Head and Wilson* [1992*b*] to calculate densities as a function of depth to be compared with the crustal densities in Table 1. For the crustal density structures implied by the surface void fractions used in Table 2, the effect can be very important on Venus, where it would cause neutral buoyancy levels to be progressively shallower than 1.4 km for total CO_2 contents in excess of 0.1 wt %. In the case of Mars and the Earth, however, the effect is much smaller. On Earth, no change in the neutral buoyancy level of 3 km occurs until the total magma CO_2 content exceeds 0.2 wt %, and a value of 0.35 wt % is needed to reduce the depth of the neutral buoyancy level to 2500 m. On Mars, changes from the 11-km depth given in Table 2 would start if the CO_2 content exceeded 0.25 wt %, and 0.35 wt % would reduce the depth to 10.4 km.

TABLE 2. Best Estimates of the Surface Void Fractions, V_0, for the Earth, Mars, and Venus and the Depths on Each Planet to the Centers of Magma Chambers Residing at the Neutral Buoyancy Level When the Density of the Magma They Contain Is 2600 kg m^{-3}

	Earth	Mars	Venus
Surface void fraction, V_0	0.24	0.325	0.15
Chamber center depth, km	3	11	1.4
Chamber center depth based on gravity scaling, km	3	7.7	2.7

Country rock density variations with depth are those given in Table 1. Also shown are the neutral buoyancy level depths which would be expected on the naive assumption that all pressures and densities scaled linearly with the planetary gravity.

In summary, despite the influence of numerous complicating factors, magma reservoirs are expected to accumulate, on average, at levels of neutral magma buoyancy in the lithosphere. The bulk density of surface rocks in a volcanic region on any planet is a function of the amount of gas released by magmas approaching the surface and hence of the surface atmospheric pressure. If the bulk density of subsurface rocks is controlled mainly by pressure-dependent compaction of void space, then the low compaction state expected for surface rocks on Mars (where the low atmospheric pressure allows high efficiency of volatile release) (Figures 1 and 2) and the probable high compaction state of surface rocks on Venus (where the high atmospheric pressure suppresses volatile release) should lead to lithospheric density profiles that are significantly different from that of the Earth (see Table 1 for examples). As a result of the differences in lithospheric bulk density profile, which in turn depend on differences in both gravity and surface atmospheric pressure, magma reservoirs are expected to be shallower on Venus than on Earth, by a factor of about 2, and deeper on Mars than on Earth, by a factor of about 4 (see Table 2). These findings will need to be combined with information on the lateral and vertical growth of magma chambers to model the long-term development of the internal plumbing systems and topography of planetary volcanoes.

2.4. Influence of Ground Ice and Groundwater on Ascent and Eruption of Magma

As magma ascends through the shallow crust on Mars, it will interact with groundwater and ground ice with several potential consequences (Figure 3), examples of some of which are known on Earth. In a passive mode the magma simply advects heat to a

TABLE 3. Gas Bubble Nucleation and Magma Fragmentation Depths on Mars and the Earth, Given as a Function of Total Magma Volatile Content for Three Magma/Volatile Combinations

Total Volatile Content, wt %	Nucleation Depths, m			Fragmentation Depths, m		
	H_2O in Basalt	H_2O in Rhyolite	CO_2 in Either	H_2O in Basalt	H_2O in Rhyolite	CO_2 in Either
			Earth			
5	8200	5000	74,000	678	546	336
3	3400	1800	44,000	387	287	196
1	815	200	15,000	116	65	62
0.3	140	15	4400	28	7	23
0.1	27	...	1500	6	...	3
0.03	2	...	440	...	...	...
			Mars			
5	21,000	13,000	196,000	1800	1460	901
3	10,000	4800	118,000	1000	771	713
1	2100	530	39,000	318	181	173
0.3	380	48	12,000	83	29	51
0.1	80	5	4000	24	4	17
0.03	14	0.4	1200	6	0.3	5

Note that the solubility of CO_2 is similar in basalts and rhyolites. A null entry implies that the relevant event does not occur.

different part of the crust, where it is then passively conducted to the surroundings; interaction with the water/ice is minimal. If magma stalls at depth in a reservoir, or locally as dikes or sills, it can change the geothermal gradient and, depending on the geometry and heat input, can potentially cause melting of ground ice and release of groundwater. In a more active mode, intimate interaction of magma and water-enriched substrate can cause vaporization leading to a range of more explosive interactions. Terrestrial examples are pseudocraters (resulting from flows over water-rich substrates [*Thorarinsson*, 1953]), maars (resulting from shallow intrusions [*Lorenz*, 1973]), and situations where large quantities of groundwater are cycled through the substrate to the vicinity of the magmatic plumbing system to produce a variety of explosive eruption styles (the basaltic plinian eruptions of Tarawera [*Walker et al.*, 1984] and the eruptions of Heimaey and Surtsey [*Thorarinsson*, 1967]). Groundwater and permafrost are known to be an important part of the upper crust of Mars [*Clifford*, 1981, 1984] and to have changed with time [*Carr*, 1990], and thus this factor must be considered throughout Martian history. The theory of large-scale volcano-ice interaction for a number of situations on Mars (Figure 3) has been treated [*Squyres et al.*, 1987], and a variety of Martian features thought to involve groundwater or ground ice interactions have been studied [*Frey et al.*, 1979; *Mouginis-Mark*, 1985; *Mouginis-Mark et al.*, 1982, 1988; *Wilhelms*, 1986; *Wilhelms and Baldwin*, 1988; *Greeley and Crown*, 1990].

2.5. Gas Exsolution at Shallow Depth and Eruption Styles

Gas release from Martian magmas will lead to a similar range of eruption styles as that encountered on Earth. The terminology used for these eruption styles is essentially identical to that employed to classify eruptions on Earth [e.g., *Fisher and Schmincke*, 1984], but we emphasize that the classification is based on physical processes, not on the characteristics of the eruption deposits or the landforms produced [*Wilson and Head*, 1981*a*, 1983; *Head and Wilson*, 1986].

Two critical events may occur as a volatile-bearing magma nears the surface and the total pressure acting on it decreases: (1) gas nucleation, where gas bubbles may begin to nucleate if the amount of the volatile present is enough to ensure a small degree of supersaturation before the magma reaches the surface, and (2) magma disruption, where the magma may disrupt into a mixture of pyroclasts and released gas if the volatile content is greater than a second limiting value [*Sparks*, 1978]. Table 3 shows the depths at which gas nucleation and magma disruption will occur in steady eruptions on Mars (and, for comparison, the Earth) for various volatile/magma type combinations and exsolved volatile fractions. Values are calculated using the methods given by *Wilson and Head* [1981*a*]. As long as gas exsolution does not occur over a large fraction of the total travel distance of a magma from its source reservoir to the surface, the vesiculation process does not greatly affect the mass eruption rate, since most of the frictional energy losses occur in the regions where the liquid is nonvesicular; gas exsolution does, however, critically control the near-surface magma rise speed [*Wilson et al.*, 1980].

Table 3 shows that the combination of the lower Martian gravity and lower atmospheric pressure ensures that both nucleation and disruption of magma occur at systematically greater depths than on Earth. An erupting magma cannot contain a given amount of a volatile unless the depth at which the magma has most recently resided is greater than the nucleation depth listed for that amount of volatile. The solubility

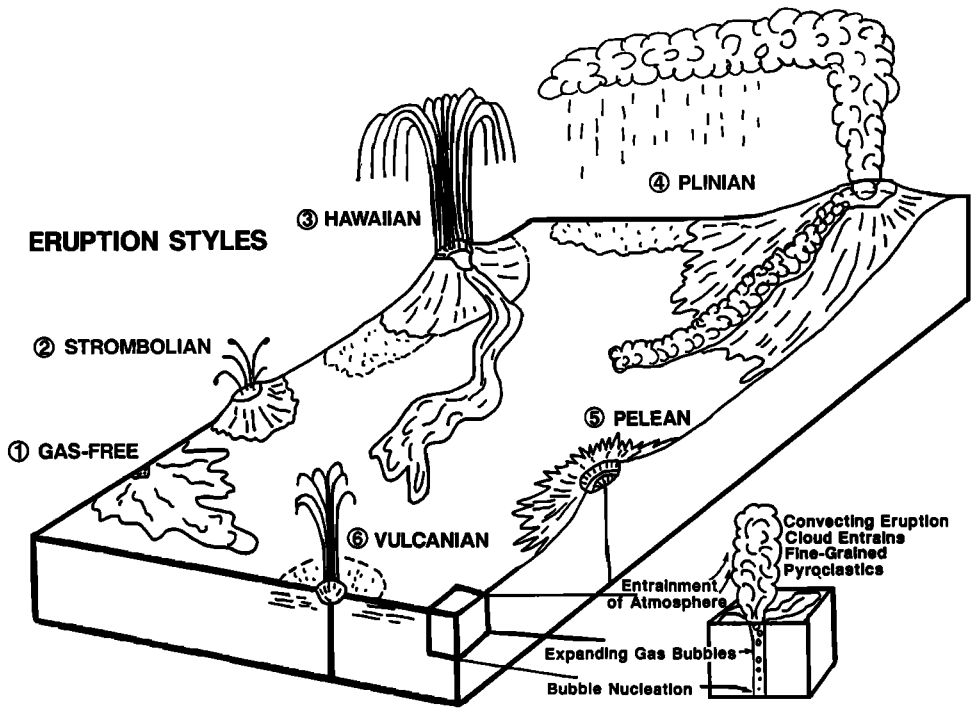

Figure 4. The important physical processes occurring in the vicinity of the vent on Mars (expanded block) and how their relative importance can result in a wide array of eruption styles: (1) Essentially gas-free magma erupts to produce a low, liquid fountain, feeding flow. (2) Strombolian eruption: Gas rise exceeds magma rise; bubbles grow and coalesce, causing intermittent disruption of lava lake surface and the near-vent accumulation of spatter. (3) Hawaiian eruption: Steady explosive eruption creates a pyroclastic fire fountain; most clasts decouple from gas and fall back to feed flow. Some cool and create scoria, building the cone; others are convected upward and create ash deposits. (4) Plinian eruption: Magma disrupts into small fragments that are locked to the gas stream; the atmosphere is incorporated and heated, and rises convectively to produce a convecting plume, which can spread laterally and deposit tephra. If insufficient atmosphere is incorporated, the density of the column exceeds that of the atmosphere, collapse occurs, and pyroclastic flows (ignimbrites) stream down slopes. (5) Pelean eruption: Low magma rise speed causes cooling and formation of a viscous dome with solid carapace; catastrophic disruption of carapace causes the formation of small convecting plume and pyroclastic flow. The aftermath, shown here, is a crater often inside a caldera. (6) Vulcanian eruption: Solidification of magma and resultant gas buildup in near-surface conduit causes an explosive disruption of solidified cap and adjacent country rock.

of CO_2 is much less than that of H_2O in all silicate melts [*Mysen*, 1977], and so CO_2 (or any other low-solubility volatile) is likely to be largely degassed from any Martian magmas which have resided for significant periods at shallow depths in the lithosphere; H_2O would then be the dominant volatile released from such magmas on eruption.

Whenever a relatively steadily erupting magma contains sufficient volatiles to ensure that it disrupts into pyroclasts at depths of at least a few meters (~0.1 wt % on Mars or ~0.3 wt % on Earth (see Table 3)), the kinetic energy produced by expansion of the released gas automatically ensures that the smaller pyroclasts and the gas emerge from the vent at eruption speeds of at least a few tens of meters per second [*Wilson*, 1980] and either a hawaiian-style, a plinian-style, or an ignimbrite-forming explosive eruption occurs. The important physical processes occurring in the vicinity of the vent on Mars and the ways in which their relative importance can result in a wide array of eruption styles are shown in Figure 4.

If the proportion of released gas is much less than the figures given above, there is little disruption of the magma and its exit velocity is small, less than about 10 m s^{-1} and comparable, in fact, to the velocity it would have had owing to buoyancy or excess pressure forces [*Wilson and Head*, 1981*a*] if it had been volatile-free. In such cases magma overflows quietly from the vent, possibly forming a low, domelike, liquid fountain at most a few meters high, and feeds directly into a lava flow.

A special case (Figure 4) occurs when a gas-poor magma rises at a low speed (less than about 1 m s^{-1} for mafic magmas on all of the terrestrial planets [*Wilson and Head*, 1981*a*]). There is then time for significant coalescence of gas bubbles to occur in the rising mag-

ma; since large bubbles rise buoyantly faster than smaller bubbles, a runaway process can develop in which large bubbles emerge intermittently from the vent, each bubble having swept a vertical column of magma almost clean of other bubbles. This is the origin of the strombolian eruption style in which magma erupts quietly during the intervals (from as little as one to many tens of seconds) between the explosive emergence of the large gas bubbles.

In relatively steady explosive eruptions, the style (hawaiian, plinian, or ignimbrite forming) is determined by a combination of the size distribution of the erupted clasts and the mass fraction of released volatiles in the eruption products (Figure 4). These factors in turn control the degree of coupling between the motions of clasts and gas, and control the bulk density of the eruption products relative to that of the surrounding atmosphere. Large clasts (whether magmatic pyroclasts or accidental lithic blocks) have a larger terminal fall velocity through the gas than smaller clasts with the same density, and high-density clasts have a larger terminal velocity than lower-density clasts of the same size; as a result, there is always a maximum size of clast of a given density which can be transported out of the vent [*Wilson*, 1976].

Hawaiian eruptions occur in hot, mafic magmas when most of the magma is disrupted into clots not much smaller than this maximum eruptable size, so that they decouple quickly from the gas stream to form a fire fountain and fall relatively near the vent (Figure 4). The fate of the accumulating clasts depends on their sizes and on the details of their passage through the fire fountain [*Head and Wilson*, 1989]. They may reach the ground cold enough to form brittle scoria deposits, hot enough to form spatter deposits, or virtually uncooled to coalesce into a lava pond which can in turn feed one or more lava flows. The upwardly directed mixture of smaller erupted clasts and magmatic gases together entrain the surrounding atmospheric gases into a convecting eruption cloud over the vent.

In contrast to hawaiian eruptions, plinian eruptions can occur in any magma type as long as most of the magma disrupts into clots so small that they are effectively locked by drag forces to the gas stream emerging from the vent. There is then no equivalent of a near-vent fire fountain. Provided the bulk density of the eruption products becomes less than the density of the atmosphere as a result of the incorporation and heating of atmospheric gases, essentially all of the eruption products ascend into an eruption cloud over the vent. It is an accidental (but very important) corollary that the small pyroclasts can transfer heat efficiently to the atmospheric gases entrained dynamically into the eruption cloud and thus maximize the buoyant convection of the cloud into the atmosphere [*Wilson*, 1976]. In cases where the bulk density of the eruption products leaving the vent is much greater than the atmospheric density, it can happen (especially if the vent is very wide [*Sparks and Wilson*, 1976]) that insufficient atmospheric gas is entrained and heated to overcome the effects of gravity; the erupted mixture then collapses back to the surface to form pyroclastic flows (ignimbrites).

For magmas of intermediate to silicic composition on Earth, it is commonly the case that the rise speed of the magma nearing the surface is small. This leads to extensive cooling of the parts of the magma in contact with the fissure walls and, if the event is extrusive rather than intrusive, those parts exposed at the surface, often in the form of an extrusive dome. There can then be quite efficient retention of gases released from the decompressing magma; also, the slow ascent speed allows time for the release of essentially all of the gas which must be exsolved to reduce the supersaturation to zero. These factors can lead to the slow buildup in the interior of a near-surface magma body or extrusive dome of a significant pressure in excess of the local hydrostatic pressure. The eventual failure in tension of the cooled carapace leads to the explosive decompression of the gas and its enclosing liquid matrix as an expansion wave spreads into the magma [*Eichelberger and Hayes*, 1982], driving a pelean eruption (Figure 4). The main characteristic of pelean explosions is that the maximum excess pressure in the trapped gas is limited (to values less than ~10 MPa) by the tensile strength of the cooled carapace retaining it [*Wilson*, 1980]. Similar characteristics apply to any other explosion driven by gas accumulation beneath a retaining layer.

Vulcanian explosions on Earth appear to be the consequence of the interaction of juvenile material with near-surface layers of water or ice [*Self et al.*, 1979]. They differ from pelean explosions mainly in that far more coarse, nonjuvenile, lithic material is incorporated into the ejecta (Figure 4). We confidently expect vulcanian activity to occur on Mars in view of the presence of significant amounts of near-surface ices in many regions (Figures 1–3) [*Clifford*, 1981, 1984, 1993; *Squyres et al.*, 1992] and assume that pelean activity will occur when (and if) high-viscosity magmas approach the surface.

There is a third mechanism by which discrete explosions may occur. Whenever a lava flow advances onto ground which contains water or ice in its near-surface layers, heat from the flow may evaporate the volatiles to produce a trapped layer of compressed gas. The pressure will rise to a value at least as large as the weight per unit area of the overlying flow, and the subsequent explosion will produce a pseudocrater in the flow [*Thorarinsson*, 1953] (Figure 3). Again, this mechanism should be at least as common on Mars as the Earth. We now review in detail each of the possible effusive and explosive eruption styles which are expected on Mars in the light of its known lithospheric and atmospheric environmental properties.

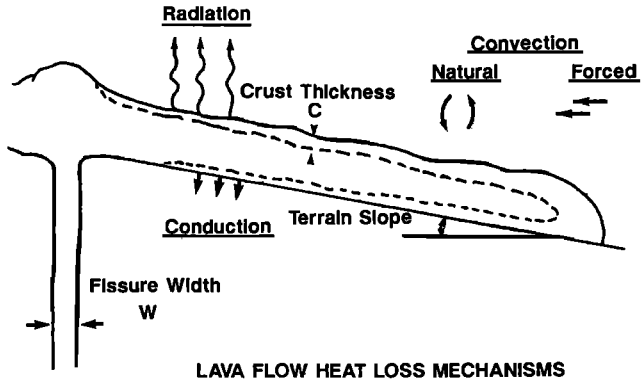

Figure 5. Heat loss mechanisms from a simple lava flow. Either natural or forced convection will eventually dominate the radiation and substrate conduction processes. The solid crust will increase with time, and therefore distance from the vent and flow motion will cease when cooling fronts have penetrated to a sufficient fraction of the flow thickness.

3. EFFUSIVE ERUPTIONS

3.1. Lava Flows: Background and Theory

Lava flows can be produced either by direct overflow of volatile-poor magma from a vent or by coalescence of hot magma clots falling from a fire fountain (Figure 4). The main difference between the two cases is that directly effused magma will be systematically hotter and hence less viscous as it leaves the near-vent region than that processed through a fire fountain (even if only by a small amount in the case of a dense fountain). When interpreting the morphological properties of lava flows, this effect may be confused with the other likely source of magma rheological variations, namely, bulk magma chemistry.

3.1.1. Flow cooling rates. Heat loss processes from the base of lava flows into the underlying surface (Figure 5) are controlled by the thermal diffusivity of the substrate and are essentially the same on all silicate planets [*Hulme*, 1982]. However, upper surface cooling is influenced by the properties of the atmosphere, if one exists. *Head and Wilson* [1986] have presented calculations of the forced and natural convection heat loss rates, and of the radiative loss rates, from the upper surfaces of lava flows on the Earth and Venus. We have used the same methods, modified for the Martian atmospheric properties, to calculate the surface temperatures and cooled skin thicknesses (defined as the depth below the surface at which the solidus temperature is reached) shown in Table 4. Values are also given for flows on the Earth for comparison.

The Martian atmosphere is seen to be about 100 times less efficient at removing heat from exposed hot surfaces by both forced and natural convection than the Earth's atmosphere, so that radiation losses dominate on Mars even at quite low excess temperatures. Graphs of flow surface temperature and cooled skin thickness as a function of time (Figure 6) show that for times between 1 hour and 1 month after eruption, a Martian lava flow surface will be at least 40 K hotter than its terrestrial counterpart. However, at times

TABLE 4. Thermal Characteristics of Lava Flows on Mars and Earth

T_0, K	F_F, W m^{-2}	F_N, W m^{-2}	F_R, kW m^{-2}	F_T, kW m^{-2}	t, s	C
			Mars			
1400	64.7	179.0	163.200	163.379	5.82	1.44 mm
1300	61.3	162.2	121.296	121.458	2.91×10^1	4.71 mm
1100	52.1	129.9	62.098	62.228	3.21×10^2	21.1 mm
900	42.9	98.9	27.736	27.835	3.10×10^3	76.5 mm
700	32.4	66.9	10.045	10.112	3.76×10^4	0.29 m
500	19.0	32.7	2.492	2.525	8.86×10^5	1.53 m
400	12.5	18.3	0.923	0.941	7.55×10^6	4.60 m
300	4.3	4.5	0.178	0.183	2.38×10^8	26.3 m
280	2.6	2.3	0.095	0.098	8.52×10^8	50.1 m
260	0.9	0.5	0.028	0.029	9.87×10^9	171.3 m
			Earth			
1400	6470	11,100	162.4	173.5	5.13	1.36 mm
1300	6100	10,000	121.0	131.0	2.54×10^1	4.38 mm
1100	5120	7880	61.9	69.8	2.53×10^2	18.8 mm
900	4140	5850	27.5	33.4	2.14×10^3	63.4 mm
700	3010	3760	9.9	13.6	2.08×10^4	0.22 m
500	1590	1600	2.3	3.9	3.73×10^5	0.99 m
400	870	700	0.7	1.6	2.61×10^6	2.69 m
330	270	150	0.16	0.43	4.02×10^7	10.8 m
310	90	34	0.05	0.14	3.90×10^8	33.8 m

Note that t is the time required for the surface of a flow erupted at 1450 K to cool to a given absolute temperature T_0. The ambient temperature is taken as 300 K on Earth and 250 K on Mars. C is the corresponding thickness of solidified crust. F_F, F_N, and F_R are the rates of heat loss from the surface by forced convection, natural convection, and radiation, respectively; F_T is the total heat loss rate, being the sum of F_R and whichever is the greater of F_F and F_N.

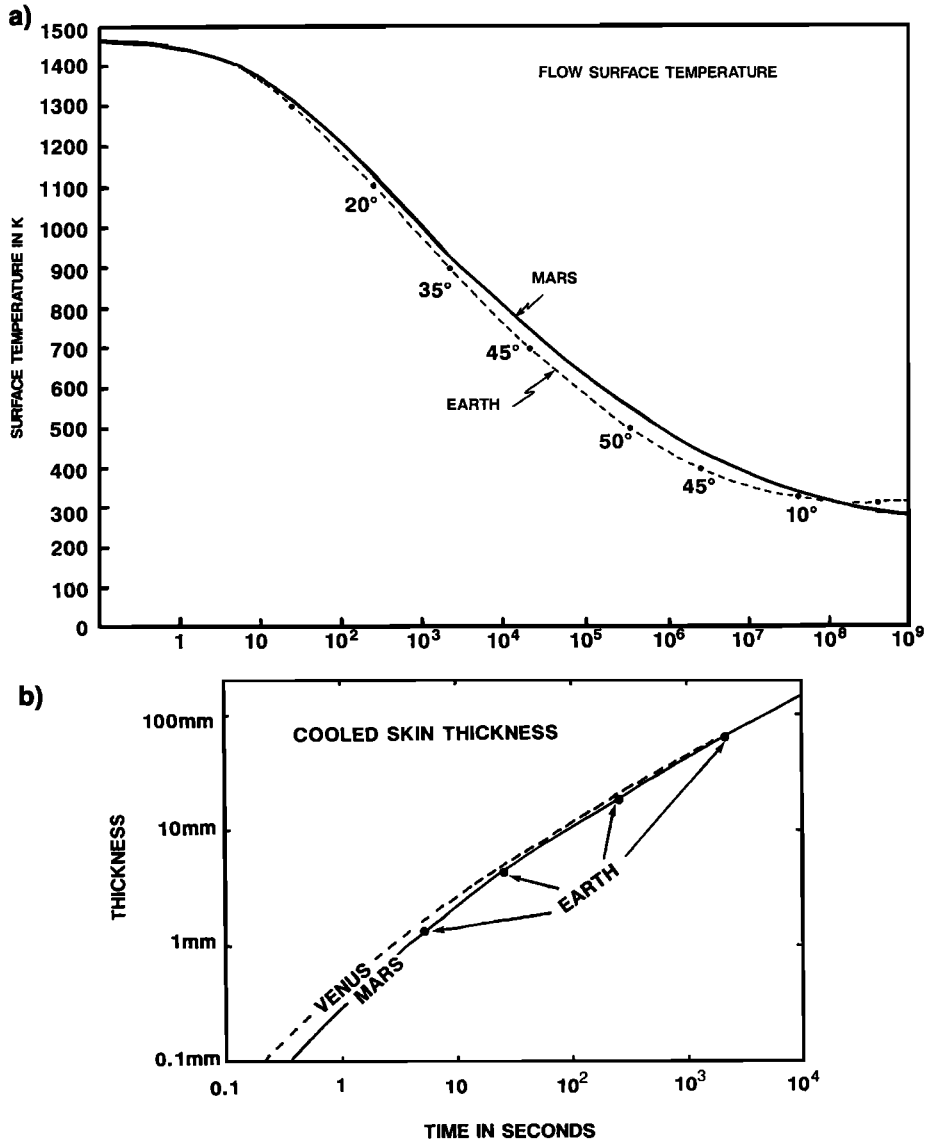

Figure 6. Comparison of lava flow cooling behavior on Mars and the Earth. (*a*) Flow surface temperatures as a function of time, showing the temperature difference at several times; between 1 hour and 1 month after eruption, Mars flows have hotter surfaces by >40°C. (*b*) Cooled skin thickness (outer thermal boundary layer) as a function of time. The dashed line illustrates the Venus case [*Head and Wilson*, 1986], and the solid line represents Mars. Because the curve for Earth is so close to that of Mars, the Earth is illustrated by four points (solid circles). Mars lava flow crust thickness is only about 2% less than that of the Earth after 10 s, and is even more similar later on.

greater than 10 s after eruption, the thickness of the cooled skin on a Martian flow is almost identical to (less than 2% smaller than) that on a terrestrial flow. It is almost certainly the cooled skin thickness (and the effect of cracks [*Crisp and Baloga*, 1990]), as the indicator of the extent to which the interior of the flow has lost heat and the flow as a whole has suffered a modification of its bulk rheology, which is the relevant thermal control on the motion of a flow. We therefore conclude that surface cooling differences are not in themselves a significant factor in causing systematic differences between the lengths and widths of lava flows on Mars and the Earth.

3.1.2. Flow surface textures. Even so, cooling effects may in principle influence the small-scale properties of lava flows, such as the pahoehoe-aa surface texture transition [*Peterson and Tilling*, 1980; *Kilburn*, 1981] and the size scales of the surface folds (ropes) which characterize pahoehoe flows. We note, however, that the pahoehoe to aa transition appears to depend on the development of the bulk rheology of a flow [*Kilburn*, 1981]. The above comments on cooled skin thicknesses then imply that the transition might be expected to occur at a similar time after eruption on Mars and the Earth.

The wavelengths and growth rates of folds on flow surfaces are influenced by thermally controlled rheological changes in the outer layers of a flow and by the local gravity [*Fink and Fletcher*, 1978]. *Head and Wilson* [1986] used the model of *Fink and Fletcher* [1978] to show that the differences between the environments of Venus and the Earth were such as to encourage somewhat longer wavelengths and more vigorously growing folds on the surface of flows on Venus for the first few hours after their eruption. We have applied the same techniques to the data in Figure 6 and find that the parameters g and R introduced by *Fink and Fletcher* [1978] are essentially identical on Mars and the Earth, whereas the parameter S, which contains the acceleration due to gravity, is about 2.5

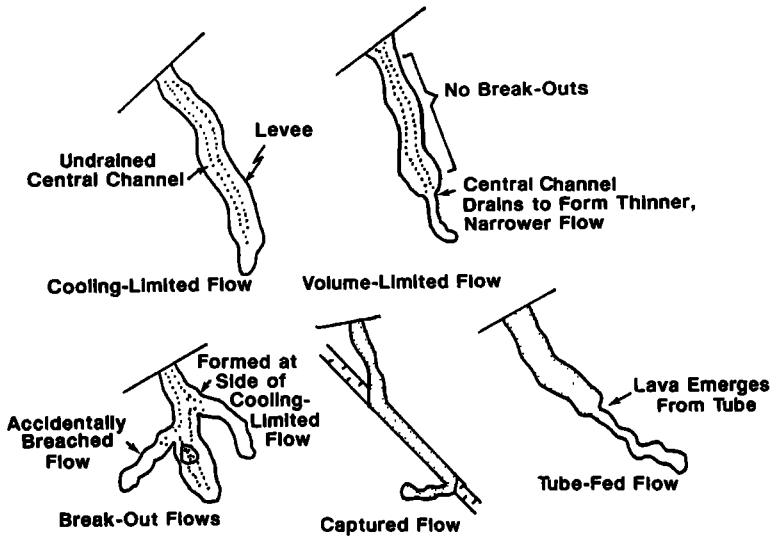

Figure 7. Summary of flow morphologies observed in several situations [after *Head et al.*, 1993]. In cooling-limited flows, effusion from the vent is relatively steady, and the flow front thickens and eventually stops because of cooling; the channel does not drain in this example [see *Pinkerton and Wilson*, 1994]. If the vent remains active, a breakout flow will form from some point on the margins of the initial flow unit (perhaps from the flow margin or central channel). In some cases, preexisting topography (e.g., a graben) may capture the flow and dictate flow geometry, while in others the central channel can become roofed over to form lava tubes, thus insulating the flow and modifying its cooling history.

times smaller on Mars. The consequence is that the growth rate of folds should be about 40% greater on Mars than on Earth; however, the dominant wavelength of the folds should be only about 15% longer than on Earth, an essentially negligible difference when the range of rope sizes on a typical terrestrial flow is considered. As a result, we endorse the findings of *Theilig and Greeley* [1986] that major "festoon" folds, forming ridges at ~100-m spacing arranged transverse to flow directions on flows extending many hundreds of kilometers from their sources, are probably the result of a combination of distal cooling, leading to apparent viscosities in excess of 10^8 Pa s, coupled with horizontal stresses developed when the flows ponded against obstacles or against their own terminal levees.

3.1.3. Flow morphology: Predictions from theory. The morphological features of lava flow deposits depend on several factors: the composition- and temperature-dependent rheological properties of the erupted materials; environmental variables such as the flow cooling rate under the ambient atmospheric conditions and surface temperature; and the physical parameters of the eruption, such as vent size and shape, total lava effusion rate, slope of the ground over which the flow advances, and planetary gravity. Effusion rate commonly varies during an eruption, flows advance down slopes which often vary systematically with distance from the vent, and lava rheology changes with progressive cooling. Thus there are many interdependencies among the above parameters.

However, some common factors appear to apply to all planetary lava flows (Figure 7). Flows generally spread laterally by a much smaller amount than they extend downslope, implying that their bulk rheology is not that of a Newtonian fluid. At relatively high effusion rates, most lava motion occurs in a central channel bounded by stationary levees; the thicknesses and widths of the levees can be characterized by a parameter with the units of stress called the yield strength. *Hulme* [1974] therefore suggested that lavas can be modeled as having the simplest non-Newtonian rheology, that of a Bingham plastic, characterized by two parameters: the yield strength, which must be exceeded for any deformation to occur, and the (constant) plastic viscosity, which is the ratio of strain rate to stress in excess of the yield strength.

This model has been applied to several Martian lava flow deposits [*Hulme*, 1976; *Moore et al.*, 1978; *Zimbelman*, 1985*a b*; *Cattermole*, 1987; *Fagents and Wilson*, 1990], producing a wide range of yield strength estimates (Table 5) that generally correspond with values deduced for flows on Earth of basaltic to andesitic composition at various distances from the vent. *Hulme* [1974] showed that a combination of measurements of levee and central channel geometry could be used to infer the product of the plastic viscosity of the lava and its effusion rate. Using the known rheological properties of terrestrial melts [*Shaw*, 1969; *Murase and McBirney*, 1973], it is possible (with caution) to use the yield strength estimated from levee geometry to infer the plastic viscosity and hence the effusion rate of a flow. Again, a wide range of values, generally consistent with mafic compositions, has been inferred for Martian lavas in this way (Table 5).

Modeling of channel-levee morphology is only possible where these features can be recognized in images of flow fields (Figure 7). Flow fields may fail to show such features because the original central channel morphology has been lost (or at least rendered unresolvable in available images) because of late stage channel overflow caused by an enhanced eruption rate or because the flows were sheetlike and fed from long fissure vents, such as may have been the case for some flood basalt eruptions on Earth [*Swanson et al.*, 1975] and for some ocean floor eruptions. No theoretical models of these conditions exist, though they probably imply high total effusion rates supplying the flows.

TABLE 5. Yield Strength and Viscosity Estimates for Lava Flows on the Earth, the Moon, and Mars

Location	*Yield Strength, Pa*	*Viscosity, Pa s^{-1}*	*Lava Type*	*Source**
		Earth		
Mauna Loa, Hawaii	3.5×10^2–7.2×10^3	1.4×10^2–5.6×10^6	basalt	10
Columbia River, N. Am.	$<7 \times 10^3$		basalt	6
Makaopuhi, Hawaii	70–8×10^3	7×10^2–4.5×10^3	basalt	14
Mount Etna, Italy	9.4×10^3	9.4×10^3	basalt	5
Mount Etna, Italy	10^3–5×10^4		basalt	11
Kilauea, Hawaii	1.5×10^3–5×10^4		basalt	8
Mauna Loa, Hawaii	0.4×10^4		basalt	4
Meru, Tanzania	6.6×10^4		phonolite	12
Hawaii	0.23–1.1×10^5		trachyte	4
Mount Saint Helens, Wash.	1.5×10^5		andesite	4
Mono Craters, Calif.	1.2–3.3×10^5		rhyolite	4
Oldoinyo Lengai, Tanzania		10–100	carbonatite	13
Columbia River, N. Am.		5.0–4×10^3	basalt	16
Mauna Loa, Hawaii		1.7×10^5	basalt	2
Paricutin, Mexico		3.6×10^6	andesite	2
Arenal, Costa Rica		1.0×10^7	basaltic andesite	14
Teide, Tenerife		4.4×10^7	phonolite	2
		Moon		
Mare Imbrium	1.5×10^2			1
Mare Imbrium	4.2×10^2			3
Aristarchus	1.3×10^4			3
Aristarchus	1.94×10^4			4
Necho	2.25×10^4			4
King	2.41×10^4			4
		Mars		
Arsia Mons	0.39–3.1×10^3			4
Alba Patera	1.9×10^3–2.8×10^4	1.7×10^5–1.9×10^6		9
Ascraeus Mons	3.3×10^3–8.3×10^4	6.5×10^5–2.1×10^8		7
Olympus Mons	8.8×10^3–4.5×10^4	2.3×10^5–6.9×10^6		2
Olympus Mons	1.8–5.3×10^4			4

Table is after *Cattermole* [1989].

*Sources are 1, *Moore and Schaber* [1975]; 2, *Hulme* [1976]; 3, *Hulme and Fielder* [1977]; 4, *Moore et al.* [1978]; 5, *Pinkerton and Sparks* [1976]; 6, *McBirney and Murase* [1984]; 7, *Zimbelman* [1985*a*, *b*]; 8, *Fink and Zimbelman* [1986]; 9, *Cattermole* [1987]; 10, *Moore* [1987]; 11, *Kilburn* [1985]; 12, P. Cattermole (unpublished data, 1993); 13, B. Dawson (unpublished data, 1993); 14, *Cigolini et al.* [1984]; 15, *Shaw et al.* [1968]; 16, *Murase and McBirney* [1973] and *Fink et al.* [1981].

Theoretical studies of lava cooling rates [e.g., *Pieri and Baloga*, 1986; *Crisp and Baloga*, 1990] and field measurements of temperatures within active flows clearly show that the apparent (i.e., bulk) rheological properties are those of some part of the cooled, outer layers of the flow and not the well-insulated interior. This fact is of great importance in considering the morphologies of flows fed from tube systems (Figure 7) formed by the roofing-over of the channels of earlier channel-fed flows [*Greeley*, 1970]. Flows of any kind fed from mature tubes can have the morphological properties of flows fed directly from a vent. However, tube formation, often with attendant breakouts of small flows from fractures in the tube roof at times of enhanced eruption rate, makes it difficult to identify the structure of a flow which develops into a tube, and so only the most distal parts of a compound flow field formed in this way may be reliably interpreted without high-resolution (meter scale) images.

The latter point is even more important when considering flows fed at low effusion rates, whether from primary vents or tubes. The deformation of lava at low-volume fluxes and hence low strain rates [*Rowland and Walker*, 1990; *Peterson and Tilling*, 1980; *Kilburn*, 1981, 1993] causes minimal disruption of the outer layers of the lava surface and produces the characteristic folded pahoehoe surface texture on networks of small (submeter) toes and larger (1–3 m) flow units fed essentially by self-generating tube systems. *Mouginis-Mark* [1992] has pointed out that it may be very difficult without very high-resolution images to distinguish compound pahoehoe flow fields produced by long-lived, low effusion rate events from sheet flows fed at much higher rates, though work on the possibly fractal nature of the plan form of flow unit margins [*Wadge and Lopes*, 1992; *Bruno et al.*, 1992] suggests an alternative approach.

The above considerations illustrate the pressing need for high (meter scale) resolution images of Martian lava flow fields which can be used to delineate unambiguously the boundaries of individual flow units and to detect the edges of central channel structures,

where these exist. Also, more detailed flow unit thickness values are needed to allow apparent yield strengths and, indirectly (see below), other rheological properties and emplacement conditions to be deduced. The difficulties associated with using shadow lengths to infer flow thicknesses [*Fagents and Wilson*, 1990] or photoclinometric methods to obtain cross-sectional profiles of flows [*Efford*, 1991] highlight the need for the use of high-resolution altimeter profiles to determine flow thickness variations.

3.1.4. Length of flows. Lava flow lengths clearly measure some combination of effusion rate, flow duration, and magma rheology and, as a result, must give some indication of the subsurface conditions within a volcano. It has been suggested on the basis of field data that flow length is controlled mainly by lava effusion rate [*Walker*, 1973] or flow volume [*Malin*, 1980], though it is clear that flow length should depend in some way on most of the variables involved [*Hulme*, 1974] and will be ultimately limited by cooling if no other factors intervene. This suggests [*Hulme and Fielder*, 1977] that the dimensionless Grätz number, Gz, which is the square of the ratio of the thickness of a flow to the distance that a thermal cooling wave will have travelled into it since the material in the flow left the vent, may be a useful parameter to characterize lava cooling. Gz is defined as

$$Gz = de^2/\kappa t = n^2Ed/(\kappa wcL), \quad (6)$$

where κ is the lava thermal diffusivity, E is the volume effusion rate from the vent, d is the average flow thickness, wc is the width of the central channel within which lava is moving, L is the flow length, and n is the ratio of the equivalent hydraulic diameter of the flow to its actual average thickness (for most flows, n is ~2). Both *Hulme and Fielder* [1977] and *Pinkerton and Wilson* [1994] found that flows cease to move when Gz has decreased from an initially high value at the start of an eruption to a critical value Gzc, ≈300. Using this relationship and treating the rheology of flows as that of a nonisothermal Bingham plastic [*Pinkerton and Wilson*, 1994], it is found that the maximum length, L_{max}, of most cooling-limited lava flows can be predicted from

$$L_{max} = [1.34/(\kappa Gzc)] \cdot (\tau/\eta)^{2/11}E^{9/11}[\tau/(\rho g)]^{6/11} \sin^{3/11}\alpha, \quad (7)$$

where τ and η are the apparent values of the yield strength and plastic viscosity, respectively, of the lava flow at its distal end, ρ is the density of the lava, g is the acceleration due to gravity, and α is the slope of the surface on which the flow is emplaced; it is found empirically that $(\tau/\eta)^{2/11}$ has a value close to 0.38 $s^{-2/11}$ near the distal ends of flows for a wide range of lava compositions [*Pinkerton and Wilson*, 1994].

This relationship is used in Figure 8 to predict the lengths of basaltic flows on Mars and Earth for a wide range of effusion rates and for three values of the slope of the substrate on which the flow is emplaced. A distal lava yield strength of 2000 Pa is used in all cases; this value is consistent within a factor of 2 with the thicknesses of most basaltic flows on Earth and Mars [*Moore et al.*, 1978; *Fagents and Wilson*, 1990]. Figure 8 shows that the lower gravity causes cooling-limited flows to travel about 1.7 times further on Mars than on Earth for the same effusion rate, mainly because they are thicker for a given lava yield strength and substrate slope. *Wilson and Head* [1988] and *Wilson and Parfitt* [1989, 1990] showed that other subsurface magma reservoir conditions being equal, higher effusion rates by a factor of 5 might be expected on Mars as a result of the up to twofold greater dike widths implied by the lower gravity (L. Wilson et al., manuscript in preparation, 1994). Taken together, these factors imply that we might expect compositionally similar cooling-limited lava flows to be about 6 times longer on Mars than on Earth.

3.2. Lava Flows: Summary of Predicted Deposits and Edifices

Although heat loss processes are such that no major differences between Mars and Earth are to be expected in terms of flow cooling rates and surface textures, the effect of lower gravity causes cooling-limited flows to be longer and dikes and vents to be wider and characterized by higher effusion rates. These factors map out into flow lengths that are about a factor of 6 longer on Mars than on Earth. This means, for example, that Laki type flows (with lengths of 35–60 km [*Thorarinsson*, 1970]) would have typical lengths of 200–350 km on Mars. If such flows built up an edifice, this would permit the construction of very large volcanoes of the order of 400–700 km in diameter.

3.3. Lava Flows: Comparison With Observations

3.3.1. Individual lava flows. Lava flows are ubiquitous in the Tharsis and Elysium region of Mars and originate mainly from the central volcanic edifices and their rift zones. A wide variety of flow types and morphologic features have been mapped [*Schaber et al.*, 1978]. For example, three main types of flows have been documented on the same volcano, Alba Patera (Figure 9): (1) short (up to about 100 km long), narrow leveed flows concentrated near the summit, (2) longer (up to about 300 km long) sheetlike flows which show terminal broadening, and (3) very long tube-fed flows [*Carr et al.*, 1977; *Cattermole*, 1987]. The very long tube-fed flows are interpreted to be flows whose channels have been roofed-over, thus retaining heat and volatiles and enhancing their extreme length. The sheetlike flows are interpreted to be large-volume high effusion rate fissure-fed flows analogous to flood basalts on Earth. The short, narrow, leveed flows produce a net-

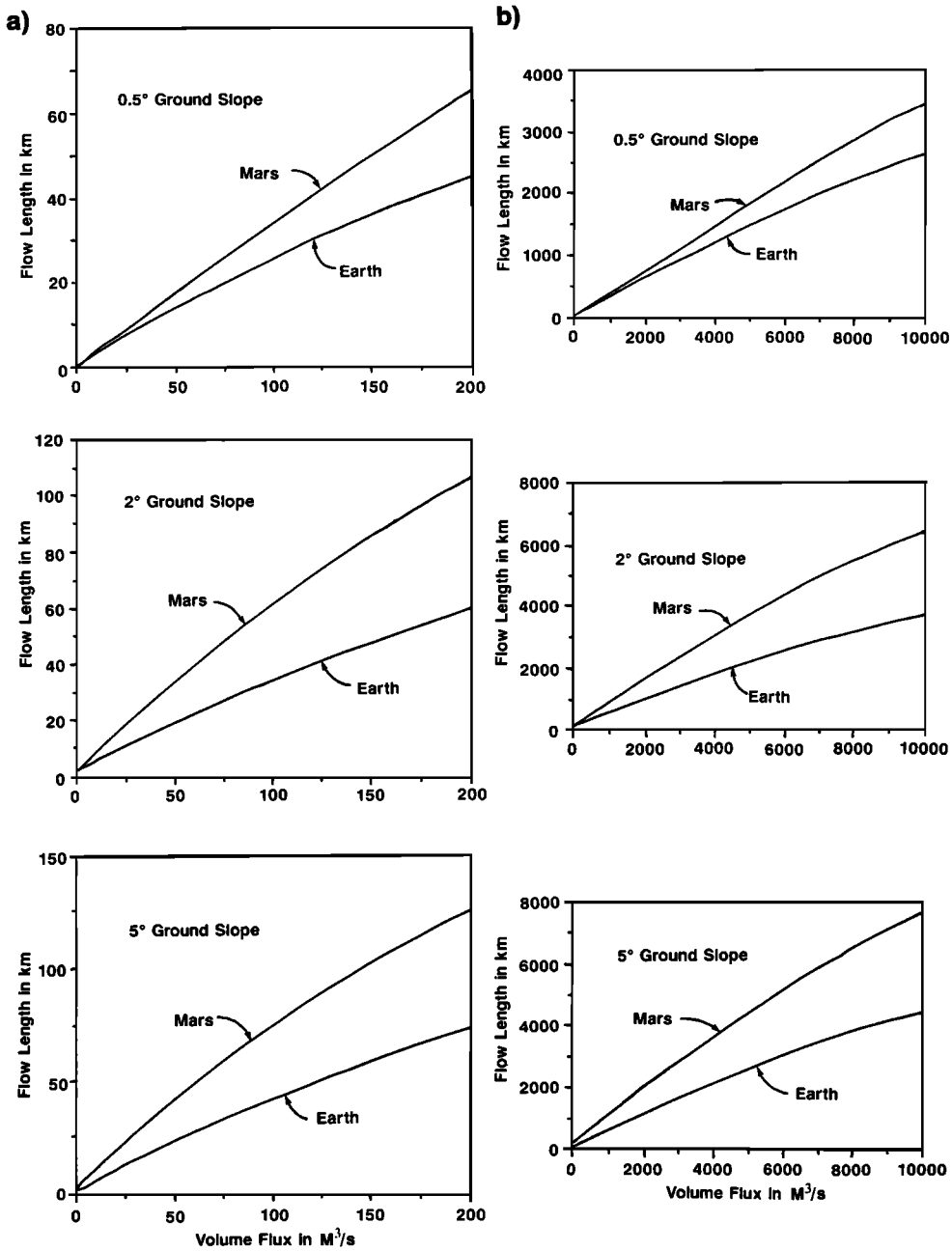

Figure 8. Lava flow lengths as a function of effusion rate for Earth and Mars for three different ground slopes (0.5°, typical of the flanks of Alba Patera; 2.0°, the East Rift Zone of Kilauea, Hawaii, measured along the rift axis; 5.0°, most parts of Mauna Loa and also the steeper parts of the Kilauea East Rift Zone, measured across the rift axis, and the flanks of the Tharsis shields). A distal lava yield strength of 2000 Pa is used in all cases. The left column shows details near the origin (the lower end of the full range); the full range of data is shown in the right column. Pu'u 'O'o type events typically have effusion rates in the range of 100–200 $m^3\ s^{-1}$. The Icelandic Laki fissure flow peaked at just over 4000 $m^3\ s^{-1}$ from a fissure about 2.5 km long. Lower Martian gravity causes cooling-limited flows to travel about 1.7 times further on Mars than on Earth for the same effusion rate, mainly because they are thicker for a given lava yield strength and substrate slope.

work of anastomosing flows in the vicinity of the vent areas. The vast majority of the flows form an overlapping network of individual flow segments and cannot be differentiated into specific flow types (Figure 9).

On Arsia Mons, *Carr et al.* [1977] mapped a series of flow units which showed increasing age as a function of distance from the summit. Length of individual flows making up the units varied inversely with elevation, as did flow width, with widths of 5–6 km close to the summit and 40–50 km at distances greater than about 400 km from the summit. Individual flows can be traced for up to 300 km and some emerging from

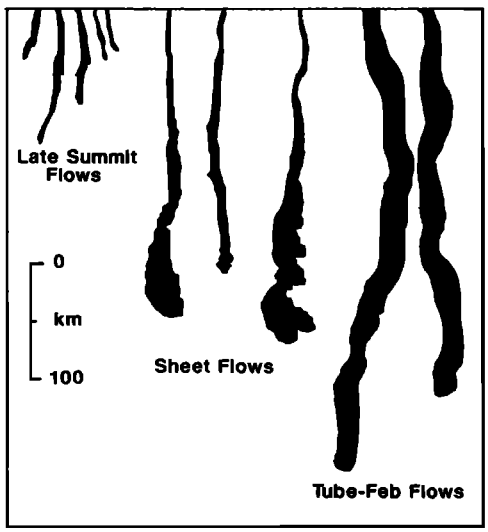

Figure 9. Spectrum of morphologies of individual lava flows on Mars as illustrated by the three main types of flows documented on Alba Patera [after *Cattermole*, 1989]. Short (up to about 100 km long), narrow leveed flows are concentrated near the summit. Longer (up to about 300 km long) sheet like flows show terminal broadening. Very long flows appear to be tube-fed flows.

underneath younger flows may have traveled as much as 800 km from the summit region. *Carr et al.* [1977] also defined discrete rift zones and associated flows on the flanks of Arsia and Pavonis Montes.

On the basis of the fact that the total volume of lava erupted to produce single flows in these cases was orders of magnitude greater than that in terrestrial lava flows, *Carr et al.* [1977] suggested that the magma generation model for these Martian examples must be rather different from any current models for Earth. On the basis of our theoretical treatment, however, the differences between the terrestrial and Martian examples may not be sufficiently different to require significantly different magma generation models. For example, the 6-times greater length expected for Martian cooling-limited flows would mean that the two shorter Alba flow types up to 100 and 300 km long (Figure 9) would map out into terrestrial flows with maximum lengths of about 17 and 38 km, respectively, values not unusual for basaltic volcanism on Earth. Although the fact that the longer flows on Alba, Arsia, and Olympus (up to 800 km) are largely tube-fed, and thus would be expected to be longer than a typical channel-fed flow, they still are only equivalent to a terrestrial flow with a length of about 133 km. Flow lengths in the Columbia River flood basalts lie within this range, with the Roza Member being of the order of 300 km in length [*Swanson et al.*, 1975].

We thus conclude that eruption rates may actually be closer to terrestrial values than previously thought. Therefore flow length alone is not a sufficient reason to require different models of magma generation and emplacement for Mars. Other factors, such as lithospheric structure and mobility, thermal evolution, crustal structure, and evolving edifice-reservoir dynamics, may be at least as important in explaining the differences in morphology of volcanic deposits and edifices on Earth and Mars.

3.3.2. Lava floods. Often lava flows take the form of flood lavas, losing the distinctive high aspect ratio of narrow flows and extending over large areas. *Plescia* [1990] has identified a very young flood lava deposit in the Cerberus Plains, covering >100,000 km^2 in southeastern Elysium and western Amazonis. These deposits (Figure 10) are characterized by lobate flow boundaries, and where high resolution is available, there is some evidence of festoons and other surface texture but little evidence of channels and levees. They have thicknesses up to about 10 m and clearly embay older terrain. They appear to originate from six eruptive vents which are interpreted to be low shields with elongate, elliptical, and symmetrical shapes, with summit vents in the 1- to 2-km-diameter range for circular vents and up to 15 km in length for elongate vents. Some of the deposits may represent late stage plains volcanism.

Several of the vents and shields are elongated along the strike of the Cerebrus Rupes, surface structures which are interpreted here to mark the near-surface manifestation of subsurface dike emplacement [see *Head and Wilson*, 1993] (Figure 10*c*). As described earlier in this section, the influence of lower Martian gravity on increasing dike widths by up to a factor of 2 and effusion rates by a factor of 5, suggests that the very extensive and floodlike nature of these deposits may be readily understood in terms of fissure-fed flood eruptions associated with dike emplacement.

3.3.3. Small lava shields and edifices. Numerous examples of small lava shields and edifices have been mapped on Mars [*Hodges and Moore*, 1994; *Plescia*, 1981; *Scott*, 1982]. A number of these ranging up to 150 km in diameter are located in the Martian western hemisphere [*Scott*, 1982] (Figure 11). Some small shields and edifices are related to linear fissures and graben (Figure 11) and may be the surface manifestation of dike emplacement. Others appear to represent the locations of larger central sources, with individual flows arrayed around a summit vent [*Scott*, 1982]. On the basis of their diameter range, and the likelihood that flows on Mars will be typically longer than on Earth, it is clear that these structures represent a variety of sources similar to those seen around small- to intermediate-sized lava shields on Earth.

3.3.4. Large lava shields and edifices. The Tharis Montes and Olympus Mons (Figure 12) are classic shield volcanoes built from thousands of lava flows over extended periods of time [*Carr et al.*, 1977; *Schaber et al.*, 1978; *Carr*, 1981; *Greeley and Spudis*, 1981; *Zimbelman and Edgett*, 1992]. *Schaber* [1982] has mapped a large low-relief shield volcano in Syrtis

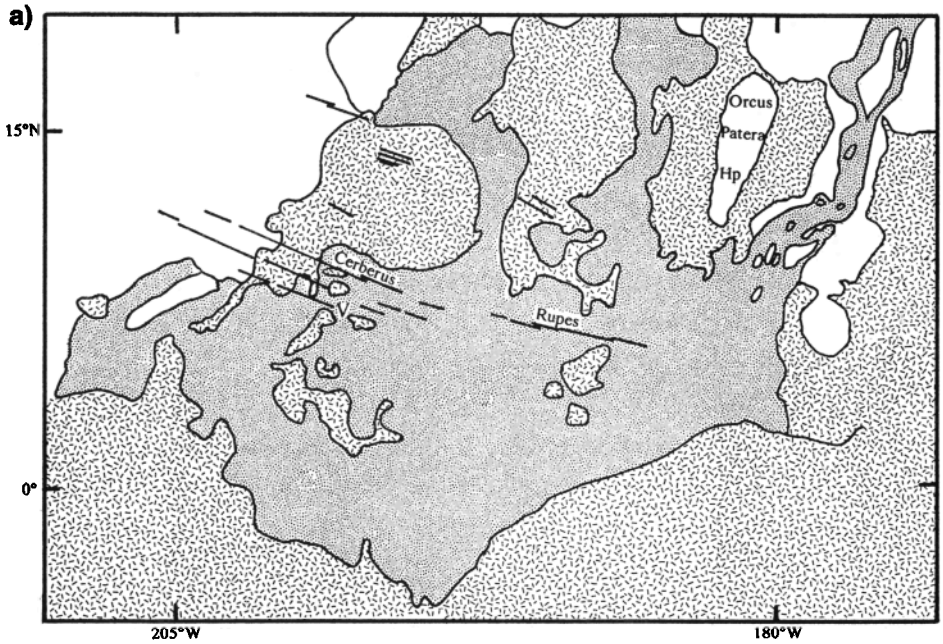

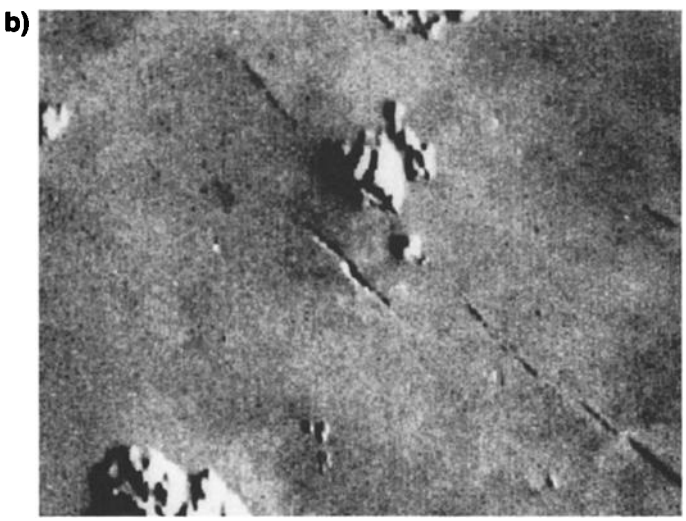

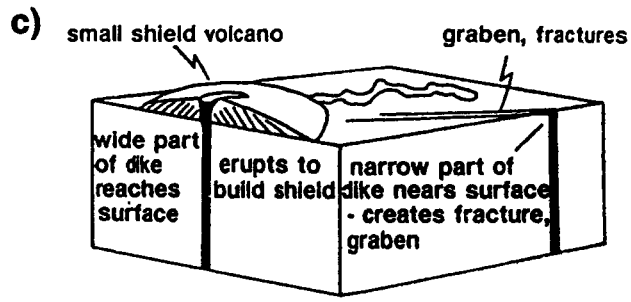

Figure 10. Lava floods in the Cerberus region of Mars. (*a*) Geologic sketch map of southeastern Elysium showing the distribution of Cerberus Plains, Cerberus Rupes, and adjacent units (white unit is undifferentiated Elysium volcanic units and ridged plains; hatched unit is heavily cratered and undifferentiated terrain; and stippled unit is Cerberus volcanic plains) [after *Plescia*, 1990]. (*b*) Candidate vent structure in the vicinity of Cerberus Rupes (VO 385S48); location is marked as V in Figure 10*a*, and the width of the image is about 72 km. (*c*) Block diagram illustrating the interpreted relationships between linear fractures and faults, volcanic vents and deposits, and dike emplacement [see *Head and Wilson*, 1993].

Major with two central calderas and associated small domes and apparent vents. Syrtis Major, along with Alba Patera [*Cattermole*, 1987], is typical of extensive volcanoes built of widespread flows emanating from a central source but where the edifice itself has not achieved and maintained heights anywhere near those of the Tharsis Montes.

In all these cases, flows emanate from near the summit region, which is often characterized by a multiple caldera structure, and extend down the flanks of the structure into the surrounding lowlands. Some of the edifices are marked by distinctive rift zones, and there is evidence for flows being emplaced on the volcano flanks at later stages than the summit regions [*Crumpler and Aubele*, 1978]. Perhaps the most remarkable aspect of these features is the extreme length of the vast majority of their flows (typically several hundreds of kilometers). A further remarkable aspect is the extreme height of many of these edifices (up to 25 km above the surrounding terrain). The flow lengths, extreme by terrestrial standards, are plausibly interpreted to be due primarily to the combination of Martian conditions (described in section 3.1.4) which result in Martian lava flows having lengths up to a factor of 6 greater than analogous terrestrial flows. The edifice elevations and volumes, also extreme by terrestrial standards, appear consistent with mantle source regions operating over hundreds of millions of years beneath a stable Martian lithosphere. Thus the combination of eruption conditions in the Martian environment, and the stable tectonic environment, may explain the characteristics of these edifices without recourse to unique petrogenetic situations or to lavas of unusual viscosity.

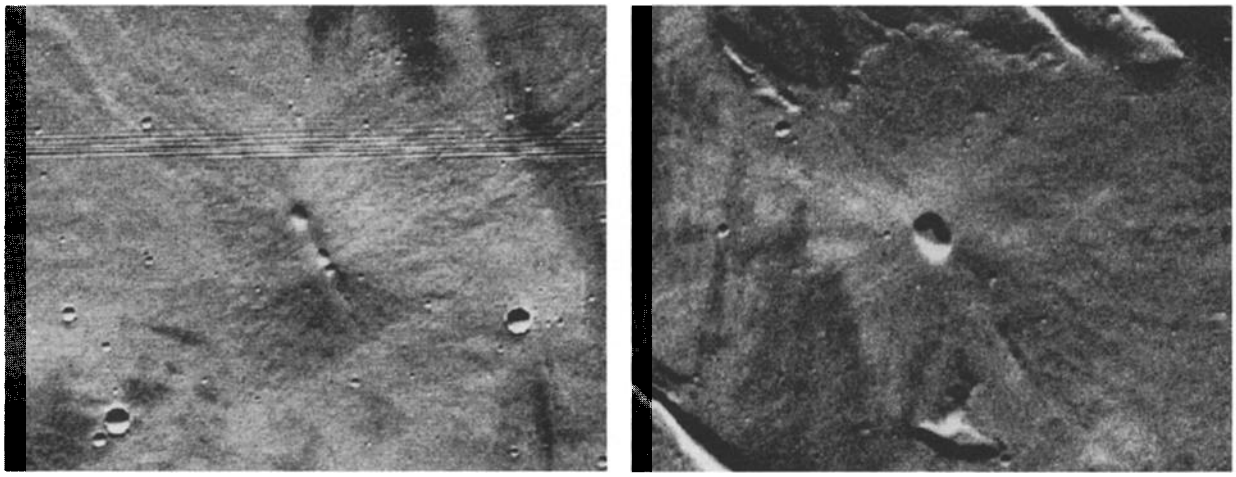

Figure 11. Examples of small lava shields and edifices from the Tempe Volcanic Province [*Plescia*, 1981]. (*a*) Elongate shield volcano with radiating flows; note linear nature of vents (VO 627A22); width of the image is about 48 km. (*b*) Equidimensional shield volcano about 20 km in diameter with radial flows emanating from a central vent area (VO 627A41).

4. EXPLOSIVE ERUPTIONS

4.1. Explosion Mechanisms

The origins of explosive activity connected with the release of magmatic volatiles (strombolian, hawaiian, plinian, and ignimbrite-forming eruption styles) and with the interaction between magma and near-surface volatiles (vulcanian and pelean styles) have been outlined (Figure 4). A common denominator that applies to all explosive eruptions on planets with appreciable atmospheres is that some of the clastic eruption products may become entrained in a mixture of released magmatic gases and atmospheric gases (and, possibly, gases derived from the thermal vaporization of near-vent volatile deposits) in such a way as to produce a convecting eruption cloud which rises into the atmo-

Figure 12. Oblique view of a portion of Olympus Mons, one of the large lava shields and edifices in the Tharsis region. Flows emanate from near the summit region, which is characterized by a multiple caldera structure, and extend down the flanks of the structure, often cascading over the major several-kilometer-high scarp at the base and onto the surrounding lowlands. The extreme flow lengths, edifice elevations, and volumes appear consistent that mantle source regions operating over hundreds of millions of years beneath a stable lithosphere in a Mars environment favoring wide dikes, high effusion rates, and extremely long lava flows (VO 641A52).

sphere over the vent. We first treat the general properties of eruption clouds on Mars and then consider in more detail the expected products of the various types of explosive eruption in the Martian environment.

4.2. Eruption Cloud Formation

An eruption cloud is a system in which atmospheric gases are entrained in sufficiently large amounts into the mixture of pyroclasts and magmatic volatiles released from a vent that a net positive buoyancy is created as the pyroclasts heat the atmospheric gas components. The entrainment process is most efficient when the magmatic materials emerge from a vent at high speed in a narrow jet [*Wilson*, 1976]; however, as long as most of the pyroclasts have the opportunity to transfer most of their heat to the atmospheric gas somewhere in the cloud before they are released from its edge, the details of the transfer process appear to be relatively unimportant [*Wilson et al.*, 1978; *Settle*, 1978], and the cloud behaves as though it were driven solely by the buoyancy generation [*Morton et al.*, 1956]. In all cases, the amount of heat injected into a cloud is proportional to the mass of material leaving the vent and to its absolute temperature.

4.3. Heights of Eruption Clouds

The maximum rise height of a cloud from a point source (conduit type) vent is then found to be proportional to the fourth root of the erupted mass flux for a maintained eruption cloud or to the fourth root of the total erupted mass for a cloud produced from a discrete explosion [*Morton et al.*, 1956]. Where the vent has an elongate geometry, the height is proportional to the mass flux or total mass, as appropriate, raised to the power one third [*Stothers et al.*, 1986; *Stothers*, 1989]. The constants of proportionality in these relations are functions of the temperature and density variations in the atmosphere into which the cloud rises. Numerical calculations [*Wilson et al.*, 1982] show that in the Martian atmosphere, eruption clouds should rise higher than in the Earth's atmosphere by a factor of about 5 for a given set of eruption conditions: detailed examples of plinian eruption cloud heights are given in section 4.6.

4.4. Strombolian Eruptions

4.4.1. Theory and predictions. These occur whenever gas bubbles can rise through a magma at a speed comparable to the ascent rate of the magma itself through the lithosphere (Figure 4). Runaway coalescence of bubbles leads to the intermittent explosive emergence of large bubbles (up to 10 m size on Earth) through a lava lake in the vent [*Blackburn et al.*, 1976]. Generally, the low viscosity of basaltic magma is needed to permit this process to occur if there is appreciable effusion, though it can take place in a nearly static lake of basaltic andesite magma; comparison of the details of this eruption style on the Earth (which has a higher atmospheric pressure and gravity than Mars) and the Moon (lower pressure and gravity) shows that the conditions under which strombolian explosions occur on Mars are very similar to the corresponding conditions on Earth [*Wilson and Head*, 1981*a*] (Figure 13).

Blackburn [1977] calculated the pressures in rising gas bubbles of various sizes in the Martian environment and found that pressures in large bubbles reaching the surface of a lava lake may be up to 2 or 3 times larger than the ambient atmospheric pressure. If the dynamics of the bubble-bursting process are the same on Mars as on Earth, the ejection velocities of gas and small pyroclasts from Martian strombolian bursts (calculated using the methods given by *Blackburn et al.* [1976]) will range up to about 250 m s^{-1}, almost exactly the same speed range as on Earth. Computation of the terminal velocities of pyroclasts in water vapor or carbon dioxide at magmatic temperatures and under Martian surface atmospheric pressure conditions (using the equations given by, for example, *Wilson* [1976]) then implies that pyroclastic fragments larger than a few centimeters in size will collect within 100 m of the vent, while smaller clasts, especially in the subcentimeter size ranges will be carried up into a convecting eruption cloud and widely dispersed (Figure 13).

Thus for strombolian eruptions on Mars, the nucleation depth is greater than on Earth, and the bubble size and pressure is greater at the surface, but the velocity range for large particles is about the same as for the Earth (Figure 13). The range of velocities as a function of particle size distribution is different, however. The main difference is that while the large particles (> a few centimeters) will remain near the vent, the finer material will be more broadly dispersed and the finest material will be carried up into a convecting cloud over the vent. This means that there would be a tendency for broader deposits of fine tephra surrounding spatter cones on Mars than on Earth. On Mars, strombolian eruption deposits should consist of cones that are slightly broader and lower relative to those on Earth and with a surrounding deposit of finer material.

4.4.2. Comparison to observations. Candidates for Martian spatter cones have been mapped by *Cattermole* [1986] in a 100- to 150-km-wide zone on the north and east flanks of Alba Patera. Here aligned ridge elements between 0.3 and 10 km in length and 100–500 m in width are characterized by small ventlike structures and associated short flows (Figure 14). Shadow measurements indicate heights of about 15 m. Interpreted by *Cattermole* [1986] as spatter ridges, these features fall in the range expected for strombolian activity and deposits. Some of the larger features, particularly those associated with flows, could represent hawaiian activity. Indeed, when fissure eruptions are initiated, spatter cones are commonly formed along the curtain of fire and the eruption

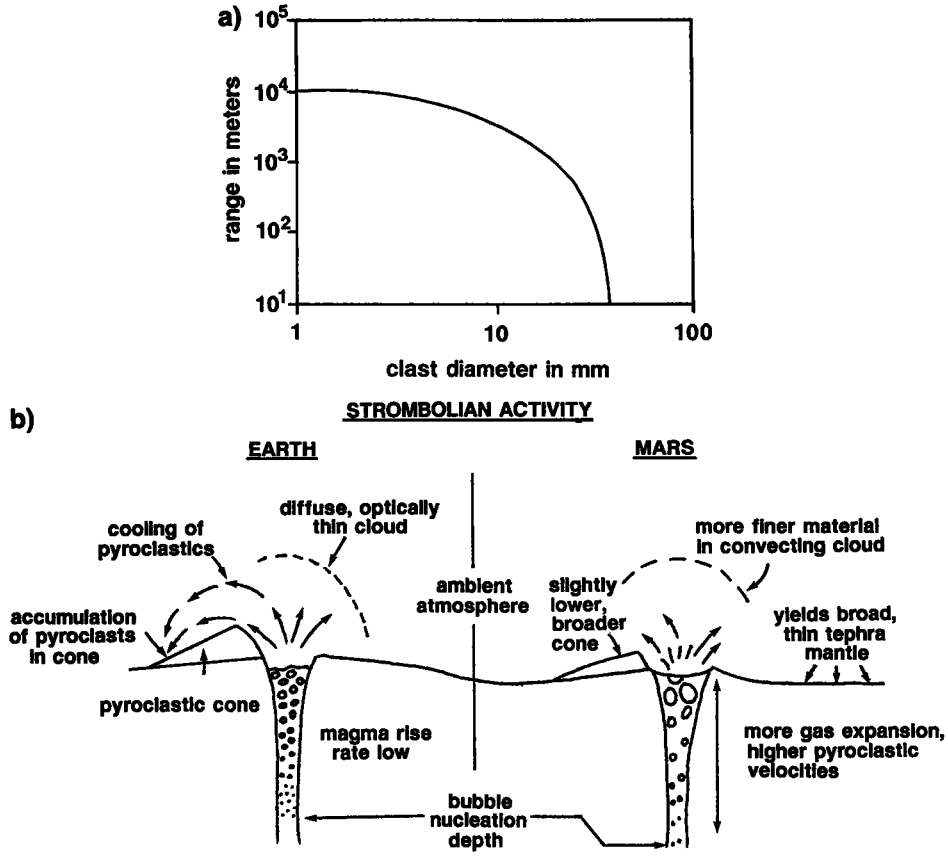

Figure 13. Strombolian eruptions on Mars. (*a*) Relationship between clast diameter and range. (*b*) Strombolian eruption cloud and clast behavior and comparison to Earth.

soon centralizes around a smaller number of vents, where a hawaiian eruption commonly continues, building a larger edifice and associated flows. Higher-resolution images of features such as these would permit delineation and distinction of strombolian deposits and their transition to hawaiian type deposits.

4.5. Hawaiian Eruptions

4.5.1. Introduction. As noted earlier, on Earth, hawaiian eruptions have fairly high effusion rates, with moderately gas-rich mafic magma forming high fire fountains [*Wilson and Head*, 1981*a*]. They represent eruption conditions which just fail to produce high plinian convection clouds, mainly because of the relatively large size of the clots into which most of the magma disrupts. For the same reason, the outer parts of the fire fountains from such eruptions are commonly optically thin on Earth [*Head and Wilson*, 1989], and significant cooling of the clots occurs before they reach the ground to form cinder or spatter cones around the vent (Figure 4). However, the central parts of such fountains can be optically dense, and magma clots landing near the vent commonly coalesce to form either rootless flows or a pond from which a lava flow issues.

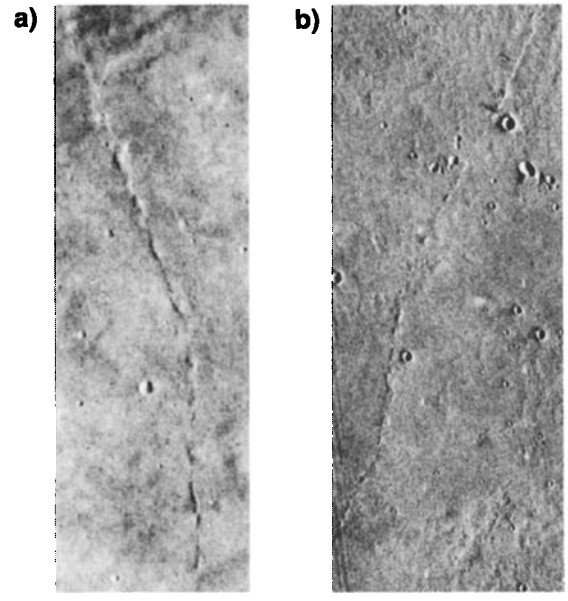

Figure 14. Examples of features interpreted to be spatter cones on Mars. (*a*) Linear constructional feature on the flank of Alba Patera (part of VO 253S44; width of the image is 12.5 km) [*Cattermole*, 1986]. (*b*) Linear chains of spatter cones no more than 50 m wide along a fissure in the Uranius Patera North region (part of VO 626A69; width of the image is about 20 km) [*Hodges and Moore*, 1994].

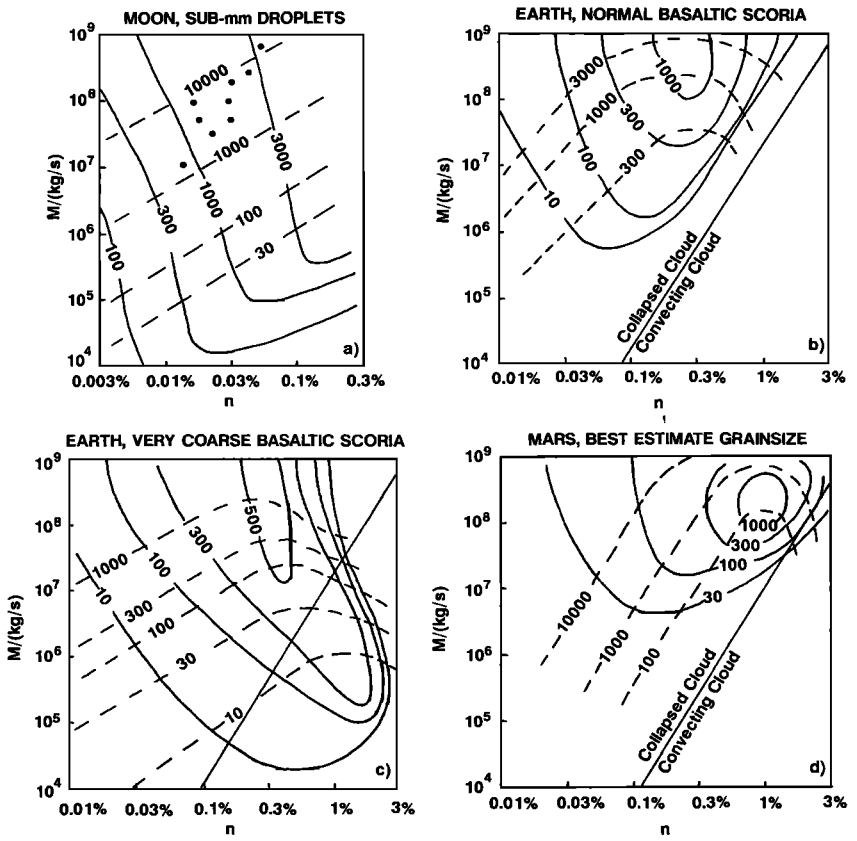

Figure 15. Formation of sinuous rilles and associated lava pools and source depressions on the Earth, Moon, and Mars. M is mass eruption rate and n is exsolved volatile content. Solid lines show maximum radii of liquid lava pools which can be formed from accumulation of hot pyroclasts at any combination of M and n. Dashed lines are contours of equal Reynolds number for the motion of lava in the pools. (*a*) Typical lunar basaltic eruptions; the dots represent the eruption conditions deduced for a number of lunar sinuous rilles [*Wilson and Head*, 1981*b*]; (*b*) Terrestrial eruptions with a size distribution of magma clots identical to that of the scoria erupted in the 1973 eruption of Heimaey [*Self et al.*, 1974]; (*c*) Terrestrial eruption with magma clots 10 times coarser than those used in Figure 15*b*; (*d*) Best estimate of magma clot sizes in Martian basaltic eruptions. In Figures 15*b*, 15*c*, and 15*d*, the boundary beyond which most of the pyroclasts would be incorporated into a convecting eruption cloud is shown.

4.5.2. Formation of sinuous rilles and associated pools and source depressions. It has been shown that the maximum sizes of gas bubbles (probably of carbon monoxide) in lunar magmas at the time of their eruption should have been sufficiently small that the magmas were disrupted into clots that were largely submillimeter in size [*Wilson and Head*, 1981*a*]. Resulting fire fountains would have been optically dense over a wider range of eruption conditions than in the case of terrestrial equivalents, and uncooled magma clots would have coalesced on landing to form lava flows. It is possible to calculate the size of the pool formed around a vent given the mass eruption rate and exsolved magma volatile content and also deduce the Reynolds number associated with the lava motion in the pool as it drains into a lava flow [*Wilson and Head*, 1981*b*]. If the Reynolds number is larger than the minimum value ($\sim 10^3$) permitting turbulent motion, thermal erosion of the substrate on which the lava is moving can occur and a sinuous rille, together with its characteristic source depression, can be formed [*Hulme*, 1973, 1982].

We investigate whether the same kind of activity can occur on the Earth or is likely to occur on Mars. The calculations involve keeping track of the thermal state and motions of coarse magma clots which are not entrained into the eruption cloud over the vent and of smaller clots which are partially sorted in the cloud before deposition. The methods described by *Wilson and Head* [1981*a*] were used to produce the results shown in Figure 15. Figure 15*a* is for typical lunar basaltic eruptions; Figure 15*b* is for terrestrial eruptions with a size distribution of magma clots identical to that of the scoria erupted in the 1973 eruption of Heimaey [*Self et al.*, 1974]; Figure 15*c* is for a terrestrial eruption with magma clots 10 times coarser than those used in Figure 15*b*; and Figure 15*d* is for our best estimate of magma clot sizes in Martian basaltic eruptions (the distribution found for terrestrial rhyolitic pumice eruptions [*Sparks et al.*, 1978] is used, on the grounds that the amount of fragmentation of mafic magmas on Mars should lie between the extremes for the Earth and Moon [*Wilson and Head*, 1981*a*]).

In each part of Figure 15 the maximum radii of liquid lava pools which can be formed for any combination of mass eruption rate and exsolved volatile content is shown by the solid lines. The largest pools are formed, in both Martian and terrestrial eruptions, for high eruption rates and some intermediate volatile content: this is because too high a volatile content produces a very strongly convecting eruption cloud, and even the larger magma clots fail to fall out in large enough numbers over a small enough area to produce an optically thick, and hence hot, zone around the vent. In contrast, convecting eruption clouds never existed on the atmosphereless Moon, and pool size increases steadily with volatile content above a threshold eruption rate [*Wilson and Head*, 1981*a*].

The dashed lines in Figure 15 are contours of equal Reynolds numbers for the motion of the lava in the pools. For all combinations of conditions which give a Reynolds number greater than about 1000, sinuous rille formation by thermal erosion is potentially possible, as long as the eruption continues for long enough to allow the underlying ground to heat up to its solidus temperature (about 2 weeks [*Hulme*, 1982]) and then for long enough to allow appreciable erosion to occur (typical erosion rates are of the order of 0.3 m d^{-1} [*Hulme*, 1973]). The solid circles marked in Figure 15*a* represent the eruption conditions deduced for a number of lunar sinuous rilles [*Wilson and Head*, 1981*b*]; the sizes of these features imply that they were all formed in events in which the rate of eruption exceeded 10^7 kg s^{-1}.

Figures 15*b* and 15*c* show that on Earth, formation of a lava pool around the vent by coalescence of hot magma clots is to be expected for a wide range of eruption conditions and clot size distributions, whether or not the erupting material is capable of driving a stable, convecting eruption cloud. For eruption rates up to 10^7 kg s^{-1} (no recorded eruption appears to have significantly exceeded this output rate from a single vent or single active section of fissure), the expected pool radii lie in the range 10 to 400 m, in good agreement with observations. However, formation of a sinuous rille on Earth with a source depression 100 m in radius would require an output rate of at least 3×10^7 kg s^{-1}; even a 10-m radius source depression would require an eruption rate of at least 3×10^6 kg s^{-1}. It seems clear that the larger terrestrial basaltic eruptions are capable of forming sinuous rilles with source depressions about 10 m in radius; however, such features are either completely hidden by the accompanying scoria fall or are not recognized as anything other than normal lava flows, because the eruptions do not continue long enough for an appreciable amount of erosion of the substrate to take place.

Figure 15*d* shows that conditions in Martian fire fountain eruptions are much more like those in terrestrial examples than in equivalent lunar events: sinuous rille formation with a source depression radius of 30 m would require an eruption rate of at least 3×10^6 kg s^{-1}, and it is unlikely that sinuous rille source depressions could ever be larger than about 2 km in diameter, even at the optimum eruption rate of about 3×10^8 kg s^{-1}. Therefore although capable of forming on Mars, sinuous rilles and associated source depressions would require very high eruption rates and sustained eruptions. Even if the small hot ponds associated with such events are not sustained at high enough rates or sufficiently long to cause thermal erosion, they may have an influence on the nature of the eruption products. For example, for a fixed gas content, if an initially very high mass flux at a vent is reduced to levels below those at which thermal erosion will take place, there will still remain a hot pond of lava up to many hundreds of meters wide surrounding the vent. If this pond continues to be fed by pyroclasts, there will be significant cooling of the pyroclasts in flight. As rootless flows develop, by overflow of the pond and incorporation of falling pyroclasts, into larger flows, their temperatures upon leaving the pond area may be substantially less than those of the pyroclasts leaving the vent. This secondary cooling phenomenon could mean that large-volume flows leaving the vicinity of pyroclastic-fed lava ponds such as these would be characterized by lower initial and subsequent flow temperatures. This could influence the interpretation of their morphology and rheology, perhaps leading to the interpretation that they were less mafic (e.g., more andesitic than basaltic) than they actually were.

4.5.3. Building of edifices. In Martian basaltic eruptions with effusion rates less than about 10^6 kg s^{-1}, Figure 15*d* shows that coalescence of hot pyroclasts could not take place. Instead, a scoria cone would be formed around the vent [*McGetchin et al.*, 1974]. For magma gas contents in the range 0.03 to 0.3 wt %, the widths of the cones which can be produced lie in the range 100 m to 10 km (Figures 15*d* and 16*a*). For two eruptions with comparable gas contents on Mars and Earth, the Martian cones should have diameters that are about a factor of 2 larger and heights that are correspondingly about a factor of 4 smaller than on Earth. Central craters in these edifices should also be broader than on Earth by a factor of up to at least 5, partly because of the wider dispersal of the pyroclasts and partly because of the greater lateral expansion, just above the vent, of the gas phase as it decompresses to the lower atmospheric pressure. Cone diameter/crater diameter ratios should be smaller on Mars than on Earth, since the vent width increase outweighs the overall clast dispersal increase. Grain sizes in Martian hawaiian edifices should be at least 1 order of magnitude finer than in terrestrial equivalents because of the enhanced magma fragmentation on Mars discussed earlier.

4.5.4. Comparison to observations: Cones and edifices. Five candidate cinder cones have been identified near the summit of Pavonis Mons [*Wood*, 1979; *Edgett*, 1990] and all are within 5 km of the inner caldera rim. Such conelike structures are apparently absent on other Tharsis Montes. The most prominent of the Pavonis cones has a basal diameter of ~1.1 km, a crater diameter of ~0.45 km, and a height of ~0.07 km, and plots in the general cinder cone field of *Wood* [1979]. Candidate cinder cones have been identified within Ulysses Patera (Figure 17), near Elysium Mons [*McBride and Zimbelman*, 1989, 1990], and elsewhere [*Scott*, 1982; *Davis and Tanaka*, 1988]. *Lucchitta* [1987, 1990] has interpreted dark interior deposits in central Valles Marineris, typically occurring along faults, to be of pyroclastic origin and has identified locally numerous features that she interprets to be cinder cones [*Lucchitta*, 1990, Figure 6c]. On the basis of stratigraphic relations, these latter features may repre-

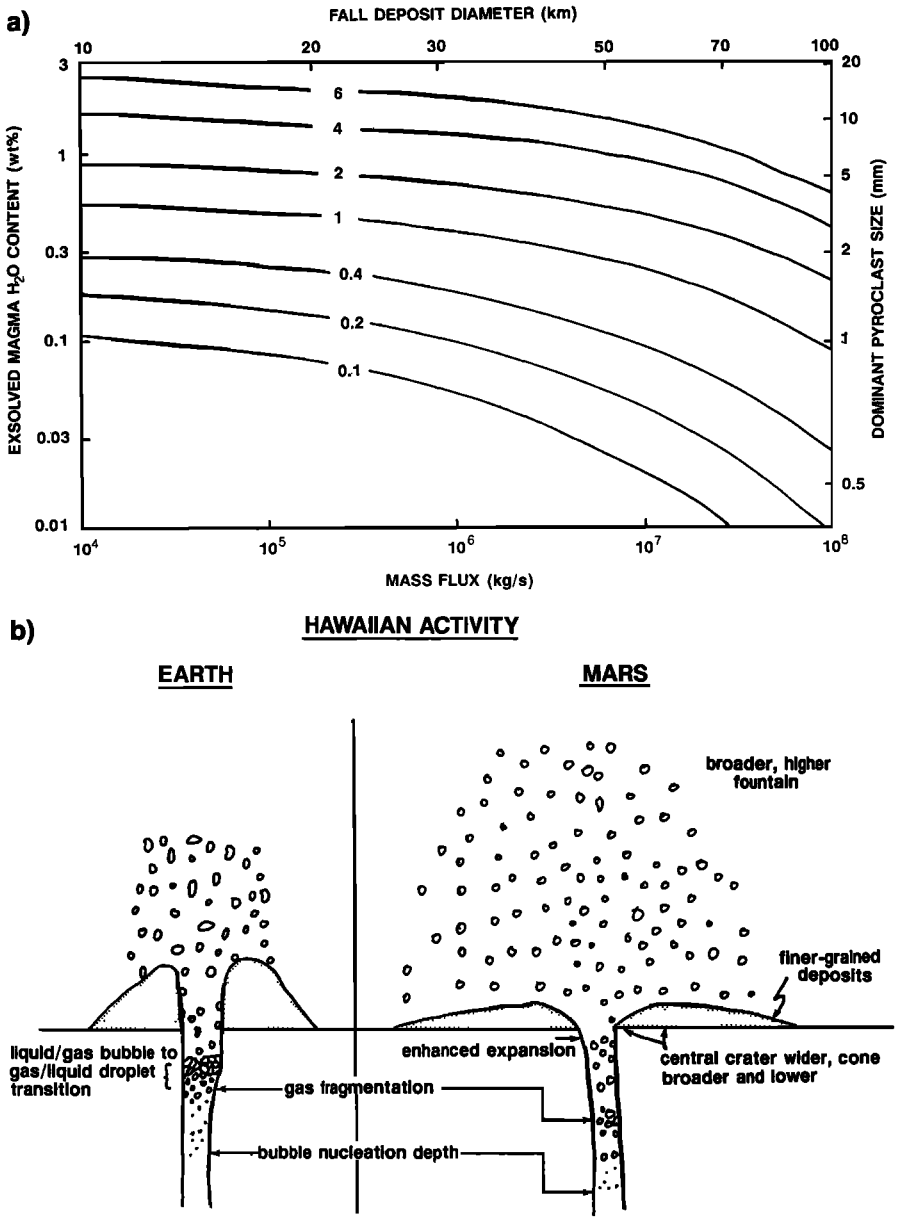

Figure 16. Hawaiian eruptions on Mars. (*a*) Fall deposit diameter as a function of exsolved gas content and mass flux. Contours are basaltic scoria cone diameters in kilometers. (*b*) Sketch illustrating the major features of hawaiian eruptions on Mars, with a comparison to Earth.

sent some of the youngest volcanism on Mars. All of these features identified in the literature are generally within the range of values suggested by the theoretical predictions for edifices produced by hawaiian eruptions, although there is virtually no data on cone heights. In an analysis of cinder cones on Earth, the Moon, and Mars, *Wood* [1979] concluded that for a given ejecta volume, Martian cinder cones have greater diameters and, on the basis of the one available measurement of cone height, that they might be only about one third as high as terrestrial cones.

On the basis of theoretical predictions, cinder cones should be relatively common occurrences and accompany many volcanic eruptions on Mars, particularly those forming the multitide of flows associated with the major edifices. The absence of high-resolution images may be one factor in the lack of detection of widespread cinder cones. However, there are several other factors that might also contribute to the paucity of documented cinder cones. First, cinder cones are predicted to be broader and flatter on Mars and thus less easily recognizable and distinguishable from small shields of effusive origin. Indeed, cinder cones averaging a factor of 2 broader and a factor of 4 lower than typical on Earth will not only be harder to detect, but will be much more readily covered by subsequent flows. Second, because of the enhanced magma fragmentation on Mars, typical grain sizes in Martian hawaiian edifices should be at least 1 order of magnitude finer than on Earth, and this will result in pyroclastic material that is very susceptible to eolian erosion. These factors, coupled with an altitude effect on the major shields that would preferentially enhance dis-

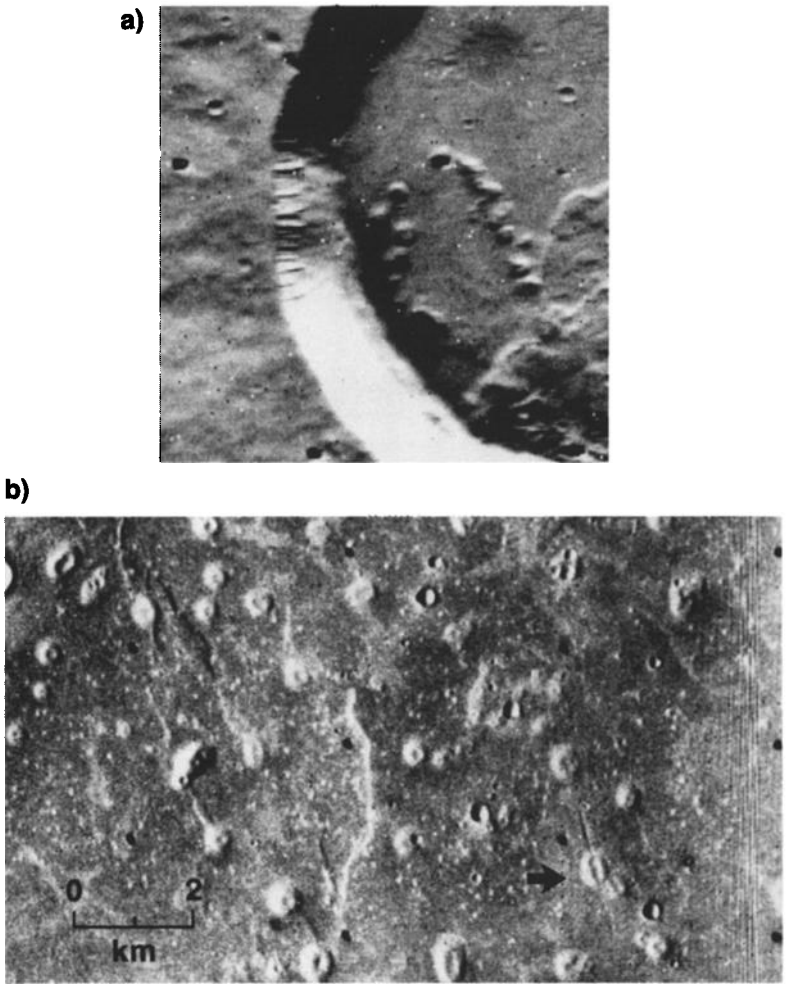

Figure 17. Examples of features interpreted to be products of hawaiian eruptions. (*a*) Features within the summit caldera of Ulysses Patera interpreted to be cinder cones (portion of VO 49B85; the width of the image is about 36 km). (*b*) Pitted cones in southern Cydonia. Although interpreted to be pseudocraters by *Frey and Jarosewich* [1982], these features generally fit the morphometric characteristics predicted for Martian cinder cones. Note the elongation and alignment of cones and summit craters, and the parallelism to fractures in the eastern part of the image (dark arrow) (portion of VO 070A04).

ruption and dispersal, may be responsible for the apparent paucity of cinder cones.

Despite this apparent general paucity, fields of small pitted domes and cones have been mapped locally in several places in the northern plains on Mars [*Frey et al.*, 1979]. There are two types of features in these fields [*Frey and Jarosewich*, 1982]: (1) small, less than 1 km diameter with summit pits that are larger relative to their basal diameters than terrestrial cones and (2) large, typically 2–5 km diameter (Figure 17). *Frey and Jarosewich* [1982] interpreted the smaller features as pseudocraters, because the cone/crater diameter ratios were similar to those of pseudocraters on Earth, even though terrestrial pseudocraters were three times smaller. The larger cones clearly fall in the range predicted for Martian cinder cones. Indeed, even the smaller cones could be cinder cones rather than pseudocraters, because their cone/crater diameter ratios are larger than those of terrestrial cinder cones and are more in the range predicted for Martian cones.

4.5.5. Comparison to observations: Sinuous rilles and source depressions. One problem in the analysis of sinuous rilles on Mars is the difficulty in distinguishing them from the ubiquitous channels thought to be linked to an aqueous origin and the possibility that any thermal erosion may be enhanced by a substrate containing water/ice and susceptible to mechanical erosion. *Carr* [1974] and *Mouginis-Mark et al.* [1984] described several candidates, particularly in the Elysium region. Figure 18 shows some possible examples of Martian sinuous rilles; the size of the largest requires eruption rates up to about 10^8 kg s^{-1}. This is comparable to the largest eruption rate yet deduced for a terrestrial basaltic eruption: the 1886 eruption of Tarawera in New Zealand seems to have had a total output rate [*Walker et al.*, 1984] of 1.6×10^8 kg s^{-1} (from an elongate fissure). However, the depths of the Martian sinuous rille channels would imply that the durations of the eruptions which formed them were very much greater than the durations of any terrestrial eruptions with comparable eruption rates. Although such eruptions are possible, the image resolution at present is insufficient to distinguish the morphology and morphometry of these deposits with enough confidence to permit a detailed quantitative treatment.

4.6. Plinian Eruptions

4.6.1. Background and predictions. Plinian eruptions occur in any magma type as long as most of the

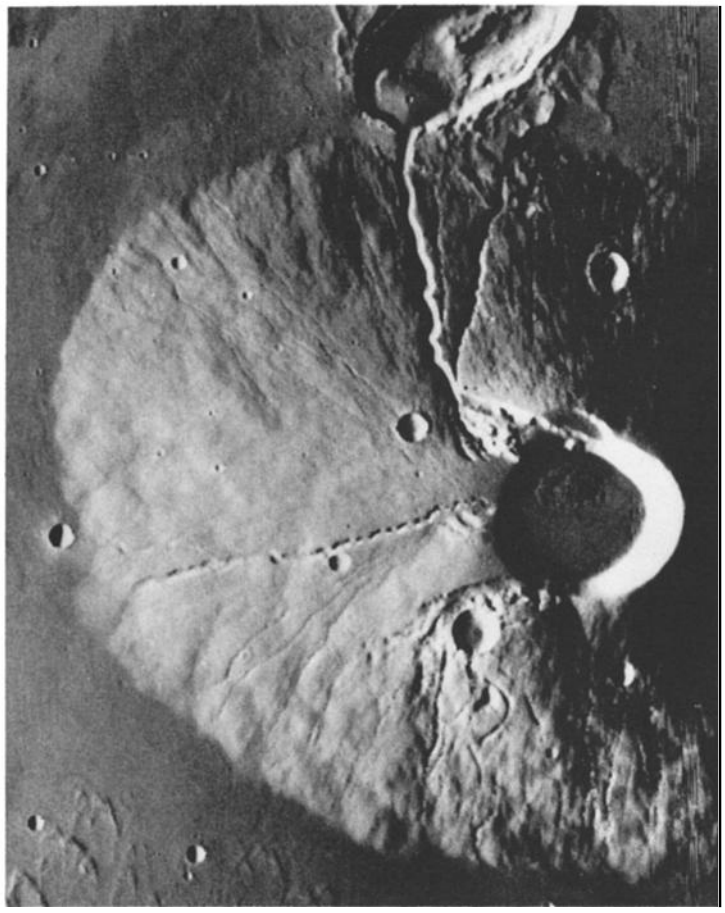

Figure 18. A feature described by *Carr* [1974] as a candidate sinuous rille formed by thermal erosion on Mars. The channel originates at the summit caldera of Ceranius Tholus in the Tharsis region and extends north (toward the top of the image) down the flank of the volcano (portion of VO 516A24; the width of the image is about 100 km).

magma disrupts into clots so small that they are effectively locked by drag forces to the gas stream emerging from the vent. Provided the bulk density of the eruption products becomes less than the density of the atmosphere as a result of the incorporation and heating of atmospheric gases, essentially all of the eruption products ascend into an eruption cloud over the vent (Figure 4). Small pyroclasts can transfer heat efficiently to the atmospheric gases entrained dynamically into the eruption cloud and thus maximize the buoyant convection of the cloud into the atmosphere [*Wilson*, 1976]. In cases where the bulk density of the eruption products is much greater than the atmospheric density, insufficient atmospheric gas is entrained and heated to overcome the effects of gravity, and the erupted mixture collapses back to the surface to form pyroclastic flows [*Sparks and Wilson*, 1976]; these cases will be discussed later.

As a basis for our predictions about plinian fall deposits we use Figure 19, which shows the results of calculations using the methods of *Wilson et al.* [1980] and *Wilson and Head* [1981*a*] of the eruption speed from a central vent of a stream of magmatic gas and all pyroclasts small enough to have a negligible terminal velocity in the gas. The speed is given as a function of the exsolved magma gas content and the magma mass flux for eruptions of highly fragmented magma with H_2O or CO_2 as the major volatile. For comparison, the equivalent information is given for the Earth. The magma is assumed to be a basalt, but the numerical results are very similar even if a rhyolitic composition is used [*Wilson*, 1980], because the rapid acceleration of the spray of pyroclasts and released gas above the fragmentation level is essentially independent of the viscosity of the magmatic liquid (which does, however, critically control the magma rise speed below the fragmentation level). The eruption velocities depend significantly on the magma mass eruption rate as well as on the volatile content, because the mass flux is an indirect measure of the width of the conduit/fissure system below the vent and frictional effects increase with decreasing conduit width [*Wilson et al.*, 1980].

On the right-hand sides of the graphs in Figure 19 are shown the sizes of the largest clasts with density 1000 kg m^{-3} which can be transported out of the vent under steady conditions at the eruption velocities given on the left-hand sides of the graphs. Eruption velocities are typically 1.5 times larger on Mars than on Earth for the same mass eruption rate and volatile content, but the lower atmospheric pressure causes the density of the erupted gas to be typically 300 times lower, and so the largest clast size transported, essentially proportional to (gas density × gas velocity^2) [*Wilson*, 1976], is about 150 times smaller on Mars.

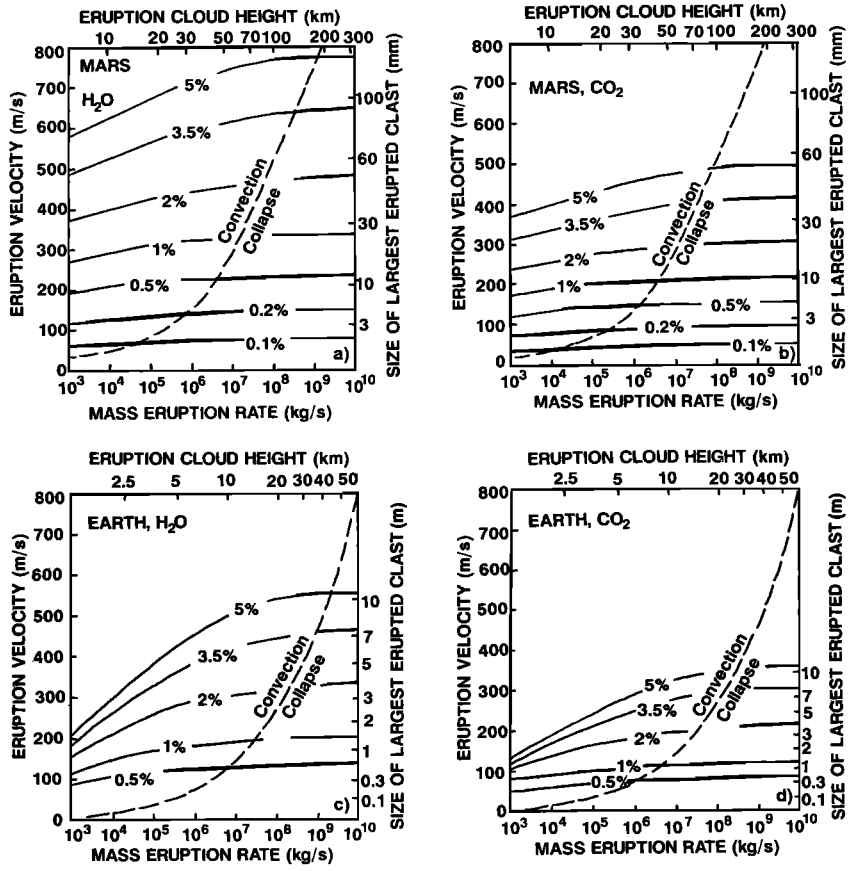

Figure 19. Eruption velocity of magmatic gas and pyroclasts from a vent as a function of mass eruption rate. Velocity is given as a function of exsolved magma gas content for H_2O and CO_2 for both Earth and Mars. The sizes of the largest clasts with density 1000 kg m^{-3} which can be transported out of the vent under steady conditions are shown along the right-hand axis. The dashed line separates convective behavior from column collapse. Eruption cloud height is shown along the top in each case.

This could, in principle, lead to more frequent episodes of vent clogging, pressure buildup, and abrupt vent clearing [*Wilson et al.*, 1980] in Martian plinian eruptions, but we expect that the increased magma fragmentation due to the lower atmospheric pressure will completely compensate for this. The net consequence of the lower atmospheric pressure therefore is that Martian plinian deposits (of any magma composition) will be systematically finer grained than plinian fall deposits on Earth by a factor of about 100. They will be almost entirely subcentimeter in size, except within a few hundred meters of their vents, and even there, clasts coarser than several centimeters should be rare.

An interesting consequence of these conditions is that basaltic plinian eruptions, rare on Earth, should be relatively common on Mars. The combination of the lower atmospheric pressure causing systematically finer grained pyroclasts and the rapid acceleration of the spray of pyroclasts and released gas above the fragmentation level (essentially independent of the viscosity of the magmatic liquid) would encourage many basaltic eruptions that would be hawaiian on Earth to be plinian on Mars.

Observations of plinian eruption clouds on Earth confirm theoretical model predictions that the height of a convecting eruption cloud formed in a high-speed pyroclastic eruption is proportional to the fourth root of the heat release rate from the vent [*Wilson et al.*, 1978; *Settle*, 1978], which is in turn proportional to the mass eruption rate. The top lines of the graphs of Figure 19 give the eruption cloud heights expected for the mass eruption rates indicated on the bottom lines. These calculations indicate that differences in the atmospheric pressure and temperature structure cause Martian plinian eruption clouds to rise about 5 times higher, for the same eruption rate, than terrestrial clouds (Figure 20).

The cross-sectional shapes of plinian eruption clouds on Earth are such [*Carey and Sparks*, 1986; *Wilson and Walker*, 1987] that the widths, measured 10 to 20 km downwind from the vent, of the air fall deposits produced by them are approximately equal to the heights of the associated eruption clouds [*Wilson*, 1978]. Essentially, the same relative shapes of eruption clouds are expected on Mars as on Earth and so the cloud-height/deposit-width relationship should also be similar. This implies that Martian fall deposits may be recognized as areas of mantled topography with widths in the range of several tens to a few hundred kilometers (Figure 20).

Mouginis-Mark et al. [1988] have given examples of the downwind transport distances expected for pyroclasts released from Martian plinian eruption clouds into a horizontal wind profile with a mean speed of 20 m s^{-1}, a value about twice as large as the mean surface wind [*Settle*, 1979]. We have used the same eruption cloud model (modified to the Martian atmospheric

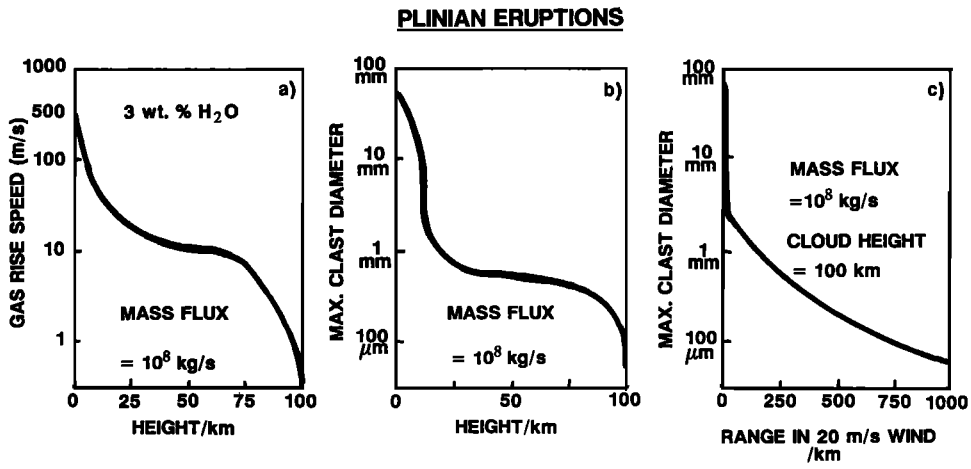

Figure 20. Plinian eruption columns and their behavior on Mars. (*a*) Gas rise speed versus eruption column height. (*b*) Maximum clast diameter versus eruption column height. (*c*) Maximum clast diameter versus range in kilometers for a 100-km-high cloud and 20 m s^{-1} wind.

environment from that used by *Wilson and Walker* [1987]) to calculate the maximum ranges expected for pyroclasts of various sizes released into a 20 m s^{-1} wind as a function of the eruption cloud height (and hence mass eruption rate) (Figure 21). The curves in this figure give an indication of the progressively finer maximum grain size which is to be expected in the distal parts of these deposits and indicate that fall deposits should extend roughly 5 times further downwind than they do at right angles to the ambient wind direction during the eruption.

It is commonly the case on Earth that the near-vent parts of plinian deposits are obliterated by caldera collapse events following, or during the latter parts of, the eruption. Similar events may occur on Mars. However, for cases where the vent regions are preserved, we give examples (Table 6) of the diameters expected for the main zones of accumulation of coarse pyroclasts around plinian vents on Mars and Earth (Figure 20). In cases where the emerging magmatic gas has decompressed to the local atmospheric pressure, this diameter will be essentially equal to that of the vent. However, in other cases the gas stream can be overpressured and the flow choked [*Kieffer*, 1984; *Wilson and Head*, 1981*a*]; when this occurs, the vent will be narrower than the diameter given, but the gas stream will rapidly expand laterally through a series of shocks over the vent, and most of the clast deposition will occur when the base of the eruption cloud has expanded to the size shown in Table 6.

4.6.2. Comparison to observations. Only one example of an air fall deposit on Mars has so far been identified and analyzed in detail [*Mouginis-Mark et al.*, 1982]: a mantled zone to the west of the summit caldera complex of Hecates Tholus (Figure 22). This deposit was recognized as a result of its obscuring effect on the background of small (500 m diameter)

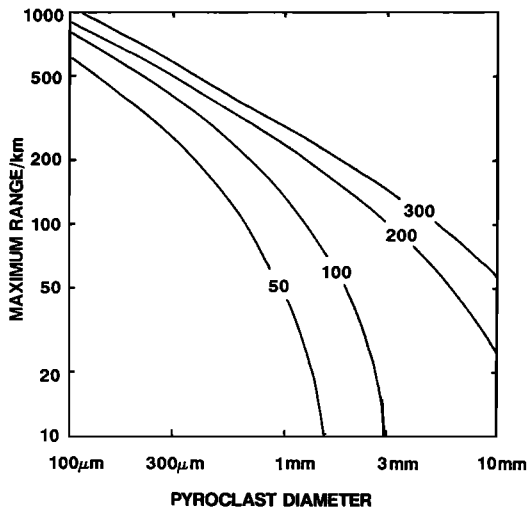

Figure 21. Maximum range expected for pyroclasts erupted into a 20 m s^{-1} wind for several values (in kilometers) of eruption cloud height.

TABLE 6. Plinian Vent Structure Diameters on Mars and Earth

Magma Volatile Content, wt %	*Mass Flux, kg s^{-1}*			
	10^4	10^6	10^8	10^{10}
		Mars		
0.1	4.14	35.0	340	3310
0.3	4.72	45.8	440	4360
1	7.20	61.0	592	5888
3	10.10	84.0	780	7750
10	12.82	109.0	1050	10,470
		Earth		
0.1	1.56	13.3	130	1268
0.3	1.68	15.8	154	1536
1	2.33	19.8	193	1880
3	2.97	24.6	229	2261
10	3.69	31.3	299	2974

Values are given in meters for various combinations of eruption mass flux and magma volatile (H_2O) content.

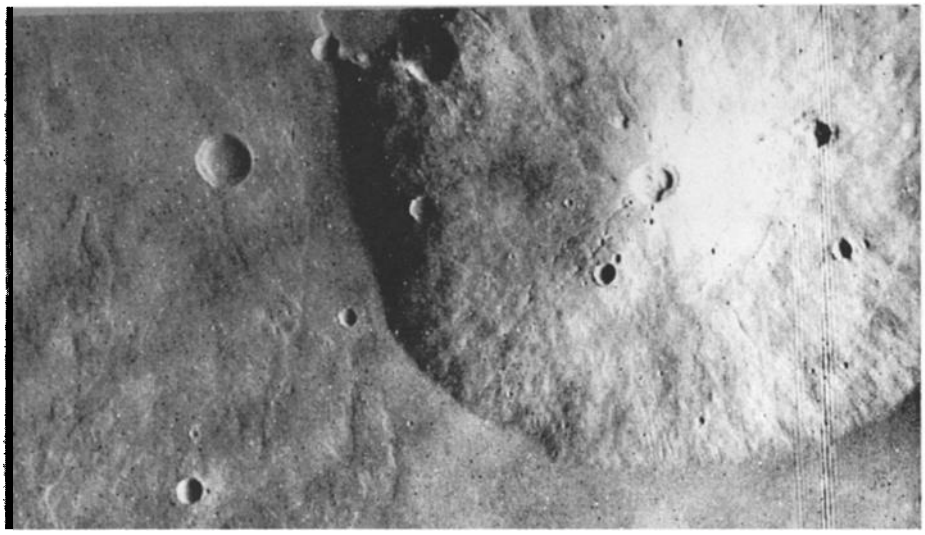

Figure 22. Hecates Tholus. The western flank, between the summit and the base, is relatively deficient in craters and has been interpreted to be the location of plinian eruption deposits [*Mouginis-Mark et al.*, 1982] (portion of VO 846A16; the width of the image is about 210 km).

impact craters in the area. It was assumed that a minimum deposit thickness of ~100 m was needed to obscure craters of this size. Combined with the deposit area of ~2000 km^2 and a bulk density estimate of 1000 kg m^{-2}, this led to a volume estimate of about 23 km^3 of dense rock equivalent, erupted at a rate (estimated from the deposit-width/cloud-height/eruption-rate correlations discussed earlier) of the order of 10^7 kg s^{-1}. We note that if this volume had been erupted at a much higher rate, say 10^9 kg s^{-1}, it would have covered an area about 200 km wide and at least 800 km long to a mean depth of 0.4 m. Clearly, a much larger volume could be erupted under such conditions without leading to significant obscuration of underlying features: even a volume of 2000 km^3 dense rock equivalent would only lead to a mean layer thickness of 35 m. It seems quite possible, therefore, that many air fall deposits on Mars may have gone unrecognized if they were produced at relatively high eruption rates and/or involved relatively small magma volumes. This, combined with the ease of erosion of such deposits in the Martian environment, may explain the paucity of readily identifiable plinian air fall deposits on Mars. In addition, air fall deposits are very likely to have accompanied eruptions associated with extensive pyroclastic deposits at Tyrrhena Patera [*Greeley and Crown*, 1990], Hadriaca Patera [*Crown and Greeley*, 1993], Alba Patera [*Mouginis-Mark et al.*, 1988], and possibly, Apollinaris Patera [*Robinson et al.*, 1993]. On the basis of the great lateral extent of the deposits associated with these volcanoes (several hundreds of kilometers), it is unlikely that the longest ones represent air fall deposits because of the extremely high eruption clouds required. The most extensive deposits are thought to be more likely emplaced as pyroclastic flows [*Reimers and Komar*, 1979; *Mouginis-Mark et al.*, 1988; *Greeley and Crown*, 1990; *Crown and Greeley*, 1993]. *Scott and Tanaka* [1982] postulated that the extensive friable deposits south of Olympus Mons and the Medusae Fossae formation are ignimbrites.

4.7. Pyroclastic Flow Formation

4.7.1. Background and theory. For all plausible magma volatile contents, the bulk density of the gas/pyroclast mixture emerging from a vent will be denser than that of the surrounding atmosphere [*Sparks et al.*, 1978]. Specifically, the exsolved gas content would have to be greater than about 16 wt % to make the densities comparable. In a density-stratified atmosphere, such as that of both Mars and Earth, an eruption cloud can only convect in a stable manner if sufficient atmospheric gas is incorporated into the lower part of the cloud and heated by the entrained pyroclasts to provide enough positive buoyancy to overcome the negative buoyancy of the eruption products. Furthermore, this entrainment must occur before the negative buoyancy causes the upward velocity to decay to a negligible value. This is only possible if the magma volatile content is sufficiently large or the mass eruption rate sufficiently small, and the critical volatile content for any given eruption rate can be calculated using methods given by *Sparks et al.* [1978] and *Wilson and Walker* [1987].

The dashed line on each graph of Figure 19 defines this boundary between eruption conditions under which convecting plinian clouds are stable (to the left of the line) and those under which the erupting mixture must, instead, form a much lower, denser fountain over the vent feeding either pyroclastic flows (if clasts are relatively cool and brittle on landing) or lava flows (if clasts can coalesce on landing). Pyroclastic flow formation is clearly inherently more likely to occur on Mars than on Earth, since eruption cloud instability occurs at a lower mass eruption rate for a given magma volatile content (Figure 19).

On Earth, both plinian ash fall activity and pyroclastic flow formation are mainly associated with silicic magmas, essentially because of their tendency, driven by their rheological response to water exsolution, to fragment into fine-grained clasts when explo-

sively disrupted. In the plinian mode this causes most of the magmatic clast size distribution to remain locked to the erupted gases long enough to be entrained into the vigorously convecting eruption cloud; the coarser-grained clasts formed in mafic eruptions, by contrast, largely avoid entrainment into an eruption cloud and form a near-ballistic lava fountain over the vent. In the ignimbrite mode at high mass eruption rates, where the gas/clast mixture collapses back to the ground near the vent, the rheology of silicic magmas minimizes clast coalescence. We have argued in section 2.5 that magma fragmentation should be more thorough on Mars than on Earth, and this should certainly lead to the relatively more common occurrence of mafic plinian deposits. The calculations summarized in Figure 19 show that for a given initial magma volatile content, eruption speeds are a factor of at least 1.5 higher on Mars, and so the fountains feeding pyroclastic flows will be rather more than twice as high as on Earth, the rise height being proportional to the square of the eruption speed [*Wilson and Heslop*, 1990]. The travel times of the materials in the outer parts of these fountains will be correspondingly 1.5 times longer than on Earth, and so, in terms of both time and distance, there will be a greater opportunity for mixing with the surrounding atmosphere and significant cooling of pyroclasts. Although hard to quantify without detailed numerical models (which have so far only been applied to terrestrial conditions [e.g., *Valentine and Wohletz*, 1989]), these facts suggest that basaltic pyroclastic flow deposits, as opposed to welded spatter deposits or rheomorphic (rootless) lava flows, should be significantly more common products of high mass flux basaltic eruptions on Mars than on Earth.

It is not easy to predict the distances to which pyroclastic flows may travel on Mars: the run-out process is not very well understood on the Earth as a result of uncertainties about the rheological properties of pyroclastic flows [*Hayashi and Self*, 1992]. However, energy conservation arguments [*Sheridan*, 1979, 1980; *Malin and Sheridan*, 1982] suggest that the final travel distance should be proportional to the square of the eruption velocity in the vent. The calculations summarized in Figure 19 show that for a given initial magma volatile content, eruption speeds are typically a factor of at least 1.5 greater on Mars than Earth, and so pyroclastic flow travel distances may be a factor of about 3 greater, leading to values up to at least a few hundred kilometers (Figure 23). *Crown and Greeley* [1993] calculated some explicit examples of run-out distances for a wide range of assumed initial velocities (all of the velocities being consistent with the range of magma gas contents shown in Figure 19). They assumed values for the basal friction coefficients for their flows of 0.05 and 0.10, somewhat less than the range (0.06 to 0.2) deduced for large-volume pyroclastic flows on Earth [*Sheridan*, 1979] on the grounds that

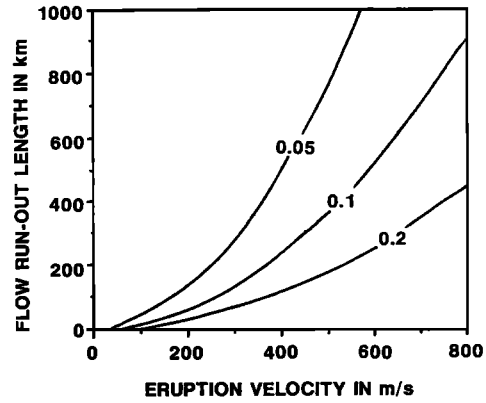

Figure 23. Distances to which pyroclastic flows will travel on Mars. Eruption velocity versus flow run-out length in kilometers for several values of the coefficient of friction. Most Martian pyroclastic flows would fall between the 0.05 and 0.1 curves.

particle/particle frictional interactions should be weaker on Mars due to the lower gravity. They found that run-out distances exceeding 1000 km were possible given favorable circumstances. Figure 23 summarizes examples of these calculations for flows traveling down a shallow incline (slope 0.3°) away from a vent for three values of the friction coefficient, 0.05, 0.1, and 0.2. Martian pyroclastic flow lengths are expected to be bracketed by the lines labeled 0.05 and 0.1; travel distances would be significantly greater on steeper substrate slopes.

Recent work on the fluid dynamics of the gas/pyroclast fountains which feed ignimbrites [*Heslop and Wilson*, 1988; *Wilson and Heslop*, 1990] has made it possible to estimate the maximum sizes of clasts which can be ejected from vents on Mars to form near-vent lag breccia deposits. The maximum clast size is found to be a function only of the exsolved magma volatile content. Because the erupted mass flux must exceed some minimum value for any given exsolved magma volatile content before an ignimbrite-forming eruption can occur, it follows that pairs of values of maximum clast size and minimum vent diameter can be calculated for a series of values of exsolved volatile content.

Table 7 shows some examples for Mars and the Earth. These indicate that fluid dynamic support for clasts would allow much larger clasts (by a factor of about 4) to be ejected from vents on Mars than on Earth. However, these potential clast sizes are so large that in practice, it is the size of the vent which acts as the limit on Mars. As a result, the maximum sizes of clasts expected in lag deposits on Mars are only up to twice those of terrestrial counterparts; diameters of about 20 to 60 m are possible for lithic clasts if exsolved magma volatile contents lie in the range 1 to 3 wt %. In lag deposits, such clasts would be embedded in the vastly finer grained matrix formed by the juvenile pyroclasts but, if partly exhumed by aeo-

TABLE 7. Properties of Ignimbrite Eruptions on Mars and Earth

n, wt %	n_b, wt %	n_r, wt %	P_v, MPa	U_v, m s^{-1}	D_m, m	D_e, m	V_m, m	V_e, m
1.0	1.17	1.57	1.93	89.4	43	10	22	34
2.0	2.28	2.81	3.91	126.4	109	28	34	81
3.0	3.37	4.00	5.93	154.8	187	51	57	132
4.0	4.46	5.16	7.99	178.7	279	79	98	179
5.0	5.54	6.31	10.08	199.8	378	110	174	215

Note that n is the exsolved magmatic water content; n_b and n_r are the implied total amounts of water in a basalt or rhyolite melt, respectively; P_v is the gas pressure in the vent; U_v is the upward speed of the gas-pyroclast mixture in the vent; D_m and D_e are the diameters of the largest supported clasts with density 2500 kg m^{-3} in the vent on Mars and Earth; V_m and V_e are the minimum vent diameter to allow an ignimbrite eruption to occur for the given magma gas content.

lian erosion, should be readily visible in suitably targeted high-resolution imaging frames of future missions.

4.7.2. Comparison to observations. *Greeley and Crown* [1990] have identified candidate pyroclastic flow deposits at Tyrrhena Patera. Although no specific flow morphology can be seen, the deposit morphology, extent, and erosional characteristics, together with the general characteristics of the edifice, are consistent with an origin by the emplacement of gravity-driven ash flows generated by magmatic or hydromagmatic explosive eruptions. *Greeley and Crown* [1990] calculated initial pyroclastic flow velocities of ~400–650 m s^{-1} (depending on the coefficient of friction) for the basal smooth plains unit that extends more than 600 km from the summit area. Other less extensive deposits were interpreted to have initial velocities in the range of ~150–450 m s^{-1}, values which are in the range of those observed [*Nairn and Self*, 1978] and predicted by theory [*Sparks and Wilson*, 1976] on Earth. In a similar analysis of Hadriaca Patera, whose deposits extend for more than 400 km, *Crown and Greeley* [1993] calculated comparable initial pyroclastic flow velocities. Thus these deposits are consistent with the theoretical predictions of pyroclastic flows extending further on Mars than on Earth for comparable conditions and extending out for distances of at least several hundred kilometers.

On the basis of spectral reflectance data, erosional morphology, and a tendency for eolian mobilization, *Geissler et al.* [1990] interpreted wall rock layers in Coprates Chasma to be composed of mafic glass and to represent an areally extensive and thick layer of mafic volcanic ash. No source vents are known.

4.8. Pelean and Vulcanian Eruptions

4.8.1. Background and theory. As outlined above, ejected country rock fragments and dense eruption clouds of gas and fine magmatic pyroclasts produced by these two eruption styles will reach essentially the same velocities on Mars and Earth, since they are driven by the near-adiabatic expansion of trapped gases decompressing from pressure levels controlled mainly by rock strengths, which will be similar (up to ~10 MPa) on the two planets. In pelean explosions (Figure 4) driven solely by magmatic volatiles, the velocities of juvenile pyroclasts will be limited to about 300 m s^{-1} (Figure 24).

In vulcanian events (Figure 4) where the mass fraction of incorporated volatiles may greatly exceed magmatic levels, gas velocities approaching 1 km s^{-1} are just possible [*Wilson*, 1980], with some clasts acquiring a substantial fraction of the gas velocity (Figure 25). Large (> meter size) clasts ejected at 300 m s^{-1} on Mars could have ballistic ranges exceeding 20 km from the vent; however, atmospheric drag forces will greatly restrict the ranges of smaller clasts of all types [*Wilson*, 1972].

The rise heights and widths of convecting eruption clouds from both of these explosion types should be much greater (by a factor of about 5 for the reasons given earlier for plinian eruption clouds) than for corresponding terrestrial events, and the dispersion of pyroclasts of a given size and density from the clouds will be somewhat greater (by a factor of about 3). The expansion geometry of the eruption clouds formed in discrete explosions (more nearly radial than in steady eruptions [*Nairn*, 1976]) is likely to be such that the incorporation of atmospheric gases is less than in, for example, plinian events. Since the bulk density of the

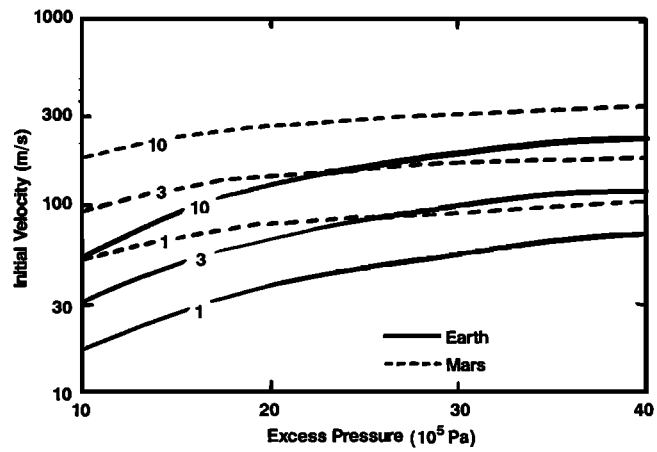

Figure 24. Pelean explosions on Mars and the Earth showing excess pressure versus initial velocity. Curves are labeled by weight percent H_2O in the eruption products.

eruption products from a pelean explosion driven by magmatic volatiles is always likely to be greater than that of the surrounding atmosphere (irrespective of the atmospheric pressure [*Sparks and Wilson*, 1976]), pyroclastic flows and/or surges (nuees ardentes) should be formed very commonly from Martian pelean eruption clouds. Small flows and surges may also form in Martian vulcanian events by the partial collapse of the eruption cloud, much as occurs on Earth [*Nairn and Self*, 1978]. Since the initial velocities of these flows will be similar on Mars and Earth, their run-out distances should also be similar, typically a few to several tens of kilometers.

4.8.2. Comparison to observations. No specific examples of pelean eruption deposits on Mars have been cited in the literature, but this is not surprising because of the strong likelihood that such deposits will be highly modified by eolian erosion or, if preserved, not easily distinguished from other flow deposits at resolutions presently available. In addition, the conditions under which such eruptions occur on Earth (viscous extrusion of low-rise speed magma forming a dome with a cooled carapace which ultimately fails, thus causing the eruption) are likely to be less common on Mars, because lower atmospheric pressure causes more significant gas exsolution, higher rise speeds near the surface, more efficient magma disruption, and systematically finer grained pyroclasts. All of these factors mean that domes produced by such conditions are highly unlikely to occur on Mars, in contrast to the Earth [*Williams*, 1932] and Venus [*Pavri et al.*, 1992] where surface atmospheric pressure is considerably higher. No specific examples of such domes on Mars have been reported in the literature.

Vulcanian eruption deposits are also not specifically identified in the literature. However, *Lucchitta* [1987, 1990] has identified dark patches typically occurring along faults on the floor of Valles Marineris and has interpreted these to be of pyroclastic origin. Although not specifically interpreted as such by *Lucchitta* [1987, 1990], these could be potential sites for vulcanian eruptions, if magma rising in dikes along major fault zones stalled, cooled, underwent volatile buildup, and then erupted.

4.9. Role of Permafrost and Groundwater in Eruption Dynamics

4.9.1. Background and theory. There is abundant evidence that permafrost and groundwater have existed in the upper crustal layers of Mars in its past history [e.g., *Carr*, 1987] (Figures 2 and 3) and that the interaction of intrusive and extrusive processes with these layers has had an important effect on near-surface processes. Magma rising to the surface may (1) stall at neutral buoyancy zones and produce large reservoirs, (2) be emplaced as a discrete dike or sill at shallow levels, and (3) continue to the surface to form

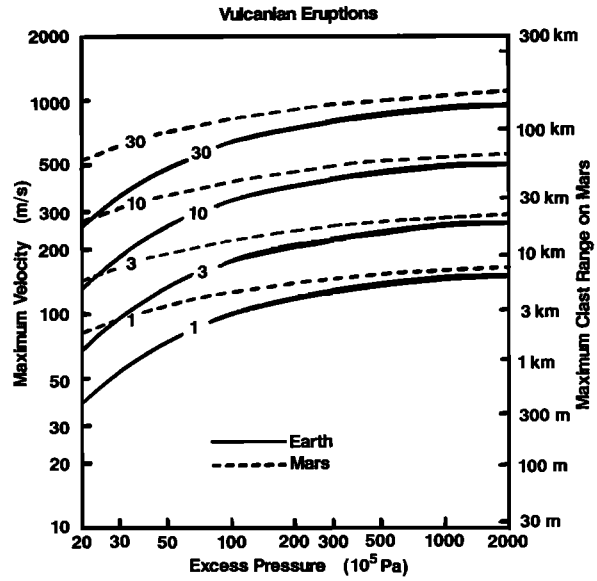

Figure 25. Vulcanian events on Mars and the Earth. Behavior of clasts in vulcanian eruptions showing the relationship between excess pressure and maximum velocity and maximum clast range. The contours are grain size.

a flow (Figure 3). In the first case, magmatic heat lost conductively from the reservoir can alter the local geothermal gradient, but not as efficiently as magma delivered in geometries with large surface areas/volumes, such as dikes and sills. Simple calculations show that a static reservoir of diameter 10 km emplaced at a depth of about 10 km will perturb the geotherms at the surface by up to about 10% within about 12 km of the area above the reservoir and that the reservoir will cool to ambient temperatures in about 1 million years. The early thermal pulse is sufficient to melt ground ice within a zone of about 25 km in diameter above the intrusion, and this might result in the formation of outflow channels and of collapse features above the intrusion.

Squyres et al. [1987] consider the thermodynamics of the interactions of volcanic intrusions (sills) and extrusions (flows) with ground ice, making quantitative estimates of the amounts and rates of liquid water and steam that might be generated or released under a variety of conditions. They then use these estimates to investigate the relation to the amount of ground subsidence predicted to occur and to compare these estimates to values inferred from fluvial channels and other features associated with volcanic complexes. The simpler case is the eruption of lava over ice-rich permafrost; as heat is conducted downward, two phase change boundaries exist, the melting front separating permafrost from wet soil and the vaporization front separating wet soil from soil plus steam. The bulk of heat is lost from the top of the flow (Figure 5), but for a 10-m-thick flow over a substrate that is 25% ice, the maximum depth of dehydration is 3.0 m beneath the base of flow, and the total amount of ice melted or

vaporized is equivalent to a column thickness of 3.7 m. As the lava flow thickness increases, the proportion of column that is only liquid increases because of the higher vaporization temperature. In general, under a variety of conditions, the total column thickness of melted water is less than half the lava flow thickness. Although not treated by *Squyres et al.* [1987], this same geometry can also lead to the explosive release of water vapor generated during substrate melting and to the disruption of the lava flow to cause rootless pyroclastic deposits and cones (pseudocraters) on the flow surface [*Thorarinsson*, 1953].

A more complex case is injection of a sill into ice-rich permafrost. The area below the sill is identical to the surface lava flow case, while in the area above the sill, the boundaries propagate upward and the water generated migrates downward and undergoes vaporization once it reaches regions where the temperature exceeds the boiling point. Therefore liquid water is only generated once the temperatures everywhere above the sill are less than the boiling temperature. Because of the lack of a "free" surface, cooling takes place much more slowly than for the flow case and significantly more liquid and vapor are generated by the sill. For a sill thickness of 10 m at a depth of 100 m in a substrate that is 25% ice, the thickness of the water column is substantially greater than the thickness of the sill, by a factor of about 2–4 (Figure 5). When the burial depth is less than approximately the sill thickness, considerable heat is lost to the surface, reducing the total column thickness. Thus sill injection into an ice-rich substrate can form net depressions (column height > sill thickness), while lava flows on the surface cannot (column height < flow thickness).

In summary, a wide diversity of interactions of igneous intrusions and volcanic extrusions with permafrost and groundwater are possible on Mars (Figure 3), and the predicted landforms include collapse depressions and outflow channels, dikes and sills possibly exhumed by erosion of surface layers, maars, and surface flows leading to melting of subsurface layers or formation of rootless explosion craters (pseudocraters).

4.9.2. Comparison to observations. Evidence for the surface effects of shallow intrusions abound on Mars. The origin and temporal relations of many of the outflow channels on Mars have been attributed to magmatic heat [e.g., *Carr*, 1979]. *Schultz and Glicken* [1979] suggested that many floor fractured craters may be the sites of sills and that there is evidence that these are also the locations of the release of groundwater. *Squyres et al.* [1987] outlined very good morphologic and stratigraphic evidence for a large flow lobe deposit in the Aeolis Mensae region of Elysium Planitia adjacent to a sill-like unit interleaved between friable deposits and now exposed by erosion. *Squyres et al.* [1987] also presented evidence for a possible lahar generated by intrusion of a sill and, just south of Hadriaca Patera, a series of channels and deposits interpreted to be generated by sill and flow emplacement. Surface lava flows can also lead to the formation of pseudocraters, and examples thus interpreted have been described by *Frey et al.* [1979] and *Frey and Jarosewich* [1982].

Tyrrhena Patera, a large low-relief volcano in the southern Martian highlands, has been interpreted to be the site of pyroclastic flow deposits possibly generated by hydromagmatic explosive eruptions involving water volumes of $\sim 7.5 \times 10^{16}$ kg and water flow rates of up to about 10^5–10^6 m^3 s^{-1} [*Greeley and Crown*, 1990]. Similar conditions are interpreted to have occurred at nearby Hadriaca Patera; the inferred high permeability of the crust of Mars apparently permitted large amounts of groundwater to be transported laterally into the region at flow rates estimated at 10^3–10^4 m^3 s^{-1} [*Crown and Greeley*, 1993] (labeled G in Figure 3a).

Maars are one distinctive type of volcanic landform that does not appear to be prominent on Mars. On Earth, maars are broad, low-rimmed volcanic craters that typically result from phreatic or phreatomagmatic eruptions. Maars form when rising magma interacts explosively with groundwater or surface water [*Lorenz*, 1973]. Maar deposits may contain little to no magmatic material (phreatic) or a mixture (phreatomagmatic), and they grade into tuff rings and tuff cones [*Cas and Wright*, 1987]. The lack of identification of abundant maars on Mars may be due to several factors, including similarity to degraded impact craters and erosion of fragmental and poorly welded deposits. One additional important factor, however, may be the lack of shallow groundwater and standing bodies of water over much of Martian history. If a cryosphere characterizes the upper several kilometers of the Martian crust [*Clifford*, 1993], then ascending magma will interact with ice, rather than groundwater, and this will considerably reduce the probability of phreatic or phreatomagmatic eruptions operating continuously enough to cause maars. However, earlier conditions on Mars may have differed, and maar deposits should be searched for wherever near-surface liquid water is suspected.

5. DISCUSSION AND CONCLUSIONS

On the basis of an assessment of the crustal configuration of Mars and a theoretical treatment of the ascent and eruption of magma through this crust in the Martian gravity and atmospheric environment, we find that the full range of volcanic eruption styles presently known on Earth is to be expected. It is clear, though, that Martian environmental conditions operate to modulate the various eruption styles and the morphology and morphometry of resulting landforms. Using these theoretical predictions as a basis, we compared observed deposits and landforms and find general agreement, as outlined above. We find that theory

provides new insight into several Martian volcanological problems. For example, the effects of gravity and cooling should cause compositionally similar cooling-limited flows on Mars to be about a factor of 6 longer than on Earth, thus providing a potential explanation for the flows several hundred kilometers long that build the major Martian edifices. Similarly, theoretical analysis of plinian air fall and pyroclastic flow emplacement provides a basis for distinguishing these types of deposits in Martian volcanoes, and analysis of the geologic record supports the view that both types of eruptions took place around several Martian volcanic centers. This analysis also provides some perspective on several other problems in Martian geology and history.

5.1. Changes in Volcanic Style in Space and Time

Variations in the areal distribution of volcanic styles have been observed on Mars, with effusive eruptions and shield building dominating the northern lowlands and explosive volcanic deposits of the paterae occurring predominantly in the southern highlands and circumbasin areas [e.g., *Greeley and Spudis*, 1981]. Our analyses underline the important influence of groundwater interactions, and one plausible interpretation of the areal differences in style is that they simply represent different crustal volatile reservoirs, with the cratered southern highlands megaregolith having a more extensive and readily replenished groundwater reservoir than the northern lowlands [*Clifford*, 1993]. Other possibilities include the role of crustal thickness and compositional variations and their influence in the development of neutral buoyancy zones, as on the Moon [*Head and Wilson*, 1992*a*], and areal variations in thermal structure [*Comer et al.*, 1985; *Solomon and Head*, 1990].

Variations in the style of volcanism with time have also been proposed, with early volcanism being characterized by more volatile-rich magma and later by volatile-depleted magma [*Francis and Wood*, 1982]. However, local depletion of groundwater reservoirs [e.g., *Greeley and Crown*, 1990; *Crown and Greeley*, 1993] seem to be at least as likely a candidate for these changes in time as are fundamental changes in the primary magmas. More detailed models of mantle depletion with time would be useful to make further progress in this area.

5.2. Changes in the Atmosphere With Time

Calculations of theoretical eruption conditions were carried out on the basis of present-day Martian atmospheric conditions, and workers basing interpretations of ancient deposits on these calculations should bear this in mind. Although there is some evidence that the Martian atmosphere has evolved with time from an early, warmer, wetter climate, many advocate models in which there has been very little change with time (see reviews by *Owen* [1992] and *Clifford* [1993]). A significant corrolary is that very large quantities of volatiles may have been injected into the atmosphere periodically by the explosive or hydromagmatic eruptions. *Robinson et al.* [1993] estimate that about 10^{15} kg of juvenile H_2O were emplaced into the Martian atmosphere during the formation of Apollinaris Patera, a quantity in excess of the current total atmospheric water budget. These and other magmatic gases would have considerable influence on the general trends of atmospheric evolution and on atmosphere-surface interactions. For example, water released into the Mars atmosphere by such eruptions will rapidly condense on the surface as ice; upon saturation, further contributions will eventually be cold-trapped at the poles [*Clifford*, 1993].

5.3. Compositional Interpretation of Volcanic Deposits

Remote sensing data and meteorites provide evidence for the composition of the Martian crust, but neither can be associated directly with individual lava flows or deposits. Thus morphology and morphometry of volcanic deposits have sometimes been used to interpret their composition. Our theoretical analysis shows that the influence of environmental conditions on eruption styles may be significant in the interpretation of composition. For example, extremely long lava flows are predicted to be primarily a consequence of Martian gravity and cooling conditions rather than viscosity and compositional factors. The production of large-scale plinian deposits may not signal the presence of more silicic compositions but, rather, may be linked to the enhanced gas exsolution and magma fragmentation of basaltic magma in the Martian environment or to the interaction of basaltic magma with groundwater. The lack of steep-sided domes potentially formed by viscous, more silicic magma cannot be cited as conclusive evidence for the absence of this composition, because enhanced magma disruption in the Martian environment may largely preclude the formation of this type of landform.

5.4. Contribution to Surface Sedimentary Deposits

Martian eruption conditions (low atmospheric pressure) favor significant gas exsolution, higher rise speeds near the surface, enhanced magma disruption, and systematically finer grained pyroclasts. These conditions mean that virtually every eruption of volatile-containing magma, regardless of composition, will be accompanied by a fine-grained pyroclastic deposit component. Many eruptions (e.g., the plinian style) will be responsible for the production of vast quantities of fine-grained tephra, the injection of it into the atmosphere, and the lateral emplacement of it for up to several hundreds of kilometers as air fall and pyroclastic flow deposits. Martian plinian deposits of any

magma composition will be systematically finer grained than plinian fall deposits on Earth by a factor of about 100. These same phenomena will favor the more common occurrence of basaltic plinian eruptions on Mars relative to the Earth. All of these factors mean that very fine grained volcanic ash should be extremely common and widespread and of a grain size susceptible to further eolian transport.

On Earth, volcanic eruption of basalt into an H_2O-rich environment or subsequent alteration of basaltic ash can produce palagonite, an amorphous ferric iron silica gel. The Martian environment, with its abundant evidence of the interaction of ascending magma and water (Figure 3), as well as the enhanced fragmentation of pyroclastic material, would favor the production of palagonite as a normal consequence of the eruption process and its aftermath. It is thus a completely logical consequence of the theoretical predictions outlined above that palagonites should be a volumetrically significant and widespread component of Martian surface material, a prediction consistent with the spectral reflectance studies of Martian bright soils and dust by *Allen et al.* [1981], *Singer* [1982], and *Roush* [1989] (see also *Soderblom* [1992] and *Murchie et al.* [1993]).

ACKNOWLEDGMENTS. We gratefully acknowledge the help of Peter Cattermole, Don Wilhelms, Gillian Thornhill, Larry Crumpler, and Jayne Aubele in providing reviews of earlier versions of this manuscript. Mike Carr and Jim Zimbelman provided formal reviews, Grant Garven provided a *Reviews of Geophysics* cross-disciplinary review, and Alan Chave, *Reviews of Geophysics* Editor-in-Chief, provided a thorough overview. Karen Plouff, Peter Neivert, and Mary Ellen Murphy provided essential help in manuscript preparation. We particularly thank Steve Benner, whose calmness and creativity in the face of rather unusual and somewhat artistic error messages insured the timely completion of the manuscript. This research was supported by National Aeronautics and Space Administration grant NAGW-2185 to J. W. H. and by the William F. Marlar Memorial Foundation. L. W. gratefully acknowledges partial support from the Royal Society through a Leverhulme Senior Research Fellowship.

Alan Chave was the editor responsible for this paper. He wants to thank Michael Carr and Jim Zimbelman for technical reviews, Grant Garven for a cross-disciplinary review, and Dan Davis for editorial advice.

REFERENCES

Adams, J. B., and T. B. McCord, Mars: Interpretation of spectral reflectivity of light and dark regions, *J. Geophys. Res.*, *74*, 4851–4856, 1969.

Allen, C. C., J. L. Gooding, M. Jercinovic, and K. Keil, Altered basaltic glass: A terrestrial analog to the soil of Mars, *Icarus*, *45*, 347–369, 1981.

Arvidson, R. E., E. A. Guinness, and A. P. Zent, Classification of surface units in the equatorial region of Mars based on Viking Orbiter color, albedo, and thermal data, *J. Geophys. Res.*, *87*, 10,149–10,157, 1982.

Baird, A. K., and B. C. Clark, On the original igneous source of Martian fines, *Icarus*, *45*, 113–123, 1981.

Bertka, C. M., and J. R. Holloway, Martian mantle primary melts: An experimental study of melt density and viscosity at 23kb, *Lunar Planet. Sci.*, *20*, 69–70, 1989.

Bertka, C. M., and J. R. Holloway, Martian mantle primary melts, *Lunar Planet. Sci.*, *21*, 73–74, 1990.

Bibring, J. P., Y. Langevin, S. Erard, O. Forni, P. Masson, and C. Sotin, The observation of the surface of Mars by the ISM instrument on board the Phobos 2 spacecraft, *Lunar Planet. Sci.*, *21*, 79–80, 1990.

Bills, B. G., and A. J. Ferrari, Mars topography and geophysical implications, *J. Geophys. Res.*, *83*, 3497–3508, 1978.

Blackburn, E. A., Some aspects of explosive volcanism on the Earth, Moon and Mars, Ph.D. thesis, Univ. of Lancaster, Lancaster, England, 1977.

Blackburn, E. A., L. Wilson, and R. S. J. Sparks, Mechanisms and dynamics of strombolian activity, *J. Geol. Soc. London*, *132*, 429–440, 1976.

Blake, S., Volcanism and the dynamics of open magma chambers, *Nature*, *289*, 783–785, 1981.

Bruno, B. C., G. J. Taylor, S. K. Rowland, P. G. Lucey, and S. Self, Lava flows are fractals, *Geophys. Res. Lett.*, *19*, 305–308, 1992.

Carey, S. N., and R. S. J. Sparks, Quantitative models of the fall-out and dispersal of tephra from volcanic eruption columns, *Bull. Volcanol.*, *48*, 109–125, 1986.

Carr, M. H., Volcanism on Mars, *J. Geophys. Res.*, *78*, 4049–4062, 1973.

Carr, M. H., The role of lava erosion in the formation of lunar rilles and Martian channels, *Icarus*, *22*, 1–23, 1974.

Carr, M. H., Formation of Martian flood features by release of water from confined aquifers, *J. Geophys. Res.*, *84*, 2995–3007, 1979.

Carr, M. H., *The Surface of Mars*, 232 pp., Yale University Press, New Haven, Conn., 1981.

Carr, M. H., Water on Mars, *Nature*, *326*, 30–35, 1987.

Carr, M. H., D/H on Mars: Effects of floods, volcanism, impacts and polar processes, *Icarus*, *41*, 159–165, 1990.

Carr, M. H., K. R. Blasius, R. Greeley, J. E. Guest, and J. E. Murray, Observations on some Martian volcanic features as viewed from the Viking orbiters, *J. Geophys. Res.*, *82*, 3985–4015, 1977.

Cas, R. A. F., and J. V. Wright, *Volcanic Successions: Modern and Ancient*, Allen and Unwin, Winchester, Mass., 1987.

Cattermole, P., Linear volcanic features at Alba Patera, Mars, *Proc. Lunar Planet. Sci. Conf. 17th*, Part 1, *J. Geophys. Res.*, *91*, suppl., E159–E165, 1986.

Cattermole, P., Sequence, rheological properties, and effusion rates of volcanic flows at Alba Patera, Mars, *Proc. Lunar Planet. Sci. Conf. 17th*, Part 2, *J. Geophys. Res.*, *92*, suppl., E553–E560, 1987.

Cattermole, P., *Planetary Volcanism: A Study of Volcanic Activity in the Solar System*, 443 pp., Ellis Horwood, Chichester, England, 1989.

Cigolini, C., A. Borgia, and L. Casertano, Intercrater activity, *aa*-block lava, viscosity and flow dynamics: Arenal volcano, Costa Rica, *J. Volcanol. Geotherm. Res.*, *29*, 155–176, 1984.

Clark, B. C., A. K. Baird, R. J. Weldon, D. M. Tsusaki, L. Schnabel, and M. P. Candelaria, Chemical composition of Martian fines, *J. Geophys. Res.*, *87*, 10,059–10,067, 1982.

Clifford, S. M., A pore volume estimate of the Martian megaregolith based on a lunar analog, in International Colloquium on Mars, *LPI Contrib.*, *441*, 46–48, 1981.

Clifford, S. M., A model for the climatic behavior of water on Mars, Ph.D. thesis, Univ. of Mass., Boston, 1984.
Clifford, S. M., A model for the hydrologic and climatic behavior of water on Mars, *J. Geophys. Res.*, *98*, 10,973–11,016, 1993.
Comer, R. P., S. C. Solomon, and J. W. Head, Mars: Thickness of the lithosphere from the tectonic response to volcanic loads, *Rev. Geophys.*, *23*, 61–92, 1985.
Crisp, J., and S. Baloga, A model for lava flows with two thermal components, *J. Geophys. Res.*, *95*, 1255–1270, 1990.
Crown, D. A., and R. Greeley, Volcanic geology of Hadriaca Patera and the Eastern Hellas region of Mars, *J. Geophys. Res.*, *98*, 3431–3451, 1993.
Crumpler, L. S., and J. C. Aubele, Structural evolution of Arsia Mons, Pavonis Mons, and Ascreus Mons: Tharsis region of Mars, *Icarus*, *34*, 496–511, 1978.
Davis, P. A., and K. L. Tanaka, Small Martian volcanoes, in MEVTV Workshop on Nature and Composition of Surface Units on Mars, *Lunar Planet. Inst. Tech. Rep.*, *88-05*, 49–50, 1988.
Delaney, P. T., and D. D. Pollard, Solidification of basaltic magma during flow in a dike, *Am. J. Sci.*, *282*, 856–885, 1982.
Dreibus, G., and H. Wanke, Accretion of the Earth and the inner planets, in *Proceedings of the 27th International Geological Conference*, vol. 11, pp. 1–20, VNU Science Press, Utrecht, Netherlands, 1984.
Edgett, K. S., Possible cinder cones near the summit of Pavonis Mons, Mars, *Lunar Planet. Sci.*, *21*, 311–312, 1990.
Efford, N. D., Sources of error in the photoclinometric determination of planetary topography: A reappraisal, *Earth Moon Planets*, *54*, 19–58, 1991.
Eichelberger, J. C., and D. B. Hayes, Magmatic model for the Mount St. Helens blast of May 18, 1980, *J. Geophys. Res.*, *87*, 7727–7738, 1982.
Elder, J. W., *The Bowels of the Earth*, 222 pp., Oxford University Press, New York, 1976.
Elder, J. W., *The Structure of the Planets*, 210 pp., Academic, San Diego, Calif., 1987.
Fagents, S. A., and L. Wilson, Yield strengths of terrestrial, Martian and lunar flows: A reassessment, *Lunar Planet. Sci.*, *21*, 341–342, 1990.
Fanale, F. P., Martian volatiles: Their degasing history and geochemical fate, *Icarus*, *28*, 179–202, 1976.
Fedotov, S. A., Mechanism of deep-seated magmatic activity below island-arc volcanoes and similar structures, *Int. Geol. Rev.*, *6*, 671–680, 1977.
Fink, J. H., and R. C. Fletcher, Ropy pahoehoe: Surface folding of a viscous fluid, *J. Volcanol. Geotherm. Res.*, *4*, 151–170, 1978.
Fink, J. H., and J. R. Zimbelman, Rheology of the 1983 Royal Garden basalt flows, Kilauea volcano, Hawaii, *Bull. Volcanol.*, *48*, 87–96, 1986.
Fink, J. H., M. C. Malin, R. E. D'Alli, and R. Greeley, Rheological properties of mudflows associated with the sprint 1980 eruptions of Mount St. Helens volcano, Washington, *Geophys. Res. Lett.*, *8*, 43–46, 1981.
Fisher, R. V., and H. U. Schmincke, *Pyroclastic Rocks*, 472 pp., Springer-Verlag, New York, 1984.
Francis, P. W., and C. A. Wood, Absence of silicic volcanism on Mars: Implications for crustal composition and volatile abundance, *J. Geophys. Res.*, *87*, 9881–9889, 1982.
Frey, H., and M. Jarosewich, Subkilometer Martian landscapes: Properties and possible terrestrial analogs, *J. Geophys. Res.*, *87*, 9867–9879, 1982.
Frey, H., B. L. Lowry, and S. A. Chase, Pseudocraters on Mars, *J. Geophys. Res.*, *84*, 8075–8086, 1979.
Geissler, P. E., R. B. Singer, and B. K. Lucchitta, Dark materials in Valles Marineris: Indications of the style of volcanism and magmatism on Mars, *J. Geophys. Res.*, *95*, 14,399–14,413, 1990.
Goettel, K. A., Density of the mantle of Mars, *Geophys. Res. Lett.*, *8*, 497–500, 1981.
Greeley, R., Lava tubes and channels in the lunar Marius Hills, *Moon*, *3*, 289–314, 1970.
Greeley, R., Mariner 9 photographs of small volcanic structures on Mars, *Geology*, *1*, 175–180, 1973.
Greeley, R., and D. A. Crown, Volcanic geology of Tyrrhena Patera, Mars, *J. Geophys. Res.*, *95*, 7133–7149, 1990.
Greeley, R., and P. Spudis, Volcanism on Mars, *Rev. Geophys.*, *19*, 31–41, 1981.
Greeley, R., and E. Theilig, Martian lava-flows: Morphology and modes of emplacement, in Reports in Planetary Geology and Geophysics Program 1985, *NASA Tech. Memo.*, *88383*, 306–308, 1986.
Gudmundsson, A., Lateral magma flow, caldera collapse, and a mechanism of large eruptions in Iceland, *J. Volcanol. Geotherm. Res.*, *34*, 65–78, 1987.
Hartmann, W. K., Ancient lunar mega-regolith and subsurface structure, *Icarus*, *18*, 634–636, 1973.
Hayashi, J. N., and S. Self, A comparison of pyroclastic flow and debris avalanche mobility, *J. Geophys. Res.*, *97*, 9063–9071, 1992.
Head, J. W., Lunar volcanism in space and time, *Rev. Geophys.*, *14*, 265–296, 1976.
Head, J. W., and L. Wilson, Volcanic processes and landforms on Venus: Theory predictions and observations, *J. Geophys. Res.*, *91*, 9407–9446, 1986.
Head, J. W., and L. Wilson, Lava fountain heights at Pu'u 'O'o, Kilauea, Hawaii: Indicators of amount and variations of exsolved magma volatiles, *J. Geophys. Res.*, *92*, 13,715–13,719, 1987.
Head, J. W., and L. Wilson, Basaltic pyroclastic eruptions: Influence of gas release patterns and volume fluxes on fountain structure, and the formation of cinder cones, spatter cones, rootless flows, lava ponds and lava flows, *J. Volcanol. Geotherm. Res.*, *37*, 261–271, 1989.
Head, J. W., and L. Wilson, Absence of large shield volcanoes and calderas on the Moon: Consequence of magma transport phenomena?, *Geophys. Res. Lett.*, *18*, 2121–2124, 1991.
Head, J. W., and L. Wilson, Lunar mare volcanism: Stratigraphy, eruption conditions, and the evolution of secondary crusts, *Geochim. Cosmochim. Acta*, *55*, 2155–2175, 1992*a*.
Head, J. W., and L. Wilson, Magma reservoirs and neutral buoyancy zones on Venus: Implications for the formation and evolution of volcanic landforms, *J. Geophys. Res.*, *97*, 3877–3903, 1992*b*.
Head, J. W., and L. Wilson, Lunar graben formation due to near-surface deformation accompanying dike emplacement, *Planet. Space Sci.*, *10*, 719–727, 1993.
Head, J. W., K. Magee Roberts, L. Wilson, and H. Pinkerton, Lava flow-field morphological classification and interpretation: Examples from Venus, *Lunar Planet. Sci.*, *24*, 627–628, 1993.
Heslop, S. E., and L. Wilson, Pyroclast sizes in terrestrial and Martian ignimbrites, *Lunar Planet. Sci.*, *19*, 483–484, 1988.
Hill, D. P., Crustal structure of the island of Hawaii from seismic-reflection measurements, *Bull. Seismol. Soc. Am.*, *59*, 101–130, 1969.

Hodges, C. A., and H. J. Moore, Atlas of volcanic landforms on Mars, *U.S. Geol. Surv. Prof. Pap.*, in press, 1993.

Hulme, G., Turbulent lava flow and the formation of lunar sinuous rilles, *Mod. Geol.*, *4*, 107–117, 1973.

Hulme, G., The interpretation of lava flow morphology, *Geophys. J. R. Astron. Soc.*, *39*, 361–383, 1974.

Hulme, G., The determination of the rheological properties and effusion rate of Olympus Mons lava, *Icarus*, *27*, 207–213, 1976.

Hulme, G., A review of lava flow processes related to the formation of lunar sinuous rilles, *Geophys. Surv.*, *5*, 245–279, 1982.

Hulme, G., and G. Fielder, Effusion rates and rheology of lunar lavas, *Phil. Trans. R. Soc. London A*, *285*, 227–234, 1977.

Johnson, A. M., and D. D. Pollard, Mechanics and growth of some lacolith intrusions in the Neary Mountains, Utah, I, Field observations, Gilbert's model, physical properties and the flow of the magma, *Tectonophysics*, *18*, 261–309, 1973.

Johnson, M. C., M. J. Rutherford, and P. C. Hess, Chassigny petrogenesis: Melt compositions, intensive parameters and water contents of Martian (?) magmas, *Geochim. Cosmochim. Acta*, *55*, 349–366, 1991.

Jones, J. H., A discussion of isotopic systematics and mineral zoning in the shergottites: Evidence for a 180 m.y. igneous crystallization age, *Geochim. Cosmochim. Acta*, *50*, 969–977, 1986.

Kieffer, S. W., Factors governing the structure of volcanic jets, in *Studies in Geophysics, Volcanism: Inception, Evolution, and Hazards*, pp. 143–157, National Academy Press, Washington, D. C., 1984.

Kilburn, C. J., Pahoehoe and aa lavas: A discussion and continuation of the model by Peterson and Tilling, *J. Volcanol. Geotherm. Res.*, *11*, 373–389, 1981.

Kilburn, C. R. J., The rheological behavior of basaltic magmas, in *Mount Etna, The Anatomy of a Volcano*, edited by D. K. Chester, A. M. Duncan, J. E. Guest, and C. R. J. Kilburn, pp. 187–228, Stanford University Press, Stanford, Calif., 1985.

Kilburn, C. J., Lava crusts, aa flow lengthening and the pahoehoe-aa transition, in *Active Lavas: Monitoring and Modelling*, edited by C. R. J. Kilburn and G. Luongo, pp. 263–280, University College London Press, London, 1993.

Longhi, J., Magmatic processes on Mars: Insights from SNC meteorites, *Lunar Planet. Sci.*, *21*, 716–717, 1990.

Longhi, J., Volatiles in SNC petrogenesis: A Sr signal?, *Lunar Planet. Sci.*, *23*, 805–806, 1992.

Longhi, J., and V. Pan, The regulation of hydrogen and oxygen escape from Mars, *Icarus*, *28*, 231–246, 1988.

Lorenz, V., On the formation of maars, *Bull. Volcanol.*, *37*, 183–204, 1973.

Lucchitta, B. K., Recent mafic volcanism on Mars, *Science*, *235*, 565–567, 1987.

Lucchitta, B. K., Young volcanic deposits in the Valles Marineris, Mars?, *Icarus*, *86*, 476–509, 1990.

Malin, M. C., Lengths of Hawaiian lava flows, *Geology*, *8*, 306–308, 1980.

Malin, M. C., and M. F. Sheridan, Computer-assisted mapping of pyroclastic surges, *Science*, *217*, 637–640, 1982.

Marsh, B. D., and I. S. E. Carmichael, Benioff zone magmatism, *J. Geophys. Res.*, *79*, 1196–1206, 1974.

Marsh, B. D., and L. H. Kantha, On the heat and mass transfer from an ascending magma, *Earth Planet. Sci. Lett.*, *39*, 435–443, 1978.

McBirney, A. R., and T. Murase, Rheological properties of magmas, *Annu. Rev. Earth Planet. Sci.*, *12*, 337–357, 1984.

McBride, K., and J. R. Zimbelman, Evidence of pyroclastic activity near Elysium Mons, Mars, *Lunar Planet. Sci.*, *20*, 651, 1989.

McBride, K., and J. R. Zimbelman, Small volcanic features in Western Elysium Planitia, *Lunar Planet. Sci.*, *21*, 746–747, 1990.

McCord, T. B., et al., Mars: Definition and characterization of global surface units with emphasis on composition, *J. Geophys. Res.*, *87*, 10,129–10,148, 1982.

McGetchin, T., and T. R. Smyth, The mantle of Mars: Some possible geologic implications of its high density, *Icarus*, *34*, 512–536, 1978.

McGetchin, T. R., M. Settle, and B. A. Chouet, Cinder cone growth modeled after Northeast Crater, Mount Etna, Sicily, *J. Geophys. Res.*, *79*, 3257–3272, 1974.

McSween, H. Y., and R. P. Harvey, Outgassed water on Mars: Constraints from melt inclusions in SNC meteorites, *Science*, *259*, 1890–1892, 1993.

Moore, H. J., Preliminary estimates of the rheological properties of 1984 Mauna Loa lava, in Volcanism in Hawaii, *U.S. Geol. Surv. Prof. Pap.*, *1350*, 1569–1588, 1987.

Moore, H. J., and G. G. Schaber, An estimate of the yield strengths of the imbrium flows, *Proc. Lunar Sci. Conf.*, *6th*, 101–118, 1975.

Moore, H. J., D. W. G. Arthur, and G. G. Schaber, Yield strengths of flows on the Earth, Moon, and Mars, *Proc. Lunar Planet. Sci. Conf.*, *9th*, 3351–3378, 1978.

Morton, B. R., G. Taylor, and J. S. Turner, Turbulent gravitational convection from maintained and instantaneous sources, *Proc. R. Soc. London A*, *234*, 1–23, 1956.

Mouginis-Mark, P. J., Volcano/ground ice interactions in Elysium Planitia, Mars, *Icarus*, *64*, 265–284, 1985.

Mouginis-Mark, P. J., Emplacement of long lava flows at Elsium Mons, Mars, *Lunar Planet. Sci.*, *23*, 939–940, 1992.

Mouginis-Mark, P. J., L. Wilson, and J. W. Head, Explosive volcanism at Hecates Tholus, Mars: Investigation of eruption conditions, *J. Geophys. Res.*, *87*, 9890–9904, 1982.

Mouginis-Mark, P. J., L. Wilson, J. W. Head, S. H. Brown, J. L. Hall, and K. D. Sullivan, Elysium Planitia, Mars: Regional geology, volcanology and evidence for volcano-ground ice interactions, *Earth Moon Planets*, *30*, 149–173, 1984.

Mouginis-Mark, P. J., L. Wilson, and J. R. Zimbelman, Polygenic eruptions on Alba Patera, Mars, *Bull. Volcanol.*, *50*, 361–379, 1988.

Mouginis-Mark, P. J., L. Wilson, and M. T. Zuber, The physical volcanology of Mars, in *Mars*, edited by H. H. Kieffer, B. M. Jakosky, C. W. Snyder, and M. S. Matthews, pp. 424–452, University of Arizona Press, Tucson, 1992.

Murase, T., and A. R. McBirney, Properties of some common igneous rocks and their melts at high temperature, *Geol. Sci. Am. Bull.*, *84*, 3563–3592, 1973.

Murchie, S., J. Mustard, S. Erard, P. Geissler, and R. Singer, Variations in the Fe mineralogy of bright Martian soil, *Lunar Planet. Sci.*, *24*, 1029–1030, 1993.

Mustard, J. F., S. Erard, J. P. Bibring, J. W. Head, S. Hurtrez, Y. Langevin, C. M. Pieters, and C. J. Sotin, The surface of Syrtis Major: Composition of the volcanic substrate and mixing with altered dust and soil, *J. Geophys. Res.*, *98*, 3387–3400, 1993.

Mutch, T. A., R. E. Arvidson, J. W. Head, K. L. Jones, and R. S. Saunders, *The Geology of Mars*, 400 pp., Princeton University Press, Princeton, N. J., 1976.

Mysen, B. O., The solubility of H_2O and CO_2 under predicted magma genesis conditions and some petrological

and geophysical implications, *Rev. Geophys.*, *15*, 351–361, 1977.

Nairn, I. A., Atmospheric shock waves and condensation clouds from Ngauruhoe explosive eruptions, *Nature*, *259*, 190–192, 1976.

Nairn, I. A., and S. Self, Explosive eruptions and pyroclastic avalanches from Ngauruhoe in February, 1975, *J. Volcanol. Geotherm. Res.*, *3*, 39–60, 1978.

Nakamura, N., D. M. Unruh, M. Tatsumoto, and R. Hutchinson, Origin and evolution of the Nakhula meteorite inferred from the Sm-Nd and U-Pb systematics and REE, Ba, Sr, Rb abundances, *Geochim. Cosmochim. Acta*, *46*, 1555–1583, 1982.

Owen, T., The composition and early history of the atmosphere of Mars, in *Mars*, edited by H. H. Kieffer, B. M. Jakosky, C. W. Snyder, and M. S. Matthews, pp. 818–834, University of Arizona Press, Tucson, 1992.

Oxburgh, E. R., Heat flow and magma genesis, in *Physics of Magmatic Processes*, edited by R. B. Hargraves, pp. 161–199, Princeton University Press, Princeton, N. J., 1980.

Pavri, B., J. W. Head, K. B. Klose, and L. Wilson, Steep-sided domes on Venus: Characteristics, geologic setting, and eruption conditions from Magellan data, *J. Geophys. Res.*, *97*, 13,445–13,478, 1992.

Peterson, D. W., and R. I. Tilling, Transition of basaltic lava from pahoehoe to aa, Kilauea volcano, Hawaii: Field observations and key factors, *J. Volcanol. Geotherm. Res.*, *7*, 271–293, 1980.

Pieri, D. C., and S. M. Baloga, Eruption rate, area and length relationships for some Hawaiian flows, *J. Volcanol. Geotherm. Res.*, *30*, 29–45, 1986.

Pieri, D., D. Schneeberger, S. Baloga, and R. S. Saunders, Dimensions of lava flows at Alba Patera, Mars, in Reports on Planetary Geology and Geophysics Program 1985, *NASA Tech. Memo.*, *88383*, 318–320, 1986.

Pinet, P., and S. Chevral, Spectral identification of geological units on the surface of Mars related to the presence of silicates from Earth-based near-infrared telescopic charge-coupled device-imaging, *J. Geophys. Res.*, *95*, 14,435–14,446, 1990.

Pinkerton, H., and R. S. J. Sparks, The 1975 sub-terminal lavas, Mount Etna: A case history of the formation of a compound lava field, *J. Volcanol. Geotherm. Res.*, *1*, 167–182, 1976.

Pinkerton, H., and L. Wilson, Factors controlling the lengths of channel-fed lava flows, *Bull. Volcanol.*, *56*, 108–120, 1994.

Plescia, J. B., The Tempe volcanic province of Mars and comparisons with the Snake River plains of Idaho, *Icarus*, *45*, 586–601, 1981.

Plescia, J. B., Recent flood lavas in the Elysium region of Mars, *Icarus*, *88*, 465–490, 1990.

Plescia, J. B., and R. S. Saunders, The chronology of the Martian volcanoes, *Proc. Lunar Planet. Sci. Conf.*, *10th*, 2841–2859, 1979.

Pollard, D. D., On the form and stability of open hydraulic fractures in the Earth's crust, *Geophys. Res. Lett.*, *3*, 513–516, 1976.

Pollard, D. D., and O. H. Muller, The effects of gradients in regional stress and magma pressure on the form of sheet intrusions in cross section, *J. Geophys. Res.*, *81*, 975–984, 1976.

Riemers, C. E., and P. D. Komar, Evidence for explosive volcanic density currents on certain Martian volcanoes, *Icarus*, *39*, 88–110, 1979.

Robinson, M. S., P. J. Mouginis-Mark, J. R. Zimbelman, S. S. C. Wu, K. K. Ablin, and A. E. Howington-Kraus, Chronology, eruption duration, and atmospheric contribution of the Martian volcano Apollinaris Patera, *Icarus*, *104*, 301–323, 1993.

Roush, T. L., Infrared transmission measurements of Martian soil analogs, in MECA Workshop on Dust on Mars III, *Lunar Planet. Inst. Tech. Rep.*, *89-01*, 52–54, 1989.

Rowland, S. K., and G. P. L. Walker, Pahoehoe and a'a in Hawaii: Volumetric flow rate controls the lava structure, *Bull. Volcanol.*, *52*, 615–628, 1990.

Rubin, A. E., Tensile fracture of rock at high confining pressure: Implications for dike propagation, *J. Geophys. Res.*, *98*, 15,919–15,935, 1993.

Rubin, A. M., and D. D. Pollard, Origins of blade-like dikes in volcanic rift zones, in Volcanism in Hawaii, *U.S. Geol. Surv. Prof. Pap.*, *1350*, 1449–1470, 1987.

Rutherford, M. J., The abundance and role of H_2O in SNC (Mars) versus Earth and Moon magmatic processes (abstract), *Eos Trans. AGU*, *72*(44), Fall Meeting suppl., 281, 1991.

Ryan, M. P., Neutral buoyancy and the mechanical evolution of magmatic systems, in Magmatic Processes: Physiochemical Principles, edited by B. O. Mysen, *Spec. Publ. Geochem. Soc.*, *1*, 259–287, 1987.

Schaber, G. G., Syrtis Major: A low-relief volcanic shield, *J. Geophys. Res.*, *87*, 9852–9866, 1982.

Schaber, G. G., K. C. Horstman, and A. L. Dial, Lava flow materials in the Tharsis region of Mars, *Proc. Lunar Planet. Sci. Conf.*, *9th*, 33,433–34,458, 1978.

Schubert, G., S. C. Solomon, S. C. Turcotte, M. J. Drake, and N. H. Sleep, Origin and thermal evolution of Mars, in *Mars*, edited by H. H. Kieffer, B. M. Jakosky, C. W. Snyder, and M. S. Matthews, pp. 147–183, University of Arizona Press, Tucson, 1992.

Schultz, P. H., and H. Glicken, Impact crater and basin control of igneous processes on Mars, *J. Geophys. Res.*, *84*, 8033–8047, 1979.

Scott, D. H., Volcanoes and volcanic provinces: Martian western hemisphere, *J. Geophys. Res.*, *87*, 9839–9851, 1982.

Scott, D. H., and K. L. Tanaka, Ignimbrites of Amazonis Planitia region of Mars, *J. Geophys. Res.*, *87*, 1179–1190, 1982.

Secor, D. T., and D. D. Pollard, On the stability of open hydraulic fractures in the Earth's crust, *Geophys. Res. Lett.*, *2*, 510–513, 1975.

Self, S., R. S. J. Sparks, B. Booth, and G. P. L. Walker, The 1973 Heimaey strombolian scoria deposit, Iceland, *Geol. Mag.*, *111*, 539–548, 1974.

Self, S., L. Wilson, and I. A. Nairn, Vulcanian eruption mechanisms, *Nature*, *277*, 440–443, 1979.

Settle, M., Volcanic eruption clouds and the thermal power output of explosive eruptions, *J. Volcanol. Geotherm. Res.*, *3*, 309–324, 1978.

Settle, M., Formation and deposition of volcanic sulfate aerosols on Mars, *J. Geophys. Res.*, *84*, 8343–8354, 1979.

Shaw, H. R., D. L. Peck, T. L. Wright, and R. Okamura, Viscosity of basaltic magma: An analysis of field measurements at Makaopuhi lava lake, Hawaii, *Am. J. Sci.*, *226*, 225–264, 1968.

Shaw, H. R., Rheology of basalt in the melting range, *J. Petrol.*, *10*, 510–535, 1969.

Sheridan, M. F., Emplacement of pyroclastic flows: A review, *Spec. Pap. Geol. Soc. Am.*, *180*, 125–136, 1979.

Sheridan, M. F., Pyroclastic block flow from the September, 1976 eruption of La Soufriere volcano, Guadeloupe, *Bull. Volcanol.*, *43*, 397–402, 1980.

Short, N. M., and M. L. Forman, Thickness of impact crater ejecta on the lunar surface, *Mod. Geol.*, *3*, 69–91, 1972.

Singer, R. B., Spectral evidence for the mineralogy of high

albedo soils and dust on Mars, *J. Geophys. Res.*, *87*, 10,159–10,168, 1982.

Singer, R. B., J. S. Miller, and W. K. Wells, Observed variations in Martian crustal composition, *Bull. Am. Astron. Soc.*, *22*, 1061, 1990.

Sleep, N., Tapping of melt by veins and dikes, *J. Geophys. Res.*, *93*, 10,255–10,272, 1988.

Soderblom, L. A., The composition and mineralogy of the Martian surface from spectroscopy observations: 0.3μm to 50μm, in *Mars*, edited by H. H. Kieffer, B. M. Jakosky, C. W. Snyder, and M. S. Matthews, pp. 557–593, University of Arizona Press, Tucson, 1992.

Soderblom, L. A., K. Edwards, E. M. Eliason, E. M. Sanchez, and M. P. Charette, Global color variations on the Martian surface, *Icarus*, *34*, 446–464, 1978.

Solomon, S. C., and J. W. Head, Heterogeneities in the thickness of the elastic lithosphere of Mars: Constraints on heat flow and internal dynamics, *J. Geophys. Res.*, *95*, 11,073–11,083, 1990.

Sparks, R. S. J., The dynamics of bubble formation and growth magmas: A review and analysis, *J. Volcanol. Geotherm. Res.*, *3*, 1–37, 1978.

Sparks, R. S. J., and L. Wilson, A model for the formation of ignimbrite by gravitational column collapse, *J. Geol. Soc. London*, *132*, 441–451, 1976.

Sparks, R. S. J., L. Wilson, and G. Hulme, Theoretical modelling of the generation, movement, and emplacement of pyroclastic flows by column collapse, *J. Geophys. Res.*, *83*, 1727–1739, 1978.

Spera, F. J., Aspects of magma transport, in *Physics of Magmatic Processes*, edited by R. B. Hargraves, pp. 265–323, Princeton University Press, Princeton, N. J., 1980.

Squyres, S. W., D. E. Wilhelms, and A. C. Moosman, Large-scale volcano-ground ice interaction on Mars, *Icarus*, *70*, 385–408, 1987.

Squyres, S. W., S. M. Clifford, R. O. Kuzmin, J. R. Zimbelman, and F. M. Costard, Ice in the Martian regolith, in *Mars*, edited by H. H. Kieffer, B. M. Jakosky, C. W. Snyder, and M. S. Matthews, pp. 523–554, University of Arizona Press, Tucson, 1992.

Stevenson, D. J., T. Spohn, and G. Schubert, Magnetism and thermal evolution of the terrestrial planets, *Icarus*, *54*, 466–489, 1983.

Stothers, R. B., Turbulent atmospheric plumes above line sources with an application to volcanic fissure eruptions on the terrestrial planets, *J. Atmos. Sci.*, *46*, 2662–2670, 1989.

Stothers, R. B., J. A. Wolff, S. Self, and M. R. Rampino, Basaltic fissure eruptions, plume heights and atmospheric aerosols, *Geophys. Res. Lett.*, *13*, 725–728, 1986.

Swanson, D. A., T. L. Wright, and R. T. Helz, Linear vent systems and estimated rates of magma production and eruption for the Yakima basalt of the Columbia plateau, *Am. J. Sci.*, *275*, 877–905, 1975.

Tanaka, K. L., M. G. Chapman, and D. H. Scott, Geologic map of the Elysium region of Mars, scale 1:5,000,000, *U.S. Geol. Surv. Misc. Invest. Map*, *I-2147*, 1992*a*.

Tanaka, K. L., D. H. Scott, and R. Greeley, Global stratigraphy, in *Mars*, edited by H. H. Kieffer, B. M. Jakosky, C. W. Snyder, and M. S. Matthews, pp. 345–382, University of Arizona Press, Tucson, 1992*b*.

Theilig, E., and R. Greeley, Lava flows on Mars: Analysis of small surface features and comparisons with terrestrial analogs, *Proc. Lunar Planet. Sci. Conf. 17th*, Part 1, *J. Geophys. Res.*, *90*, suppl., E193–E206, 1986.

Thorarinsson, S., The crater groups in Iceland, *Bull. Volcanol.*, *14*, 3–44, 1953.

Thorarinsson, S., *Surtsey—The New Island in the North Atlantic*, pp. 1–47, Viking, New York, 1967.

Thorarinsson, S., The Lakagigar eruption of 1783, *Bull. Volcanol.*, *33*, 910–927, 1970.

Toulmin, P., A. K. Baird, B. C. Clark, K. Keil, H. J. Rose Jr., R. P. Christian, P. H. Evans, and W. C. Kelliher, Geochemical and mineralogical interpretation of the Viking inorganic chemical results, *J. Geophys. Res.*, *84*, 4625–4634, 1977.

Treiman, A. H., The parental magma of the Nakha achondrite: Ultrabasic volcanism on the shergottite parental body, *Geochim. Cosmochim. Acta*, *50*, 1061–1070, 1986.

Valentine, G. A., and K. H. Wohletz, Numerical models of plinian eruption columns and pyroclastic flows, *J. Geophys. Res.*, *94*, 1867–1887, 1989.

Wadge, G., and R. M. C. Lopes, The lobes of lava flows on Earth and Olympus Mons, Mars, *Bull. Volcanol.*, *54*, 10–24, 1992.

Walker, G. P. L., Lengths of lava flow, *Phil. Trans. R. Soc. London A*, *274*, 107–118, 1973.

Walker, G. P. L., S. Self, and L. Wilson, Tarawera, 1886, New Zealand—A basaltic plinian fissure eruption, *J. Volcanol. Geotherm. Res.*, *21*, 61–78, 1984.

Weertman, J., Theory of water-filled crevasses in glaciers applied to vertical magma transport beneath oceanic ridges, *J. Geophys. Res.*, *76*, 1171–1183, 1971.

Wilhelms, D. E., Lava-ice interactions on Mars, in Reports on Planetary Geology and Geophysics Program 1985, *NASA Tech. Memo.*, *88383*, 491–493, 1986.

Wilhelms, D. E., and R. J. Baldwin, The role of igneous sills in shaping the Martian uplands, *Proc. Lunar Planet. Sci. Conf.*, *19th*, 355–365, 1988.

Williams, H., The history and character of volcanic domes, *Univ. Calif. Publ. Geol. Sci.*, *21*, 51–146, 1932.

Wilson, L., Explosive volcanic eruptions, II, The atmospheric trajectories of pyroclasts, *Geophys. J. R. Astron. Soc.*, *30*, 381–392, 1972.

Wilson, L., Explosive volcanic eruptions, III, Plinian eruption columns, *Geophys. J. R. Astron. Soc.*, *45*, 543–556, 1976.

Wilson, L., Energetics of the minoan eruption, in *Proceedings of 2nd International Conference on Thera and the Aegean World*, edited by C. Doumas, pp. 221–228, Thera and the Aegean World, London, 1978.

Wilson, L., Relationships between pressure, volatile content and ejecta velocity in three types of volcanic explosion, *J. Volcanol. Geotherm. Res.*, *8*, 297–313, 1980.

Wilson, L., The influences of planetary environments on the eruption styles of volcanoes, *Vistas Astron.*, *27*, 333–360, 1984.

Wilson, L., and J. W. Head, Ascent and eruption of basaltic magma on the Earth and Moon, *J. Geophys. Res.*, *86*, 2971–3001, 1981*a*.

Wilson, L., and J. W. Head, The formation of eroded depressions around the sources of lunar sinuous rilles: Theory, *Lunar Planet. Sci.*, *12*, 427–429, 1981*b*.

Wilson, L., and J. W. Head, A comparison of volcanic eruption processes on Earth, Moon, Mars, Io and Venus, *Nature*, *302*, 663–669, 1983.

Wilson, L., and J. W. Head, The influence of gravity on planetary volcanic eruption rates, *Lunar Planet. Sci.*, *19*, 1283–1284, 1988.

Wilson, L., and S. E. Heslop, Clast sizes in terrestrial and Martian ignimbrite lag deposits, *J. Geophys. Res.*, *95*, 17,309–17,314, 1990.

Wilson, L., and E. A. Parfitt, The influence of gravity on planetary volcanic eruption rates: A reappraisal, *Lunar Planet. Sci.*, *20*, 1213–1214, 1989.

Wilson, L., and E. A. Parfitt, Widths of dikes on Earth and Mars, *Lunar Planet. Sci.*, *21*, 1345–1346, 1990.

Wilson, L., and G. P. L. Walker, Explosive volcanic eruptions, VI, Ejecta dispersal in plinian eruptions: The control of eruption conditions and atmospheric properties, *Geophys. J. R. Astron. Soc.*, *89*, 657–679, 1987.

Wilson, L., R. S. J. Sparks, T. C. Huang, and N. D. Watkins, The control of volcanic column heights by eruption energetics and dynamics, *J. Volcanol. Geotherm. Res.*, *83*, 1829–1836, 1978.

Wilson, L., R. S. J. Sparks, and G. P. L. Walker, Explosive volcanic eruptions, IV, The control of magma properties and conduit geometry on eruption column behavior, *Geophys. J. R. Astron. Soc.*, *63*, 117–148, 1980.

Wilson, L., J. W. Head, and P. J. Mouginis-Mark, Theoretical analysis of Martian volcanic eruption mechanisms, Proceedings of Workshop on the Planet Mars, *Eur. Space Agency Spec. Publ., ESA SP-185*, 107–113, 1982.

Wood, C. A., Monogenetic volcanoes of the terrestrial planets, *Proc. Lunar Planet. Sci. Conf., 10th*, 2815–2840, 1979.

Wood, C. A., and L. D. Ashwal, SNC meteorites: Igneous rocks from Mars?, *Proc. Lunar Planet. Sci. Conf., 12th*, 1359–1375, 1981.

Zimbelman, J. R., Estimates of rheologic properties for flows on the Martian volcano Ascraeus Mons, *Proc. Lunar Planet. Sci. Conf. 16th*, Part 1, *J. Geophys. Res.*, *90*, suppl., D157–D162, 1985*a*.

Zimbelman, J. R., Estimates of rheologic properties for six Martian lava flows, *Lunar Planet. Sci.*, *16*, 932–933, 1985*b*.

Zimbelman, J. R., and K. S. Edgett, The Tharsis Montes, Mars: Comparison of volcanic and modified landforms, *Proc. Lunar Planet. Sci. Conf., 22nd*, 31–44, 1992.

J. W. Head III, Department of Geological Sciences, Brown University, Box 1846, Providence, RI 02912.

L. Wilson, Environmental Science Division, Institute of Environmental and Biological Sciences, Lancaster University, Lancaster LA1 4YQ, England.